AGRICULTURAL WASTES AS ADSORBENTS FOR THE REMOVAL OF TOXIC METAL IONS FROM INDUSTRIAL EFFLUENTS

Submitted in the partial fulfillment of the requirement

for the Degree of

Doctor of Philosophy

by

Joginder Singh

(Roll No. 950909003)

SCHOOL OF CHEMISTRY AND BIOCHEMISTRY

THAPAR UNIVERSITY

(Formerly, Thapar Institute of Engg. & Tech.)

PATIALA – 147 004

July (2013)

ACKNOWLEDGEMENTS

I am highly indebted to the Almighty who has given me the strength to accomplish this big task.

It is my proud privilege to put on record my deep sense of gratitude to my revered guide and mentor, Dr. Amjad Ali, School of Chemistry and Biochemistry, Thapar University, Patiala, for his kind support, guidance, constructive criticism and timely advice from preliminary to the concluding level of my Doctoral Research. He guided me through out my work with patience and knowledge whilst allowing me the room to work in my own way. He has always been a pillar of support and constant source of inspiration. His commitment and sense of mission has molded my work to provide it direction and substance.

I am extremely thankful to the Director, Thapar University, Dean (Research & Sponsored Projects) and Head, School of Chemistry and Biochemistry for extending the opportunity to undertake this doctoral research.

I am indebted to Shri Tarsem Garg Ji, Founder and President, M.M. University Trust, Director and Principal M.M.E.C, Registrar M.M. University, Mullana, Ambala for providing me the opportunity to carry on this research.

I would like to acknowledge Dr. Satnam Singh and Dr. Dinesh Goyal, Thapar University, Patiala for providing their expertise to the study and mentoring me professionally as well as personally. I am highly obliged to Dr. Susheel Mittal, Dr. Bomanali Pal, Dr. Manmohan Chibber, Dr. N. Tejo Prakash, Dr. Ranjana Prakash & Dr. Rajesh Kumar for directing my study through valuable inputs.

Pal, Dr. Manmohan Chibber, Dr. N. Tejo Prakash, Dr. Ranjana Prakash & Dr. Rajesh Kumar for directing my study through valuable inputs.

Grateful acknowledgement is made to my senior Dr. Dinesh Kumar, Dr. Nirankar Singh, Mr. Vishal, Mr. Pawan Kumar and my friends Rohit, Mandeep, Madhu, Navjot, Alka, Nidhi, Rishu.

I am extremely grateful to my parents and parents' in-law, my elder brother & sister and my wife for their infinite patience and unending support.

Joginder Singh

CERTIFICATE

This is to certify that thesis entitled "AGRICULTURAL WASTES AS ADSORBENTS FOR THE REMOVAL OF TOXIC METAL IONS FROM INDUSTRIAL EFFLUENTS", being submitted by Joginder Singh, to the School of Chemistry and Biochemistry, Thapar University, Patiala for the award of degree of DOCTOR OF PHILOSOPHY, is a record of bonafide research work carried out by him. Mr. Joginder Singh has worked under my guidance and supervision and has fulfilled the requirements for the submission of this thesis, which to my knowledge has reached the requisite standard.

The results embodied in the thesis have not been submitted in part or full to any other University or Institute for the award of any degree or diploma.

Dr. Amjad Ali
Associate Professor
School of Chemistry and Biochemistry,
Thapar University,
Patiala, Punjab,
India.

Thesis Approval Sheet

Thesis entitled **"AGRICULTURAL WASTES AS ADSORBENTS FOR THE REMOVAL OF TOXIC METAL IONS FROM INDUSTRIAL EFFLUENTS"** by Joginder Singh is approved for the degree of DOCTOR OF PHILOSOPHY.

.....

Head, SCBC

Preceptor

.....

.....

DEAN, R&EP

Date: 10-10-2013

List of Abbreviations

Abbreviation	Description
AAHSP	Activated *Arachis hypogea* shell powder
AAS	Atomic absorption spectrophotometer
AHSP	*Arachis hypogea* shell powder
BOD	Biological oxygen demand
ANDB	Aspergillus niger decomposed biomass
BDST	Bed depth service time
BTP	Breakthrough point
COD	Chemical oxygen demand
CPCB	Central pollution control board standards
ESD	*Eucalyptus sp.* saw dust
EDX	Energy dispersive x-ray
FTIR	Fourier transform infra red
FESEM	Field emission scanning electron microscope
kJ mol^{-1}	Kilo joule per mole
kJ $mol^{-1}K^{-1}$	Kilo joule per mole per Kelvin
mg	Milligram
M	Molar
mg L^{-1}	Milligram per litre
min	Minute
mL	Milli litre
M_a	Mass of the adsorbent
mL min^{-1}	Milli litre per minute
NTU	Nephelometric turbidity unit
nm	Nanometer
ppm	Parts per million
pH_{PZC}	Point of zero charge
rpm	Rotation per minute
T	Temperature
TABP	*Trifolium alexandrinum* biomass powder
t	Time
L	Litre
h	Hour
V	Volume
USEPA	United States Environmental Protection Agency
WHO	World Health Organization

List of Symbols

Symbol	Description
α	Initial adsorption rate
B	Langmuir constant (L mg^{-1})
B	Desorption constant
C	Celsius
C_e	Equilibrium metal ion concentration (mg L^{-1})
C_i	Initial metal ion concentration (mg L^{-1})
$^\circ$	Degree
G	Gram
ΔG°	Gibb's free energy change (kL mol^{-1})
ΔH°	Enthalpy change (kL mol^{-1})
K	Kelvin
k_1	pseudo-first-order rate constant (g $mg^{-1}min^{-1}$)
k_2	pseudo-second-order rate constant (g $mg^{-1}min^{-1}$)
K_F	Freundlich constant (L g^{-1})
K_a	Rate constant for BDST model (L mg^{-1} h^{-1})
k_{th}	Thomas constant (mL min^{-1} mg^{-1})
K_d	Equilibrium constant
N	Freundlich constant
N_o	Adsorption capacity (mg L^{-1})
%	Percentage
q_e	Metal uptake capacity (mg g^{-1})
q_t	The amount of metal ions adsorbed at time t (mg g^{-1})
q_{max}	Maximum biosorption capacity of the biosorbent (mg g^{-1})
R	Flow rate in column studies (mL min^{-1})
R	Gas constant (J mol^{-1} K^{-1})
R^2	Correlation Coefficient
R_L	Separation Factor
S	Amount of adsorbent in gram (Thomas model parameter) (g)
ΔS°	Entropy change (kL $mol^{-1}K^{-1}$)
t_b	Breakthrough service time (h)
V_{eff}	Effluent volume (mL)
Z	Bed depth (cm)

CONTENTS

Abstract

Millions of people worldwide are suffering with the scarcity of fresh and clean drinking water, which is a fundamental need for all human beings. Freshwater resources are continuously degrading mainly due to the hasty pace of unplanned urbanization, industrialization, population growth, over exploitation and poor management. The main sources of freshwater pollution can be attributed to discharge of untreated sanitary and toxic industrial wastes, dumping of industrial effluent and runoff from agricultural fields. It is well known that 70-80% of diseases in developing countries are due to the consumption of contaminated water. Metal ions are one of the main categories of water pollutants as they are toxic for humans when penetrated the food-chain pyramid. Various toxic heavy metals (Chromium, Nickel, Copper, Zinc, Lead, Cadmium, Mercury, Arsenic, Molybdenum, Cobalt and Uranium) discharged into the environment through different industrial activities are the major causes of water pollution. These metals are highly toxic and it is compulsory to treat the industrial wastewater to permissible limits before disposal into normal water bodies. Several treatment technologies such as membrane processes, ion exchange, precipitation and coagulation have been applied in past to remove heavy metal ions from industrial wastewater. However, these methods posses various disadvantages such as lack of cost effectiveness, production of toxic chemical sludge etc. Therefore the removal of toxic heavy metals from industrial effluents in a cost effective and environment friendly manner is of greater significance. Biosorption of metal ions by agricultural residues seems to be an ecofriendly technology to clean up contaminated water.

In this context, present work envisaged to prepare, characterize and evaluate the metal uptake capacity of the agricultural residues from synthetic and industrial wastewater. Mainly four different biosorbents viz., *Arachis hypogea* shell powder, *Trifolium alexandrinum* biomass powder, *Eucalyptus sp.* saw dust and *Citrus limetta* peel powder have been prepared and employed for the water treatment. *Arachis hypogea* shell powder used was activated using different concentration of hydrochloric acid and in one of the experiment, the fungus *Aspergillus niger* was employed on *Citrus limetta* peel powder for decomposing it and the decomposed, dead biomass was employed for biosorption purposes.

The influence of pH, initial metal ion concentration, adsorbent dose, and contact time were studied and the experimental data obtained were evaluated and fitted using equilibrium isotherms and kinetic models. FTIR analyses of the biosorbents were done to study the functional groups

involved in metal binding. SEM-EDX was employed to study the surface morphology and to analyze the biosorbed metal ions. Mechanistic aspect of metal biosorption were investigated via chemical blocking of the functional groups and the release of alkali and alkaline earth metals during biosorption of the metal ions. This study supported that ion-exchange mechanism is involved in metal biosorption.

Under optimized conditions for different metal ions, column studies were conducted in both down flow and up flow mode using the electroplating, lead acid battery and paint manufacturing industrial wastewater. The column breakthrough curves were analyzed at different flow rates and bed depths, and best fittings were obtained by following the Thomas and BDST models. To demonstrate the reusability of the biosorbents, they have been regenerated by different desorption agents viz., HCl, H_2SO_4 , HNO_3, NaOH and EDTA.

Thus, it could be concluded from the present work that biosorbents prepared from agricultural wastes have excellent potential for the removal of Cr(VI), Cu^{2+}, Ni^{2+}, Zn^{2+}, Pb^{2+} and Cd^{2+} from different industrial effluents with high biosorption capacity.

Keywords: Metal toxicity, agricultural residues, *Trifolium alexandrinum, Citrus limetta, Aspergillus niger*, chemical blocking, functional groups, ion exchange process, paint manufacturing industries wastewater, up flow column studies.

"Thesis Configuration"

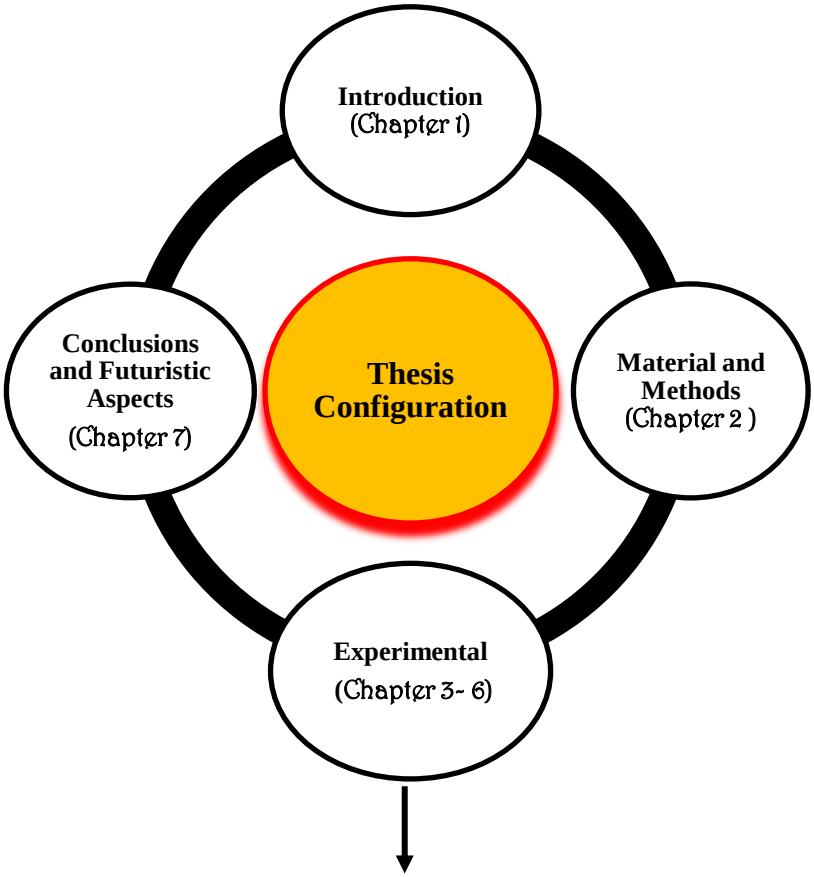

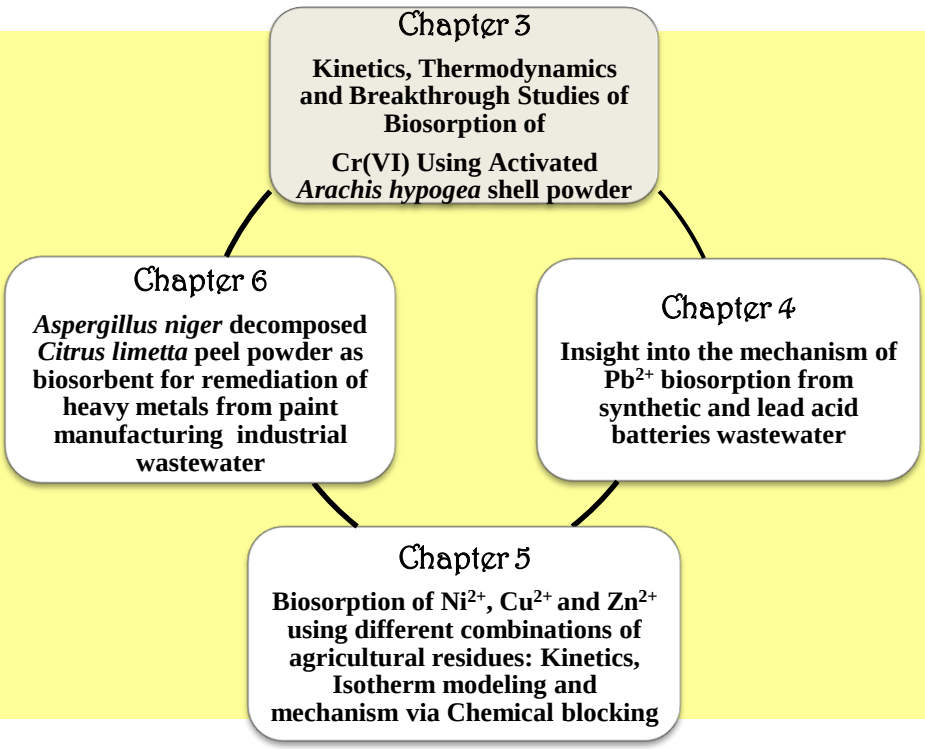

Chapter 1

Introduction and Literature Review

Contents

Abstract

Wastewater from industrial processes such as electroplating, painting, dyeing, food and drug manufacturing typically contains metals (Chromium, Cobalt, Nickel, Copper, Zinc, Lead Cadmium, Mercury) that must be removed prior to discharge into open water sources. These metals are stable and persistent water contaminants since they cannot be degraded and destroyed. They can lead to different diseases in human beings. Although, human beings require trace amounts of some metals, including manganese, iron, cobalt, copper, zinc, molybdenum, vanadium, strontium but excessive levels of these metals can also be harmful and injurious to health. Non-essential heavy metals of particular concern to surface water systems are chromium (VI), cadmium, mercury, lead, arsenic and antimony.

Several conventional treatment technologies such as ion exchange, membrane separation, ultra-filtration, ion flotation, electro-coagulation, electrodylysis, sedimentation and reverse osmosis have been employed, in recent past to treat contaminated waters. However these methods involve high operating cost and produce large volume of toxic sludge. In this context, biosorption using agricultural residues could be helpful and is emerging as a potential alternative to the existing technologies for the removal and recovery of metal ions from aqueous solutions. The major advantages of biosorption over conventional treatment methods include high efficiency, minimization of chemical sludge, low cost in regeneration of biosorbents and possibility of metal recovery. Agricultural waste materials rich in cellulose, hemicellulose and lignin are an excellent source for metal biosorption. They have different functional groups *viz.*, hydroxyl, carboxyl and phenolic having affinity for metal ions to form chelates and metal complexes. The mechanism of biosorption process includes chemisorption, complexation, ion exchange and surface adsorption.

The main aim of this chapter is to give an overview about the toxicity and health hazards of different metal ions found in the industrial effluents and removal of the same using different agricultural residues.

Keywords*:* Industrial wastewater, essential metals, toxic chemical sludge, biosorption, agricultural waste materials, ion exchange.

1.1 Introduction

Water pollution is a major environmental problem faced by modern society that leads to ecological disequilibrium and health hazards (Mishra *et al*., 2010; Ali, 2011; Gupta *et al*., 2006). Metals, a major category of globally-distributed pollutants, are natural elements that have been extracted from the earth and harnessed for human needs. They are non biodegradable and therefore tend to accumulate in the tissues of the human body and have potential to be toxic even at relatively minor levels of exposure (Jain *et al*., 2013, Visa *et al*., 2012; Martin *et al*., 2009; Jain *et al*., 2000).

Every essential element follows a dose–response curve which indicates that at lowest dosages the organism does not survive, whereas in deficiency regions the organism exists with less than optimal functioning. After the concentration plateau of the optimal dosage region, higher dosages causes toxic effects in the organism, eventually leading to lethality. The dose response curve of selenium is shown in Figure 1 (Roat - Malone, 2007).

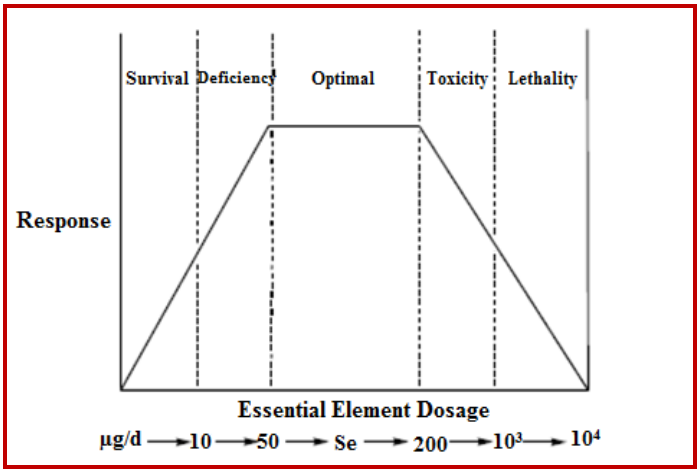

Figure 1: Dose-response curve for selenium (Source: Roat - Malone, 2007)

There are number of industries (Table 1) responsible for discharging metal ions to the water bodies. Among these industries, fertilizer, pesticides, electroplating, paint, pulp and paper industrial effluents are rich in maximum of the metals ions.

Table 1. General distributions of heavy metals in particular industrial effluents

Industries	Ti	Cr	Mn	Fe	Ni	Cu	Zn	As	Se	Ag	Cd	Hg	Pb
Electronics									✓	✓			
Fertilizers		✓	✓	✓	✓	✓	✓				✓	✓	✓
Electroplating		✓			✓	✓	✓				✓		✓
Fibers						✓	✓						
General Industry		✓	✓	✓		✓	✓						✓
Insecticides /Pesticides						✓		✓				✓	
Dye/Paint	✓	✓									✓		✓
Pulp and Paper	✓	✓			✓	✓	✓					✓	✓
Photographic		✓								✓			
Tanning		✓						✓					

The metal ions such as magnesium, iron, cobalt, nickel, copper, zinc and arsenic are required in trace and ultra-trace amount in human body as given in Table 2 where as metal such as lead, silver, cadmium and mercury are toxic even if present in ultra-trace concentrations in biological systems (Malakootian *et al*., 2008; Onundi *et al*., 2010).

Table 2: Four major categories of essential elements and their weight percentage in human body.

Elements	Wt. %	Elements	Wt. %
Bulk elements: Oxygen	53.6	Silicon, Magnesium	0.04
Carbon	16.0	**Trace elements:** Iron, Fluorine	0.005
Hydrogen	13.4	Zinc	0.003
Nitrogen	2.4	Copper, Bromine	2.0×10^{-4}
Macrominerals and Ions:		**Ultra-trace elements**: Selenium,	
Sodium, Sulphur, Potassium	0.10	Manganese, Arsenic, Nickel	2.0×10^{-5}
Chlorine	0.09	Lead, Cobalt	9.0×10^{-6}

Figure 2 gives in details, the permissible limits and health hazards of different metal ions found in water bodies.

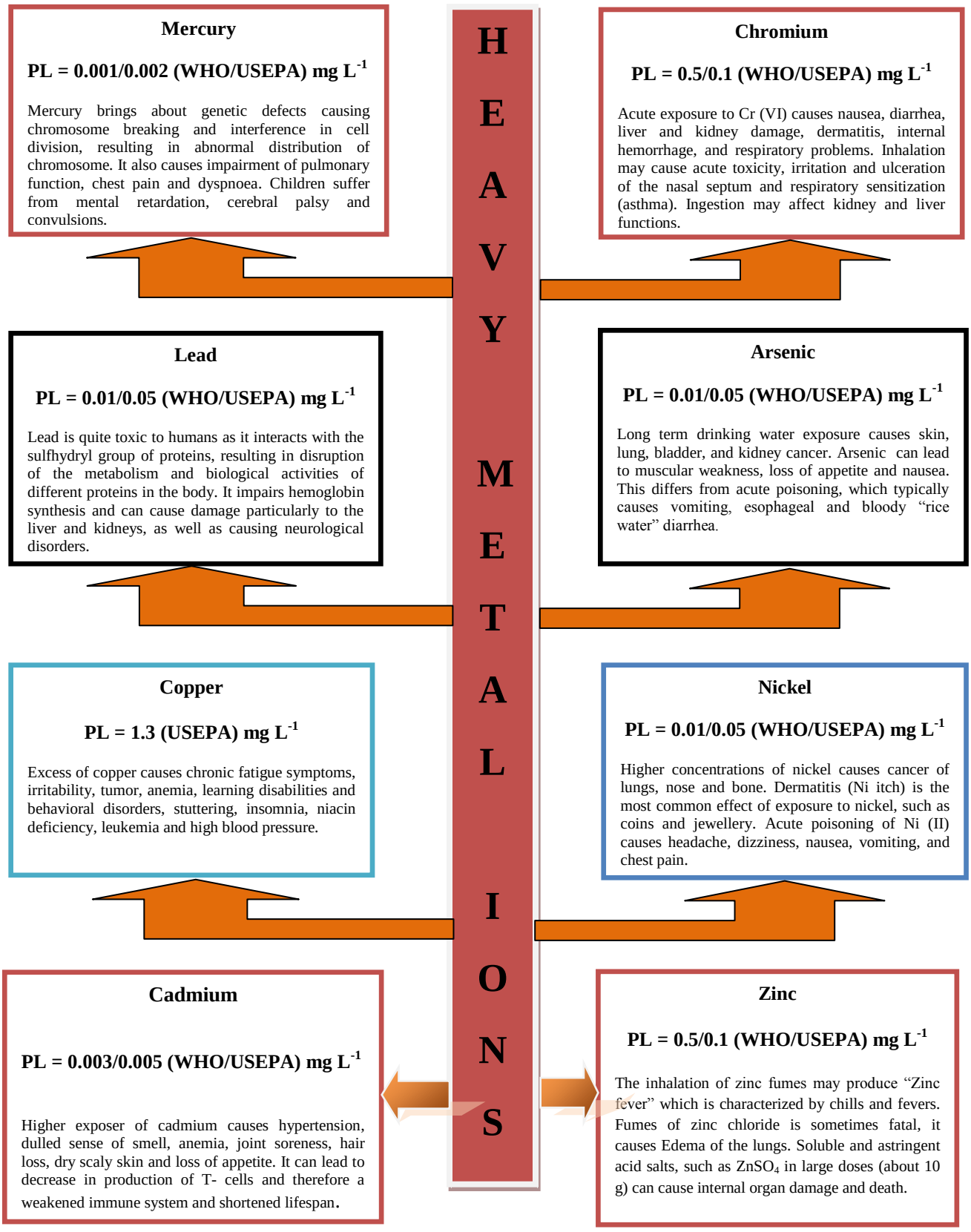

Figure 2: The permissible limits (PL) given by WHO/USEPA and health hazards of heavy metal ions.

1.2 Literature Review

For several years now, it is mandatory for each industry to make their wastewater free from different pollutants before discharging it to ponds, rivers and seas. The commonly used technologies for removing metal ions from aqueous streams include ion exchange, chemical precipitation, coagulation/flocculation, flotation, complexation and reverse osmosis. The main advantages and disadvantages of these processes have been discussed in Table 3.

Table 3: Advantages and disadvantages of different treatment technologies for the biosorption of heavy metals from aqueous systems

Technologies	**Advantages**	**Disadvantages**	**References**
Ion exchange	Its equipments require very limited space. It avoids the generation of sludge and allows convenient recovery of the metals. It has high regeneration capacity.	Metallic fouling on the ion exchange media due to oil, grease, silt, clay, colloidal silica, organic materials, and microbes. It has fairly high operational and maintenance cost.	Srivastava *et al*., 1988; Gupta *et al*., 1985.
Chemical precipitation	It has low cost for high volumes and is reliable process, well suited to osmotic control.	Produces toxic sludge, require the stoichiometric chemical addition and it is not readily applicable to small and intermittent flows.	Blais, 2008.
Coagulation /Flocculation	Bacterial inactivation capability Good sludge settling and dewatering characteristics	High chemical consumption, large volume of sludge formation, pH and temperature dependent.	Crittenden *et al*, 2005; Sinha *et al.*, 2004.
Flotation	It is metal selective and has low retention times. It is applicable to waters containing very fine particles.	It is dependent on pH, conditioning time, ionic strength and solution metal concentration. It leads to the generation of toxic sludge.	Liu *et al*., 2009

Complexation	Process simplicity, applicable to different metals and has low capital cost.	It is pH dependent and leads to the generation of toxic sludge.	Bhatt *et al*., 2012.
Membrane process	Low solid waste generation, low chemical consumption and small space requirement.	It has high operational and maintenance cost. It has membrane fouling and limited flow rates defects.	Madaeni and Mansourpanah, 2003.

The excessive numbers of disadvantages of the above mentioned technologies has directed the attention towards biosorption for desalinating metal ions from aqueous systems. The biosorption process involves an interaction between solid phase (biosorbent) and a liquid phase (solvent, normally water) containing dissolved metal ions to be removed (Joshi *et al*., 2011). The process continues till equilibrium is established between the amount of solid-bound adsorbate species and its portion remaining in the solution. Biosorption has certain advantages when compared with other conventional techniques (Volesky, 1999). Some of these are listed below:

- Biosorption can be operated at ambient conditions of pH and temperature.
- It has low operating cost.
- The biosorbents used for biosorption can be regenerated and reused in different biosorption cycles.
- The volume of chemical or biological sludge can be minimized.
- In this process the supply of nutrients is not required.
- The biomass which is to used as a biosorbent can also be procured from agricultural waste as well as industrial waste.
- The metals biosorbed can be recovered from the biosorbents after being removed from the solution.

Hence it can be said that the biosorption process is comparatively better than other technologies. Further biosorption using agricultural waste material has gained impetus recently, as it has two fold benefits to avoid environmental pollution. First, the volume of agricultural waste materials could be partly reduced and secondly, prepared adsorbents can treat toxic industrial effluents at a realistic cost.

Agricultural residues are mainly composed of cellulose, hemicellulose and lignin as shown in Figure 3 (Brown, 2003; Qi and Aldrich, 2008). Lower concentrations of various other compounds, such as proteins, simple sugars, starches, pectin (citrus plants), water, hydrocarbons are also present. The primary metal elements include Ca, K, P, Mg, Si, Al, Fe and Na.

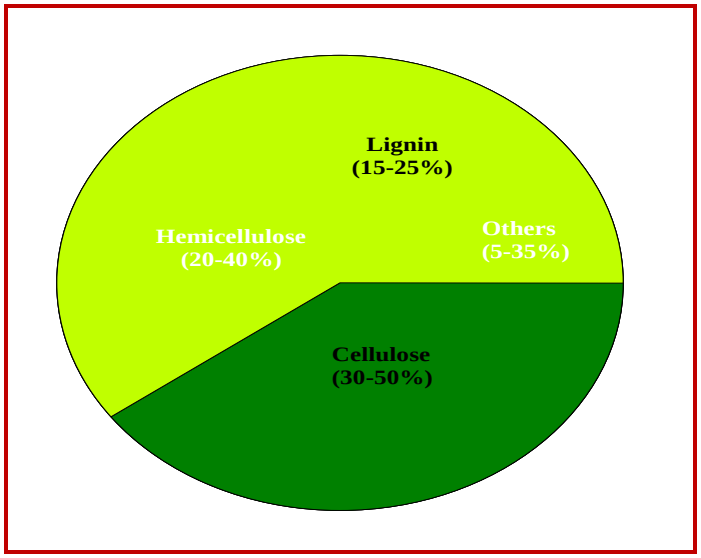

Figure 3: Pie chart of chemical composition of agricultural residues (Source: Brown, 2003).

Cellulose (Figure 4) is a polysaccharide made up of β- D-glucose molecules. The cellulose chain bristles with polar -OH groups. These groups form many hydrogen bonds with OH groups on adjacent chains, bundling the chains together. The chains also pack regions that give the bundled chains even more stability and strength. Hemicelluloses are derived mainly from chains of pentose sugars, and act as the cement material holding together the cellulose micelles and fiber (Demirbas, 2008). The polymer chains of hemicelluloses have short branches and are amorphous. Because of the amorphous morphology, hemicelluloses are partially soluble in water. After cellulose, lignin is the most abundant renewable carbon source on Earth (Mantanis *et al*., 1995). Between 40 and 50 million tons per annum of lignin are produced worldwide as a mostly non commercialized waste product. It is composed of up to three different phenyl propane monomers, depending on the species as shown in Figure 4. Coniferyl alcohol occurs in all species and is the dominant monomer in conifers (softwoods). Deciduous (hardwood) species

contain up to 40% syringyl alcohol units while grasses and agricultural crops may also contain coumaryl alcohol units.

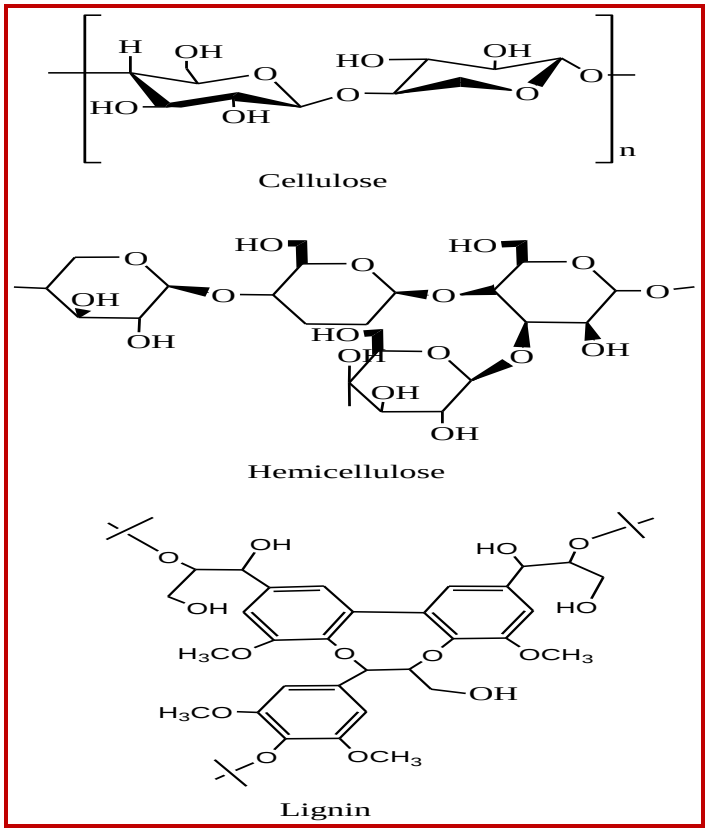

Figure 4: The structures of repeating units of cellulose, hemicellulose and lignin**.**

The four agricultural residues viz., *Arachis hypogea* shell powder (AHSP), *Trifolium alexandrnium* biomass powder (TABP), *Eucalyptus sp.* saw dust (ESD) and *Citrus limetta* peels (CLPP) are used for metal biosorption in the present study and the chemical composition of same are given in Table 4.

Table 4: Chemical composition of AHSP, TABP, ESD and CLLP

Agricultural biomass	Cellulose (%)	Hemicellulose (%)	Lignin (%)	Proteins (%)	Pectin (%)	Others (%)	References
AHSP	35.7	18.7	30.2	-	-	2.0	Raju and Kumarappa, 2011.
TABP	12.0	18.0	9.0	20.0	-	3.0	Bishnoi and Hughes, 1979.
ESD	51.7	15.4	27.2	-	-	10.4	Couto, 2009.
CLPP	13.0	7.0	3.0	6.0	30.0	2.0	Aravantinos-Zafiris and Oreopoulou, 1992.

Above mentioned constituents of agricultural residues and structural properties of cellulose, hemicellulose and lignin reveals that the agricultural waste material containing them have the potential to be used as possible adsorption substrate to remove metal ions from wastewater. Numbers of adsorbents as mentioned in Table 5 have been derived from agricultural wastes for the removal of different metal ions

Table 5: Different agricultural wastes as biosorbent for the removal of heavy metal ions from aqueous solutions

Adsorbent	Metal ion removed	References
Modified corn stalk	Cr(VI)	Chen *et al*., 2012.
Modification of corncob with citric	Cd(II)	Leyva-Ramos *et al*., 2012.
Arachis hypogea shell powder	Cr(VI)	Singh *et al.*, 2012.
Dalbergia sisoo pods	Cr(VI)	Mahajan and Sud, 2012.
Peanut hull	Cu(II)	Johnson *et al*., 2002.
Brown Algae	Cd(II), Pb(II), Ni(II)	Montazer-Rahmatia *et al*., 2011.
Modified orange peel	Pb(II), Cd(II), Ni(II)	Feng *et al*., 2011.
Neem saw dust	Cr(VI)	Vinodhini and Dass, 2010.
Mango peel waste	Cd (II), Pb(II)	Muhammad *et al*., 2009.
Symphoricarpus albus	Pb(II)	Akara *et al*., 2009.
Irish peat moss	Cu(II), Ni(II)	Gupta *et al*., 2009.
Barley straws	Cu(II), Pb(II)	Pehlivan *et al*., 2009.

Neem bark	Pb(II)	Naiya *et al*., 2008.
Okra waste	Pb(II)	Hashem, 2007.
Modified sunflower stalk	Hg(II)	Hashem *et al*., 2006.
Wheat bran	Cd(II), Cd(II)	Singh *et al.*, 2005.
Waste tea leaves	Ni(II), Pb(II), Fe(II), Zn(II)	Ahluwalia and Goyal, 2005.
Modified lignin	Cr(III), Cr(VI)	Demirbas, 2005.
Hazelnut shells	Co(II)	Demirbas , 2003.
Modified sugar beet pulp	Ni(II), Cu(II)	Reddal *et al*., 2002.
Hazelnut shell activated carbon	Ni(II)	Demirbas *et al*., 2002.
Coconut husk	Zn(II), Cd(II)	Babarinde, 2002.
Modified cellulosic materials	Cu(II)	Acemıoglu and Alma, 2001.
Rice hulls	Cr(VI)	Low *et al.*, 1999.
Pinus bark	Cu(II)	Ajmal *et al*., 1998.
Different bark samples	Cd(II)	Al-Asheh and Duvnjak, 1997.
Corncobs	Cu(II)	Hawrhorne-Costa, 1995.
Maple sawdust	Cu(II), Pb(II)	Bin, 1995.
Palm kernel husk	Pb(II), Zn(II)	Omgbu and Iweanya, 1990.
Bark	Hg(II)	Deshkar and Dara, 1988.
Tea leaves	Pb(II), Cd(II), Zn(II)	Tee and Khan, 1988.
Peanut husk	Cu(II)	Randall *et al.*, 1975.
Chemically modified cotton	Hg(II)	Roberts and Rowlandd, 1973.

1.2.1 Mechanism of metal biosorption

The actual challenge in the field of biosorption process is to identify the mechanism of metal uptake by the biosorbent. The most commonly reported mechanisms for metal ion sorption are ion exchange, electrostatic interaction, chelation, precipitation and complexation. One of the mechanisms suggested by Iqbal *et al*. (2009) to be involved in sorption of Cd^{2+} and Pb^{2+} removal by mango peel waste was the ion exchange process between protons and/or light metals as counter ions present on the biomass and heavy metal ions taken-up from the metal containing aqueous solution (Figure 5). The results showed a significant release of Na^{+}, K^{+}, Mg^{2+}, Ca^{2+} and H^{+} from mango peel waste due to the uptake of Cd^{2+} and Pb^{2+} and the same process was proved by the EDX analysis of mango peel waste before and after metal sorption. Bin (1995) suggested ion-exchange mechanism for the removal of copper by adsorption on sawdust where divalent heavy metal ion (M^{2+}) attaches itself to two adjacent hydroxyl groups and two oxyl groups which could donate two pairs of electrons to metal ions, forming four coordination number compounds

and releasing two hydrogen ions into solution. Similar mechanism was proposed by Saeeda *et al.* (2009) and Pehlivan and Altun (2007).

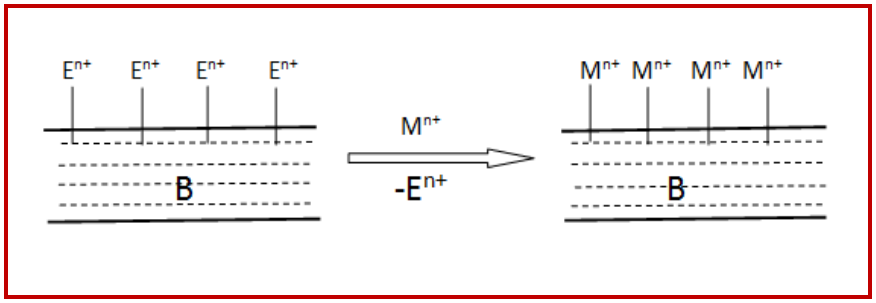

Figure 5: The ion exchange mechanism between the exchangeable ions and the metal ions present in the solution (B = Biomolecules in the biomass used, E^{n+} = Exchangeable ions (Na^{+}, K^{+}, Mg^{2+}, Ca^{2+}, H^{+}), M^{n+} = Metal ions such as Ni^{2+}, Cu^{2+} Zn^{2+} etc).

Biosorption of Cr(VI) and Cr(III) on different biosorbents have been explained by number of authors (Dinoex, 1996; Barrera *et al*., 2006; Mohan and Pittman Jr, 2006). Chromium exists in different oxidation states (+2, +3 and +6) depending upon the pH of the solution. Among the three oxidation states, Cr(VI) compounds are toxic than Cr(III) due to their high water solubility and mobility. Cr(VI) gives different anionic species (CrO_4^{2-}, $HCrO_4^{2-}$, $Cr_2O_7^{2-}$) at different pH values as shown in Figure 6.

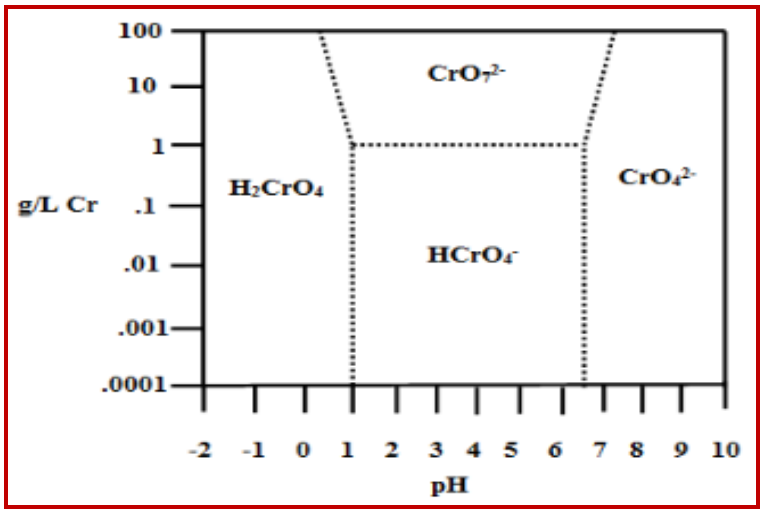

Figure 6: Speciation diagram of Cr(VI) (Source: Dinoex, 1996; Mohan and Pittman Jr, 2006).

The adsorption of Cr(VI) from aqueous solutions by adsorbents/biosorbents consists mainly of two steps: Firstly the Cr(VI) ions are removed by adsorption onto the interior surface of the adsorbent and secondly the Cr(VI) ions are reduced into Cr(III) and this trivalent state adsorbs at the external surface of the biosorbent. The pH, temperature, adsorbent particle size, dose, total chromium concentrations are the major parameters which governs the adsorption mechanism of Cr(VI) / Cr(III).

Park *et al*. (2008) suggested both direct and indirect reduction mechanisms for the removal of Cr(VI) from aqueous solutions by using banana skin. In direct reduction mechanism, Cr(VI) was directly reduced to Cr(III) in the aqueous phase by contact with electron-donor groups of banana skin and the reduced Cr(III) remained in the aqueous phase or formed complexes with Cr-binding groups of the same. Barrera *et al*. (2006) pointed out that at pH 4, the *Ectodermis* of *Opuntia* surface was positively charged due to protonation, while the sorbate, dichromate ion, exists mostly as an anion leading to the electrostatic attraction between sorbent and sorbate as shown in Figure 7.

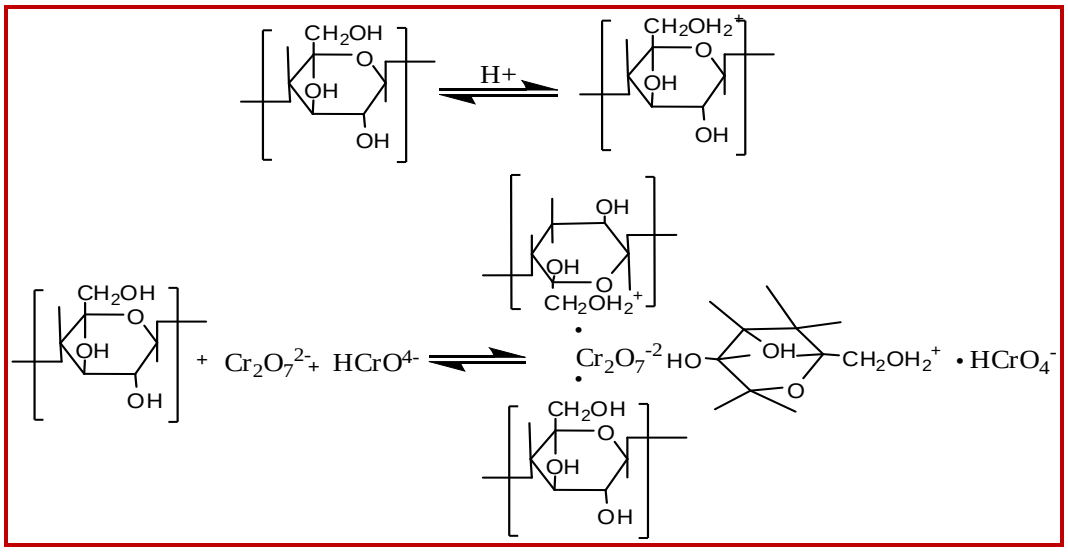

Figure 7: Scheme of the possible electrostatic interaction of Cr(VI) by cellulose of *Ectodermis* of *Opuntia* (Source: Barrea *et al*., 2006; Mohan and Pittman Jr, 2006).

Barrea *et al*. further highlighted that at pH values below 4, the main specie was Cr(III) and they interacted with the –OH groups of cellulose as shown in Figure 8. Demirbas (2008) suggested that cellulose molecules collectively form microfibrils and water containing dissolved species can filter through the microfibrils along with hemicelluloses and lignin. The dissolved species get entrapped into these microfibrils forming complexes, resulting the desalination of the liquid phase. Along with this entrapment, the several functional groups present in the biomass have the affinity for metal complexation. Some biosorbents are non-selective and bind to a wide range of heavy metals with no specific priority, whereas others are specific for certain types of metals depending upon their chemical composition.

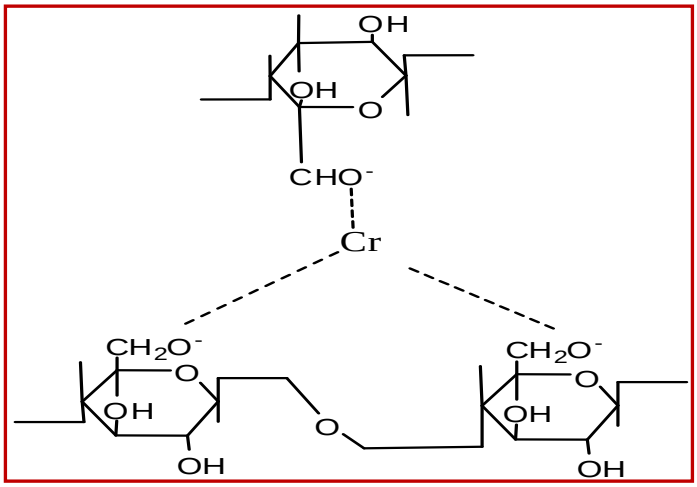

Figure 8: Scheme of the possible interaction of Cr(III) by cellulose of *Ectodermis* of *Opuntia* (Source: Barrea *et al*., 2006; Mohan and Pittman Jr, 2006).

1.3 Conclusion

Biosorption using agricultural residues has shown significant contribution for the removal of contaminants from aqueous effluents. The importance of biosorption over other technologies have been studied and it has been concluded that biosorption using low cost natural and waste biomasses constitutes the basis for a new cost effective technology that can find its largest application in the bioremediation of heavy metals from industrial effluents. Application aspects of biosorption are being aimed at biosorption process optimization. The ion exchange, electrostatic interaction, chelation, precipitation and complexation are the main mechanism of biosorption. The process of biosorption requires further investigation in the direction of

modeling, regeneration of biosorbent, recovery of metal ions, immobilization of the waste materials in order to make the process economic viable at industrial scale with focus for enhanced efficiency and recovery.

1.4 Research Gaps

On the basis of above mentioned literature survey following research gaps were identified:

1. Numbers of biosorbents have been prepared from agricultural products and waste products in recent past but most of them were further treated with certain expensive chemicals to increase their biosorption capacity. This treatment of biosorbents with expensive chemical increases the cost of the biosorption process and moreover is time consuming. The chemical activation could be a problem, if larger volume of the biosorbent has to be prepared.

2. The mechanism involved during biosorption on agricultural residues have not been studied and fully discussed in the literature. Further, the effect of the solution pH on the biosorption process has not been studied using the point of zero charge in literature for most of biosorbents.

4. Most of the researcher carried out batch biosorption processes which cannot be used at large industrial scale.

5. In most of the reported studies, a single adsorbent has been employed for the metal removal. However, the combination of different adsorbents can be effective for the removal of multi metal ions from the industrial effluents.

On the basis of these research gaps, following objectives have been identified for the present thesis.

1.5 Objectives

- To develop economically feasible adsorbents from agricultural wastes for the removal of different toxic metal ions (e.g. Cr, Ni, Cu, Zn and Pb) from industrial effluents.
- To study the effect of various parameters of adsorption in batch and continuous adsorption process.
- To study the desorption of toxic metal ions and safe disposal of metal loaded waste.

References

Acemıoglu, B. and Alma, M.H.; Equilibrium studies on the adsorption of Cu(II) from aqueous solution onto cellulose; *J. Colloid Interface* Sci; **2001**, 243, 81–84.

Ahluwalia, S.S. and Goyal, D.; Removal of heavy metals from waste tea leaves from aqueous solution; *Eng. Life Sc.;* **2005,** 5, 158–162.

Ajmal, M.; Khan, A.H.; Ahmad, S. and Ahmad, A.; Role of sawdust in the removal of copper (II) from industrial wastes; *Water Res*; **1998**, 22, 3085–3091.

Akara, S.T.; Gorgulu, A.; Anilan, B.; Kaynak, Z. and Akara, T.; Investigation of the biosorption characteristics of lead(II) ions onto Symphoricarpus albus: batch and dynamic flow studies; *J. Hazard. Mater.*; **2009**, 165, 126–133.

Ali, I.; The quest for active carbon adsorbent substitutes, inexpensive adsorbent for toxic metal ions removal from wastewater; *Sepr. Purif. Rev*.; **2011**, 39, 95e171.

Al-Asheh, S. and Duvnjak, Z.; Sorption of cadmium and other heavy metals by pine bark; *J. Hazard. Mater*, **1997**, 56, 35–51.

Aravantinos-Zafiris, G. and Oreopoulou, V.; The effect of nitric acid extraction variables on orange pectin; *J. Sci. Food Agric*; **1992**, 60, 127–129.

Babarinde, N.A.A.; Adsorption of zinc(II) and cadmium(II) by coconut husk and goat hair; *J. Pure Appl. Sci.*; **2002,** 5, 81–85.

Barrera, H.; Ure˜na-N´u˜nez, F.; Bilyeu, B. and Barrera-D´ıaz, C.; Removal of chromium and toxic ions present in mine drainage by *Ectodermis* of *Opuntia; J. of Hazard.Mater.*, **2006**, B136, 846–853.

Bhatt, R.R.; Shah, B.A. and Shah, A.V.; Uptake of heavy metal ions by chelating ion-exchange resin derived from p-hydroxybenzoic acid-formaldehyde-resorcinol; *The Malaysian Journal of Analytical Sciences*, **2012**, 16 (2), 117 – 133.

Blais, J. F.; Djedidi, Z.; Ben Cheikh, R; Tyagi, R. D. and Mercier, G; Metals Precipitation from Effluents: Review; *Practice Periodical of Hazardous; Toxic and Radioactive Waste Management* ; **2008**, 137–149.

Bin, Y.; Adsorption of copper and lead from industrial wastewater by maple sawdust; *Thesis, Lamar University; Beaumont*; USA; **1995.**

Bishnoi, U.R. and Hughes, J.L.; Agronomic Performance and Protein Content of Fall-planted Triticale, Wheat and Rye. *Agron. J*., **1979**; 71, 359–360.

Boddu, V.M.; Abburi, K.; Talbott, J.L. and Smith, E.D.; Removal of hexavalent chromium from wastewater using a new composite chitosan biosorbent; *Environ. Sci. Technol.* **2003,** 37(19) 4449–4456.

Brown, R.C.; Biorenewable resources; Engineering new products from agriculture; Iowa State Press; Ames. ; **2003**.

Chen, S.; Yue, Q.; Gao, B.; Li, Q.; Xu, X. and Fu, K.; Adsorption of hexavalent chromium from aqueous solution by modified corn stalk; A fixed-bed column study; *Bioresource Technology* **2012**, 113, 114–120.

Couto, G.; Utilização da serragem de Eucalyptus sp. Dissertation; Minas Gerais; Brazil; **2009**.

Crittenden, J.C.; Trussel, R.R.; Hand D.W.; Howe, K.J. and Tchobanoglous, G. (eds), Coagulation; mixing and flocculation; in: Water Treatment: Principles and Design; second ed., John Wiley & Sons; New Jersey; **2005**, 643-779.

Demirbas, E.; Kobya, M.; Oncel, S. and Sencan, S.; Removal of Ni(II)from aqueous solution by adsorption onto hazelnut shell activated carbon: equilibrium studies; *Biores. Technol;* **2002**, 84, 291–293.

Demirbas, E.; Adsorption of Cobalt(II) from aqueous solution onto activated carbon prepared from hazelnut shells. *Adsorp. Sci. Technol*; **2003**, 21, 951–963.

Demirbas, A.; Adsorption of Cr(III) and Cr(VI) ions in aqueous solutions onto modified lignin. *Energy Sour*.; **2005,** 27, 1449–1455.

Demirbas, A.; Heavy metal adsorption onto agro-based waste materials: A review; *Journal of Hazard. Mater.;* **2008**, 157, 220–229.

Deshkar, A.M. and Dara, S.D.; Sorption of mercury by Techtona grandis bark. *Asian Environ,* **1988,** 10, 3–11.

Dionex, Determination of Cr (VI) in water, wastewater and solid waste extracts, Technical Note 26; LPN 34398-011M7/96, Dionex Corporation, **1996.**

Feng, N.; Guo, X.; Lianga, S.; Zhub, Y. and Liub, J.; Biosorption of heavy metals from aqueous solutions by chemically modified orange peel, *J. of Hazard. Mater.;* **2011**, 185, 49–54.

Gupta, B. S.; Curran, M.; Hasan, S. and Ghosh, T.K.; Adsorption characteristics of Cu and Ni on Irish peat moss; *J. Environ. Manag*.; **2009,** 90, 954–960.

Gupta, D.C and Tiwari U.C.; Aluminum oxide as adsorbent for removal of hexavalent chromium from aqueous waste; *Ind. J. Environ. Health;* **1985,** 27, 205–215.

Gupta, S.S and Bhattacharyya , K.G; Removal of Cd(II) from aqueous solution by kaolinite, montmorillonite and their poly(oxo zirconium) and tetrabutylammonium derivatives; *Journal of Hazardous Materials*; **2006**, B128, 247–257.

Hashem, A.; Abou-Okeil, A.; El-Shafie, A. and El-Sakhawy, M.; Grafting of high cellulose pulp extracted from sunflower stalks for removal of Hg (II) from aqueous solution; *Polym. Plast. Technol. Eng*.; **2006**, 45, 135–141.

Hashem, M.A.; Adsorption of lead ions from aqueous solution by okra wastes; *Int. J. Phys. Sci*.; **2007,** 2, 178–184.

Hawrhorne-Costa, E.T.; Winkler Hechenleitner, A.A. and Gomez- Pineda, E.A.; Removal of cupric ions from aqueous solutions by contact with corn cobs; *Sep. Sci. Technol;* **1995**, 30, 2593–2602.

Iqbal, M.; Saeed, A. and Zafar, S.I; FTIR spectrophotometry, kinetics and adsorption isotherms modeling; ion exchange, and EDX analysis for understanding the mechanism of Cd^{2+} and Pb^{2+} removal by mango peel waste; *J. of Hazard. Mater,* **2009**, 164, 161–171.

Jain, C.K. and Ali, I.; Arsenic: occurrence, toxicity and speciation techniques; *Water Res.;* **2000**, 34, 4304–4312.

Jain, M.; Garg, V.K. and Kadirvelu, K.; Chromium Removal from Aqueous System and Industrial Wastewater by Agricultural Wastes; *Bioremediation Journal;* **2013**,17 (1), 30–39.

Johnson, P.D.; Watson, M.A.; Brown, J., and Jefcoat, I.A.; Peanut hull pellets as a single use sorbent for the capture of Cu(II) from wastewater; *Waste Manage*.; **2002,** 22, 471– 480.

Joshi, P.K.; Swarup, A.; Maheshwari, S., Kumar, R. and Singh, N.; Bioremediation of heavy metals in liquid media through fungi isolated from contaminated sources; *Indian. J.Microbiol* **2011,** 51(4), 482-487**.**

Leyva-Ramos, R.; Landin-Rodriguez, L.E.; Leyva-Ramos, S. and Medellin-Castillo N.A.; Modification of corncob with citric acid to enhance its capacity for adsorbing cadmium(II) from water solution; *Chemical Engineering Journal***; 2012,** 180, 113– 120.

Low, K.S.; Lee, C.K.; and Ng, A.Y.; Column study on the sorption of Cr(VI) using quaternized rice hulls; *Biores. Technol*; **1999**, 68, 205–208.

Liu, Z. and Doyle, M.F.; Ion Flotation of Co^{+2}, Ni^{+2}, and Cu^{+2} using dodecyldiethylenetriamine (Ddien); *Langmuir*; **2009**, 25, 8927–8934.

Madaeni, S.S. and Mansourpanah, Y.; COD removal from concentrated wastewater using membranes; *Filtration and Separation;* **2003**, 40 (6), 40–46.

Mahajan, G. and Sud, D.; Modified agricultural waste biomass with enhanced responsive properties for metal-ion remediation: a green approach; *Appl Water Sci.;* **2012,** 299– 308.

Mantanis, G.I.; Young, R.A. and Rowell, R.M.; Swelling of compressed cellulose fiber webs in organic liquids; *Cellulose;* **1995,** 2, 1–22.

Malakootian, M.; Almasi, A. and Hossaini, H.; Pb and Co removal from paint industries effluent using wood ash; *Int. J. Environ. Sci. Tech.;* **2008**, 5 (2), 217-222.

Mohan, D.; Singh, K.P.; Singh, V.K.; Removal of hexavalent chromium from aqueous solution using low-cost activated carbons derived from agricultural waste materials and activated carbon fabric cloth; *Ind. Eng. Chem. Res.*; **2005,** 44, 1027–1042.

Mohan, D. and Pittman Jr. C.U.; Review Activated carbons and low cost adsorbents for remediation of tri- and hexavalent chromium from water, *J. Hazard. Mater.;* **2006**, B137, 762–811.

Montazer-Rahmatia, M. M.; Rabbania, P.; Abdolalia, A.; Keshtkar, A.R.; Kinetics and equilibrium studies on biosorption of cadmium, lead, and nickel ions from aqueous solutions by intact and chemically modified brown algae; *J. of Hazard. Mater.;* **2011**, 185, 401–407.

Muhammad, I.; Saeeda, A. and Zafar, S. I.; FTIR spectrophotometry, kinetics and adsorption isotherms modeling, ion exchange, and EDX analysis for understanding the mechanism of Cd^{2+} and Pb^{2+} removal by mango peel waste; *J. of Hazard. Mater.;* **2009**, 164, 161–171.

Naiya, T.K.; Bhattacharya, A.K. and Das, S.K.; Adsorption of Pb(II) by sawdust and neem bark from aqueous solutions; *Environ. Prog.*; **2008**, 27, 313–328.

Omgbu, J.A. and Iweanya, V.I.; Dynamic sorption of Pb^{2+} and Zn^{2+} with Palm (*Eleasis guineensis*) kernel husk; *J. Chem. Ed.*; **1990**, 67, 800–801.

Onundi, Y. B.; Mamun, A. A.; Al Khatib, M. F. and Ahmed, Y. M.; Adsorption of copper, nickel and lead ions from synthetic semiconductor industrial wastewater by palm shell activated carbon; *Int. J. Environ. Sci. Tech.;* **2010**, 7 (4), 751-758.

Mishra, S.; Meda, V.; Dalai, A. K.; Headley, J. V.; Peru, K. M. and McMartin, D. W.; Microwave treatment of naphthenic acids in water; *J. of Environ. Science and Health, Part A;* **2010,** *45*, 10.

Park, D.; Lim, S. R.; Yun, Y.S. and Park, J.M.; Development of a new Cr(VI)- biosorbent from agricultural biowaste; *Bioresource Technology;* **2008,** 99, 8810–8818.

Pehlivan, E. and Altun, T.; Biosorption of chromium(VI) ion from aqueous solutions using walnut; hazelnut and almond shell; *J. of Hazard. Mater.;* **2007,** 155, 378–384.

Perez Martin, A.B; Aguilar, M.I.; Meseguer, V.F; Ortuno, J.F.; Saez, J. And Lorens, M.; Biosorption of chromium (III) by orange (Citrus cinensis) waste: Batch and continous studies, *Chemical Engineering Journal;* **2009,** 155, 199– 20.

Qi, B.C. and Aldrich C.; Biosorption of heavy metals from aqueous solutions with tobacco dust; *Bioresource Technology;* **2008**, 99, 5595–5601.

Raju, G.U. and Kumarappa, S.; *J. Reinf. Plast. Comp.*, **2011**, 30, 1029.

Randall, J.M.; Reuter, F.W. and Waiss Jr.,A.C.; Removal of cupric ions from solution with peanut skins; *J. Appl. Polym. Sci*.; **1975,** 19, 1563–1571.

Reddal, Z.; Gerente, C.; Andres, Y.; Ralet, M.C.; Thibault, J.F. and Cloirec, P.L.; Ni (II) and Cu (II) binding properties of native and modified sugar beet pulp; *Carbohyd. Polym*.; **2002,** 49, 23–31.

Roberts, E.J. and Rowland, S.P.; Removal of mercury from aqueous solution by nitrogen-containing chemically modified cotton; *Environ. Sci. Technol*; **1973**, 7, 552–555.

Roat-Malone, R. M.; Bioinorganic Chemistry; John Wiley & Sons; New Jersey; **2007**, 1-539.

Saeeda, A.; Iqbal, M. and Hölla, W.H.; Kinetics, equilibrium and mechanism of Cd^{2+} removal from aqueous solution by mung bean husk; *J. of Hazard. Mater;* **2009**, 168, 1467–1475.

Srivastava, K.; Bhattacharjee, G.; Tyagi, R., Pant, N. and Pal, N.; Studies on the removal of some toxic metal ions from aqueous solutions and industrial waste; Part I (Removal of lead and cadmium by hydrous iron and aluminium oxide); *Environ. Technol. Lett*.; **1988**, 9, 1173–1185.

Singh, J. and Ali. A.; Kinetics, Thermodynamics and Breakthrough Studies of Biosorption of Cr(VI) Using Arachis hypogea Shell Powder; *Res. J. Chem. Environ*.; **2012**,16 (1), 69–79.

Singh, K.K.; Rastogi, R.; Hasan, S.H.; Removal of cadmium from waste water using agricultural waste using rice polish; *J. Hazard.Mater*.; **2005**, A 121, 51–58.

Sinha, S.; Yoon, Y.; Amy, G. and Yoon, J.; Determining the effectiveness of conventional and alternative coagulants through effective characterization schemes; *Chemosphere*; **2004**, 57, 1115–1122.

Tee, T.W. and Khan, R.M.; Removal of lead, cadmium and zinc by waste tea leaves; *Environ. Technol. Lett*.; **1988**, 9, 1223–1232.

U.S.EPA; Control and treatment technology for the metal finishing industry: Sulphide precipitation; EPA – 625/8-80-003; Cincinnati; Ohio; **1980**.

Vinodhini, V. and Dass, N.; Packed bed column studies on Cr(VI) removal from tannery wastewater by neem sawdust; *Desalination*; **2010,** 264, 9–14.

Volesky, B.; Biosorption for the next century; Bio hydrometallurgy and the Environment Toward the Mining of the 21st Century; *Internat*.; **1999.**

Visa, M.; Isac, L. and Duta, A.; Fly ash adsorbents for multi-cation wastewater treatment; *Applied Surface Science;* **2012**, 258, 6345– 6352.

WHO; Environmental Health Criteria 118; Inorganic Mercury; Geneva, World Health Organization **1991**.

Chapter 2

Material and Methods

Contents

2.1 Chemicals

Potassium dichromate, nickel nitrate, copper chloride, zinc sulphate, lead nitrate, cadmium sulphate, hydrochloric acid, nitric acid, ethylene diamine tetra acetic acid, sulphuric acid, sodium carbonate and sodium hydroxide of analytical grade (> 99% purity) were purchased from Merch, India and used as such without any further treatment.

2.2 Collection and preparation of the biosorbents

In the present study four different agricultural residues *viz.*, *Arachis hypogea* shells, *Eucalyptus sp.* saw dust, *Trifolium alexandrinum* biomass and *Citrus limetta* peels, were collected from different local sources. *Arachis hypogea* shells and *Eucalyptus sp.* saw dust were collected from Trilok oil industry and Dinesh Wood Works, Mustafabad, Haryana, India respectively. *Trifolium alexandrinum* biomass was collected from Sandhu farms, village Khera, Ambala, Haryana. *Trifolium alexandrinum* is used as fodder for domestic animals like cow, buffalo, horses etc. but in many part of Haryana and Punjab it is cultivated for seeds only as a cash crop. In that case, large amount of biomass is left after harvesting. Maximum of the farmers burn it to clear their fields, this leads to air pollution to a major extent. *Citrus limetta* peels were collected from Multani's juice corner, Yamuna Nagar, India. These waste materials are either burned in open air or dumped somewhere, which creates environmental and disposal problems. Therefore, use of these wastes as biosorbents offers a dual assistance in solving water pollution and waste disposal problem.

2.2.1 Preparation of *Arachis hypogea* shell powder

The *Arachis hypogea* shells were washed extensively in running tap water to remove dirt and other particulate matter, dried in an electric hot air oven at 105 $^{\circ}$C for 24 h and finally grinded in a vegetable grinder. Resulting powder was sieved through a 600 µm mesh sized sieve and powder (500.0 g) thus obtained was boiled in deionised water (2.5 L) for 5 h to remove the coloring materials. The *Arachis hypogea* shell powder was recovered by filtration through ordinary filter paper and then activated chemically by treating it with 1.0 M HCl (2.0 L) at 80 $^{\circ}$C for 5 h. The activated *Arachis hypogea* shell powder (AAHSP) (500.0 g) thus obtained was dried in an electric air oven at 105 $^{\circ}$C for 24 h and employed for the removal of Cr(VI) from synthetic and industrial wastewater as mentioned in chapter 3.

2.2.2 Preparation of different combinations of *Arachis hypogea* shell powder, *Trifolium alexandrinum* biomass, *Eucalyptus sp.* saw dust

All the three agricultural residues were initially washed extensively with deionised water to remove dirt and other adhering matter and then dried in an electric hot air oven at 105 $^{\circ}$C for 24 h. *Trifolium alexandrinum* biomass and *Arachis hypogea* shells were finally grinded separately in a vegetable grinder to obtain the biomass powder. Resulting powders and *Eucalyptus sp.* saw dust were separately sieved through a 600 µm mesh sized sieve and powders (500 g each) thus obtained were heated in an electric hot air oven at 105 $^{\circ}$C for 12 h. The dried *Trifolium alexandrinum* biomass powder (TABP), *Eucalyptus sp.* saw dust (ESD) and *Arachis hypogea* shell powder (AHSP) were mixed in different wt % to prepare the various combinations used in chapter 4 and 5.

2.2.3 Preparation of *Citrus limetta* peel powder and *Aspergillus niger* cultivation

The *Citrus limetta* peels were washed properly first in tap water to remove dirt and other particulate matter and then in deionised water. The peels were then dried in the hot air oven at 60 $^{\circ}$C for 48 h and finally grinded in a vegetable grinder to obtain the powder. Resulting powder was sieved through a 150 µm mesh sized sieve and powder (100 g) thus obtained was used for the cultivation of *Aspergillus niger.*

Aspergillus niger obtained from microbiology department, M.M.M.C, M.M.U, Mullana, Ambala was grown in medium containing 200.0 mL deionised water and 100.0 g *Citrus limetta* peel powder at room temperature. After 20 days of incubation, living fungi biomass was killed by autoclaving (at 121°C) for 20 min. The biomass thus obtained washed thrice using deionized water to removal the residual growth medium and then dried at room temperature. The dried *Aspergillus niger* decomposed biomass (ANDB) (88.5 g) was grinded in a mortar and pestle and sieved through a 150 µm sieve. The final biomass obtained was used for removal of lead and cadmium from synthetic and industrial wastewater in chapter 6.

2.2.4 Preparation of stock solution

An aqueous stock solutions (1000 mg L^{-1}) of Cr(VI), Ni^{2+}, Cu^{2+}, Zn^{2+}, Pb^{2+} and Cd^{2+} ions was prepared by dissolving requisite amount of potassium dichromate, nickel nitrate, copper chloride, zinc sulphate, lead nitrate, cadmium sulphate, in 1.0 L deionised water. The stock solutions have

been further diluted with deionized water to prepare the solutions of the desired concentrations. The pHs of the solutions were adjusted by adding the appropriate amounts of 0.1 M HCl or 0.1 M NaOH solutions.

2.3 Instruments and software

2.3.1 UV-visible and Atomic absorption spectrophotometer

The quantification of the Cr(VI) in solutions has been performed on Perkin-Elmer, Lamba-35 UV-visible spectrophotometer and that of Ni^{2+}, Cu^{2+}, Zn^{2+}, Pb^{2+} and Cd^{2+} was done on Atomic Absorption Spectrophotometer (AAS) AA630, Shimadzu.

2.3.2 Fourier transform infrared (FTIR)

Thermo, Nicolet Is10 FTIR spectrophotometer was used to study the different functional groups present on the surface of the biosorbents used in the present study.

2.3.3 Field emission scanning electron microscopy (FESEM)

The surface topography of the biosorbents and qualitative analysis of the adsorbed metal ions were performed with the help of JEOL JSM 6510LV Field emission scanning electron microscope.

2.3.4 The pH meter and Orbital shaker incubator

The pH of the solution has been measured by Cyber scan, Eutch pH meter and the orbital shaker incubator by Metrex scientific instruments has been used for shaking the samples during batch studies at desired temperature and rpm.

2.3.5 Software

Software Sigma plot 11 and Origin 8 has been used for the data analysis and fitting the values in various models.

2.4 Batch Biosorption studies

Batch biosorption experiments for Cr(VI), Ni^{2+}, Cu^{2+}, Zn^{2+}, Pb^{2+} and Cd^{2+} onto different biosorbents prepared were conducted in 250 mL screw-cap conical flasks. The mixtures so

obtained were agitated in orbital shaker at different agitation speed, time and temperatures. The effect of solution pH, initial metal ion concentration, contact time and biosorbent dose was studied. The suspensions obtained were filtered through Whatman no. 40 filter paper, centrifuged and the filtrates were analyzed by UV-visible spectrophotometer and atomic absorption spectrophotometer.

The percent of metal removal (*R%*) was calculated for each experiment using equation 1.

$$R(\%)=[(C_i - C_e)/C_i] \times 100 \quad (1)$$

where C_i and C_e was the initial and equilibrium metal ion concentrations respectively in the solution. The metal uptake capacity (q_e = mg g^{-1}) of the biosorbent was calculated using equation 2.

$$q_e = \frac{(C_i - C_e)}{M_a} \times V \quad (2)$$

where V is the volume of the solution (L) and M_a is the mass of the biosorbent (g) used.

2.4.1 Point of zero charge

The charge on the biomass surface is a function of pH. The pH at which the charge on the solid surface is zero is referred as the point of zero charge (pH_{PZC}) (Rivera *et al.,* 2001). The pHpzc of the biosorbents were determined by following the procedure as described by Rivera *et al.* (2001). In a typical experiment, 50 ml of 0.01 M NaCl solution was taken in 6 different conical flasks of 100 mL capacity. The pH of the solutions in the flasks was adjusted to 2, 4, 6, 8, 10 and 12 by adding appropriate amounts of 0.1M HCl or 0.1 M NaOH solutions. To these flasks 0.15 g of the desired biosorbent was added, and agitated for 48 h at 30 °C and after stipulated time the final pH of the mixture was measured with the help of pH meter. The graph was plotted between the initial and final pH values and the pH_{PZC} was obtained as mentioned in chapter 4 and 6.

2.4.2 Biosorption kinetics studies

Biosorption kinetics, which describes the solute biosorption rate, is an important characteristic in evaluating the efficiency of the biosorption. In order to clarify the biosorption kinetics of the studied metal ions onto different biosorbents, pseudo-first-order and pseudo-second-order kinetic models as proposed by Lagergren (1898) were applied to the experimental data. The pseudo-first-order is represented by equation 3.

$$\frac{d_q}{d_t} = k_1(q_e - q_t) \quad (3)$$

where q_t (mg g^{-1}) is the amount of metal ions biosorbed at time t, q_e is the amount of metal ions biosorbed at equilibrium (mg g^{-1}), and k_1 is the rate constant of the biosorption (g $mg^{-1}min^{-1}$). The equation 3 was integrated and rearranged to equation 4.

$$In(q_e - q_t) = Inq_e - k_1 t \quad (4)$$

The pseudo-second-order kinetic model is given by the equation 5.

$$\frac{dq_t}{dt} = k_2(q_e - q_t)^2 \quad (5)$$

where k_2 (g $mg^{-1}min^{-1}$) is the rate constant of the second order equation; q_t (mg g^{-1}) the amount of biosorption at time t (min), and q_e (mg g^{-1}) is the amount of biosorption at equilibrium. The equation was integrated and rearranged to equation 6.

$$\frac{t}{q_t} = \frac{1}{k_2 q_e^{\,2}} + \frac{t}{q_e} \quad (6)$$

Straight line in the graphs of *ln* ($q_e - q_t$) versus t and t/q_t versus t suggests the applicability of the pseudo first order and the pseudo-second-order kinetic models, respectively. The value of q_e and rate constants can be determined from the intercept and slope of the plots, respectively.

2.4.3 Biosorption isotherms modeling

The biosorption isotherms models helps to establish the relationship between the amounts of metal ions adsorbed on the biosorbent and its equilibrium concentration in aqueous solution. Among various biosorption isotherms models, Langmuir and Freundlich isotherm models are preferred in this study. The Langmuir (1916) model assumes that the uptake of the metal ions occurs on a homogenous surface by monolayer biosorption without any interaction between adsorbed ions and is given by equation 7.

$$q_e = \frac{q_{\max} b C_e}{1 + b C_e} \quad (7)$$

The linear form of the Langmuir equation can be represented by equation 8.

$$\frac{C_e}{q_e} = \frac{C_e}{q_{\max}} + \frac{1}{b q_{\max}} \quad (8)$$

where q_e (mg g^{-1}) is the amount of metal ions adsorbed per unit mass of biosorbent and C_e is the equilibrium concentration of the metal in the solution (mg L^{-1}), q_{max} represents the maximum biosorption capacity(mg g^{-1}) under the experimental conditions and b is a constant related to the affinity of the binding sites (L mg^{-1}).

Further, the shape of isotherm can be used to predict whether a sorption system is favorable or not. The essential features of the Langmuir isotherm can be expressed in terms of a dimensionless constant or separation factor (R_L) (Singh and Ali, 2012) and the same could be defined by using the equation 9.

$$R_L = \frac{1}{1+bC_i} \tag{9}$$

where C_i (mg L^{-1}) is the initial amount of the adsorbate in the solution and b (L mg^{-1}) is the Langmuir constant described above. There are four probabilities for the R_L value, viz., for (i) favorable biosorption $0 < R_L < 1$, (ii) unfavorable biosorption $R_L > 1$, (iii) linear biosorption $R_L = 1$ and (iv) irreversible biosorption $R_L = 0$.

On the other hand, Herbert Max Finley Freundlich (1906) derived an empirical biosorption isotherm equation, which is based on the biosorption on a heterogeneous surface and is given by equation 10.

$$q_e = K_F (C_e)^{1/n} \tag{10}$$

The linear form of the same could be used conveniently by taking the logarithmic of equation 10 as given in the following equation 11.

$$Inq_e = \frac{1}{n} InC_e + InK_F \tag{11}$$

where K_F and n are the Freundlich constants and are indicators of biosorption capacity and biosorption intensity, respectively.

2.4.4 Biosorption thermodynamics

The effect of temperature on the biosorption of metal was studied at different temperatures, with fixed initial metal ion concentration, biosorbent dose and pH. The spontaneity of the biosorption process was decided by several thermodynamic parameters viz., Gibb's free energy change (ΔG°), enthalpy change (ΔH°) and entropy change (ΔS°). These thermodynamic parameters were calculated using the following equations.

$$\Delta G^{\circ} = -RT \ In \ K_d \tag{12}$$

where R is the gas constant (8.314 J mol^{-1} K^{-1}) T is the temperature (K), and K_d is the equilibrium constant. The value of K_d was calculated using equation 13.

$$K_d = \frac{q_e}{C_e} \tag{13}$$

where q_e and C_e are the equilibrium concentrations of metal ions on the biosorbent and in the solution, respectively. The enthalpy change (ΔH°) and entropy change (ΔS°) of biosorption were calculated using equation 14.

$$\Delta G^{\circ} = \Delta H^{\circ} - T\Delta S^{\circ} \tag{14}$$

The equations (12) and (14) can be combined together as:

$$In K_d = \frac{\Delta S^{\circ}}{R} - \frac{\Delta H^{\circ}}{RT} \tag{15}$$

A plot between $ln \ K_d$ versus $1/T$, would give the values of the ΔH° and ΔS° from slope and intercept, respectively and the values of ΔG° were calculated from Equation 12.

2.5 Column studies

Batch biosorption assays give fundamental information related to biosorption equilibrium and kinetics. However, in most industrial aqueous treatment units, a continuous flow biosorption experiments are preferred. Therefore, in present study biosorption experiments were performed in continuous flow columns. The overall performance of the column is usually described through the concept of breakthrough curve, which is obtained by plotting the measured effluent concentration divided by the influent concentration (C_e/C_i) versus time (t).

The column performance was studied by varying the flow rate and bed depth at specific metal ion concentration in glass columns (internal diameter = 1.5, 2.5, 3.0 cm and length 25.0, 50.0 cm) filled with biosorbents up to the required bed depth. The biosorbents in the columns were packed properly to avoid any channels, cracks and empty spaces in the bed. The biosorbents packed columns were held vertically with the help of stands and clamps and connected with peristaltic pump to control the flow rates. The operation and the response of the column could be explained with the help of the breakthrough time. Breakthrough occurs when the metal concentration in the effluent from the column remain ~ 3-5% of the original concentration (Paul

et al., 2003). Bed depth service time (BDST) model (Hutchins, 1973) and Thomas model (1944) were applied to the column study.

The BDST model is one of the mathematical models proposed by Hutchins which states that bed depth (Z) and breakthrough service time (t_b) of a column bears a linear relationship. The equation can be expressed as follows.

$$t_b = (\frac{N_o}{C_i R})Z - (\frac{1}{K_a C_i})\, In(\frac{C_i}{C_b} - 1) \tag{16}$$

where C_b (mg L^{-1}) is the breakthrough metal ion concentration, N_o (mg L^{-1}) is the biosorption capacity, K_a (L $mg^{-1}h^{-1}$) is the rate constant in BDST model and the R (mL min^{-1}) is the flow rate. Equation 16 could be written in the form of the following equation 17

$$t_b = mZ - K \tag{17}$$

where m is the slope of the BDST line ($m=N_o/C_iR$) and K is the intercept of this equation.

$$K = \frac{1}{k_a C_i}\left(In\frac{C_i}{C_b} - 1 \right) \tag{18}$$

The values of biosorption capacity N_o and rate constant K_a were evaluated from the slope and intercept of the plot of t_b versus Z. The value of K_a could be used to describe the capacity of biosorption column.

The Thomas model assumes the Langmuir second order reversible reaction kinetic model of sorption and desorption, with no axial dispersion. The expression by Thomas for the column biosorption is given in equation 19.

$$\frac{C_e}{C_i} = \frac{1}{1 + \exp\left(\frac{k_{TH} q_e s}{R} - k_{TH} C_i t \right)} \tag{19}$$

where k_{TH} is the Thomas rate constant (mL $min^{-1}mg^{-1}$), q_e is the equilibrium metal uptake per gram of the biosorbent (mg g^{-1}), s is the amount of biosorbent in gram in the column, C_i and C_e are the influent and the effluent concentrations (mg L^{-1}) of metal, respectively, at time t (min), $t=V_{eff}/R$ where V_{eff} is the effluent volume (mL) and R is the flow rate (mL min^{-1}).

References

Freundlich, H.; Over the biosorption in solution; *J. Phys. Chem*.; **1906**, 57, 385–470.

Hutchins, R.A.; New method simplifies design of activated carbon system; *Chem. Eng.*; **1973,** 80, 133–135.

Lagergren, S.; About the theory of so-called adsorption of solution substances; *Handlinge*; **1898,** 24 (4), 147–156.

Langmuir, I.; The constitution and fundamental properties of solids and liquids; *Am. Chem. Soc*; **1916,** 38, 2221–2295.

Paul, Chen J.; Yoon, J.T. and Yiacoumi, S.; Effects of chemical and physical properties of influent on copper sorption onto activated carbon fixed- bed columns; *Carbon;* **2003,** 41, 1635–1644.

Rivera-Utrilla, J.; Bautista-Toledo, I.; Ferro-Garcy'a, M.A. and Moreno- Castilla, C., Activated carbon surface modifications by Biosorption of bacteria and their effect on aqueous lead adsorption. *J. Chem. Technol. Biotechnol*.; **2001,** 76, 1209–1215.

Singh, J. and Ali. A.; Kinetics, Thermodynamics and Breakthrough Studies of biosorption of Cr(VI) Using Arachis hypogea Shell Powder; *Res. J. Chem. Environ*.; **2012**,16 (1), 69–79.

Thomas, H.C; Heterogeneous ion exchange in a flowing system; *J Am. Chem. Soc*; **1944**, 66, 1446-1664**.**

Chapter 3

Kinetics, Thermodynamics and Breakthrough Studies of Biosorption of Cr(VI) as Hydrogen Chromate anion Using Activated *Arachis hypogea* shell powder

Contents

Abstract

In this chapter, activated *Arachis hypogea* shell powder was applied for studying kinetics, isotherm modeling, thermodynamics and breakthrough studies of biosorption of Cr(VI) as hydrogen chromate from synthetic and electroplating chrome wastewater in batch and column studies. To optimize the conditions for maximum biosorption in batch process, the pH, contact time, biosorbent dose and initial Cr(VI) concentration have been varied. Both Freundlich and Langmuir isotherm models have been used to study the batch equilibrium data. The best fitting was observed following Langmuir isotherm model with 111.11 mg g^{-1} maximum biosorption capacity and correlation coefficient of 0.99.

The experiments were performed to study the kinetics of Cr(VI) biosorption and the same was best described with pseudo-second-order kinetic model supporting that the rate limiting step may be chemical sorption. The thermodynamic parameters viz., Gibbs free energy (ΔG°), enthalpy (ΔH°) and entropy (ΔS°) changes were also calculated, and the observed values supported the spontaneity of the biosorption process.

Column studies were carried out to study the effect of bed depth and flow rate on continuous biosorption process. Thomas and Bed Depth Service Time models were applied to study the breakthrough curves for successive sorption-desorption cycles.

Keywords: *Arachis hypogea* shell powder, Langmuir isotherm model, correlation coefficient, Gibbs free energy, Bed Depth Service Time model, electroplating chrome wastewater.

3.1 Introduction

Most heavy metals are well-known toxic and carcinogenic agents and when discharged into the wastewater represent a serious threat to the human population and the fauna and flora of the receiving water bodies (Jain *et al*., 2013; Ali *et al*., 2012; Visa *et al*., 2012). Among these metal ions, chromium is dominant in most of the effluent streams in India and all over the world (Mohan *et al*., 2005). It is widely used in a range of industries for instance metal finishing, corrosion inhibitors, electroplating, paints, metallurgical, tanning and mining (Mohan *et al*., 2005). Chromium exists usually in both trivalent and hexavalent forms in aqueous solutions. The trivalent form is relatively insoluble and required in small quantities by microorganisms. It acts as an essential trace metal nutrient, while hexavalent is hazardous by all exposure routes. Hexavalent chromium exists primarily as salts of chromic acid, hydrogen chromate and chromate ion, depending on the pH of the medium. Acute exposure to Cr(VI) causes nausea, diarrhea, liver and kidney damage, dermatitis, internal hemorrhage and respiratory problems. Hence the elimination of Cr(VI) from waste water is a priority concern.

In the present study activated *Arachis hypogea* shell powder (AAHSP) was used for the removal of Cr(VI) from synthetic and industrial wastewater. The effect of contact time, pH, adsorbent dose and initial chromium ions concentration were studied in batch studies and effect of different flow rates and bed depth were studied column operations.

3.2 Experimental section

3.2.1 Batch biosorption studies

Batch experiments for Cr(VI) biosorption onto AAHSP (activated *Arachis hypogea* shell powder, preparation mentioned in chapter 2) from synthetic solutions were carried out at different pH values viz., 1.0 to 8.0 by agitating a biosorbent dose of 0.25 g/0.1 L with 100 mg L^{-1} initial Cr(VI) concentration in 250 mL screw-cap conical flasks. The mixtures so obtained were agitated in orbital shaker at 225 rpm for 720 min at 25 $^{\circ}$C. The suspensions were filtered after every ten minutes of agitation through Whatman no. 40 filter paper and the filtrates were analyzed spectrophotometrically using diphenly carbazide as the complexing agent at 540 nm (Aksu *et al*., 2002). Further experiments were conducted by varying the Cr(VI) concentration in the range of 50 to 300 mg L^{-1} and contact time of 1 to 720 min. The effect of biosorbent dose was studied from 0.050 to 0.750 g/0.1 L and temperature from 15 to 30 $^{\circ}$C. The reduction rate of

Cr(VI) to Cr(III) by AAHSP at different pH (1.0 – 8.0) was also studied by taking the biosorbent dose of 0.25 g/0.1 L with 100 mg L^{-1} initial Cr(VI) concentration. The total chromium was estimated by AAS and Cr (III) concentration of the sample was calculated as a difference of total chromium and Cr(VI) of the sample solutions. The percent removal (*R%*) of Cr(VI) and the metal uptake capacity (q_e = mg g^{-1}) was calculated for each experiment using equation 1 and 2 as mentioned in chapter 2.

3.2.2 Down flow column studies

Down flow column studies were conducted in glass columns (internal diameter = 1.5 cm and length 50.0 cm) filled with AAHSP up to the required bed depth. The AAHSP packed columns were washed twice by circulating 1.0 L deionised water through them. The effect of bed depths on the breakthrough curves were investigated using bed depths of 13.0, 17.0, and 20.0 cm made by the uniform packing of 6.5, 8.5, and 10.0 g of AAHSP respectively. The feed solution having 50 mg L^{-1} initial Cr(VI) concentration was allowed to flow through the column to study the effect of an effluent flow rate of 2.0, 4.2 and 5.4 mL min^{-1}. Effluents were collected in conical flask in 60.0 mL fractions and analyzed for the residual metal ion concentration spectrophotometrically. The electroplating chrome wastewater rich in Cr(VI) was passed through the column of AAHSP with fixed bed depth of 20.0 cm at pH 2.0 and flow rates of 2.0 mL min^{-1}. The Thomas model was applied to the data obtained to find the value of q_{max} and the effluent was treated till the values reached to satisfy the Central pollution control board standards (CPCB, 1998).

3.2.3 Desorption of Cr(VI) and regeneration of exhausted AAHSP

The exhausted AAHSP in batch mode was regenerated using different desorbing agents (NaOH, Na_2CO_3, EDTA, HCl, HNO_3 and deionised water). The desorbing efficiency of these desorbing agents were evaluated and compared. The best eluting agent obtained was used for the regeneration of the exhausted columns.

3.3 Results and Discussion

3.3.1 Characterization of the AAHSP

The AAHSP used in the column studies for Cr(VI) biosorption from the aqueous solution has been recovered, dried and analyzed by the FTIR, SEM and EDX instruments.

3.3.1.1 FTIR analysis

To determine the main functional groups of AAHSP responsible for Cr(VI) binding from the solution, FTIR spectra of the biosorbent before and after Cr(VI) binding have been recorded and given in Figure 1.

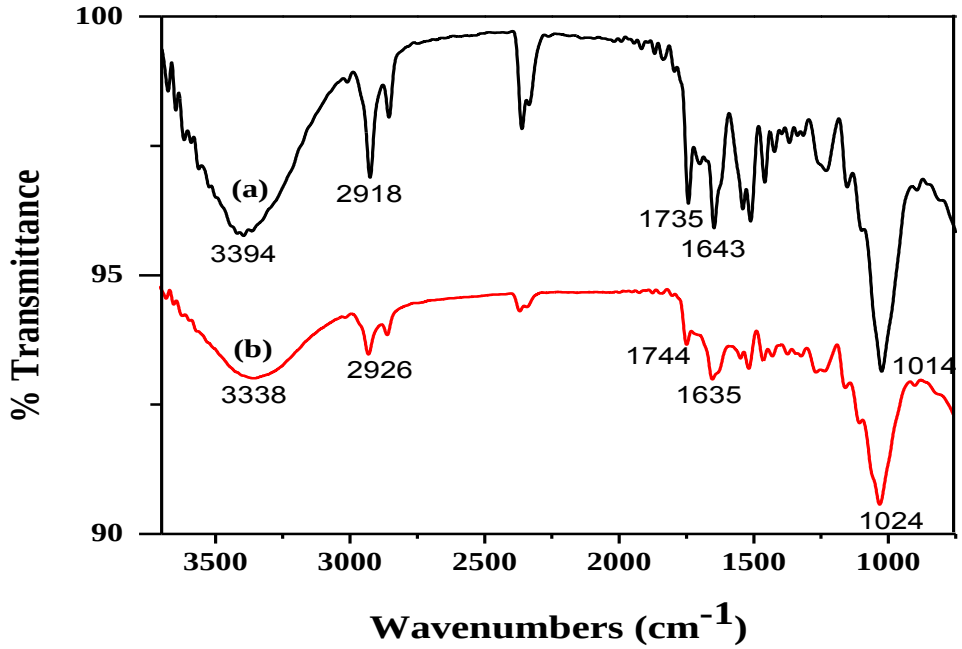

Figure 1: IR spectra of AAHSP (a) before and (b) after biosorption of Cr(VI) ions.

In Figure 1a, the broad and strong band at 3394 cm^{-1} indicates the presence of bonded hydroxyl group that can be of cellulose, pectin, absorbed water, hemicellulose and lignin (Feng *et al*., 2009; Perez Marin *et al*., 2009). This peak was consistent with the peak at 1014 cm^{-1} assigned to alcoholic C–O stretching vibrations (Pavan *et al.*, 2006). Another band observed at 2918 cm^{-1} can be assigned to the C–H group and the band observed at 1735 and 1643 are indicative of the carbonyl groups (Jacques *et al*., 2007; Vaghetti *et al*., 2009). In the spectra of chromium-loaded AAHSP (Figure 1b), the original bands of biosorbent observed at 3394, 2918, 1735, 1643 and

1014 cm^{-1} were shifted to 3338, 2926, 1744, 1635 and 1024 cm^{-1} respectively. The shift in band position supports that –OH and C=O groups have interacted with Cr(VI) during the biosorption process. The possible biosorption on AAHSP may be due to physical biosorption, complexation with functional groups, ionic exchange or chemical reaction with biosorbent sites (Ashkenazy *et al*., 1997).

3.3.1.2 SEM and EDX analysis

To study the surface morphology of the AAHSP, the scanning electron microscopy of the same has been performed before and after the chromium biosorption and are shown in Figures 2a and 2b. The SEM images of the AAHSP gave a porous structure with rough surface before biosorption and the surface became bit smoother after Cr(VI) biosorption. The EDX analysis of the recovered AAHSP (from the column studies) was found to have a 1.24 wt% of chromium and hence, supported the biosorption of chromium by the AAHSP.

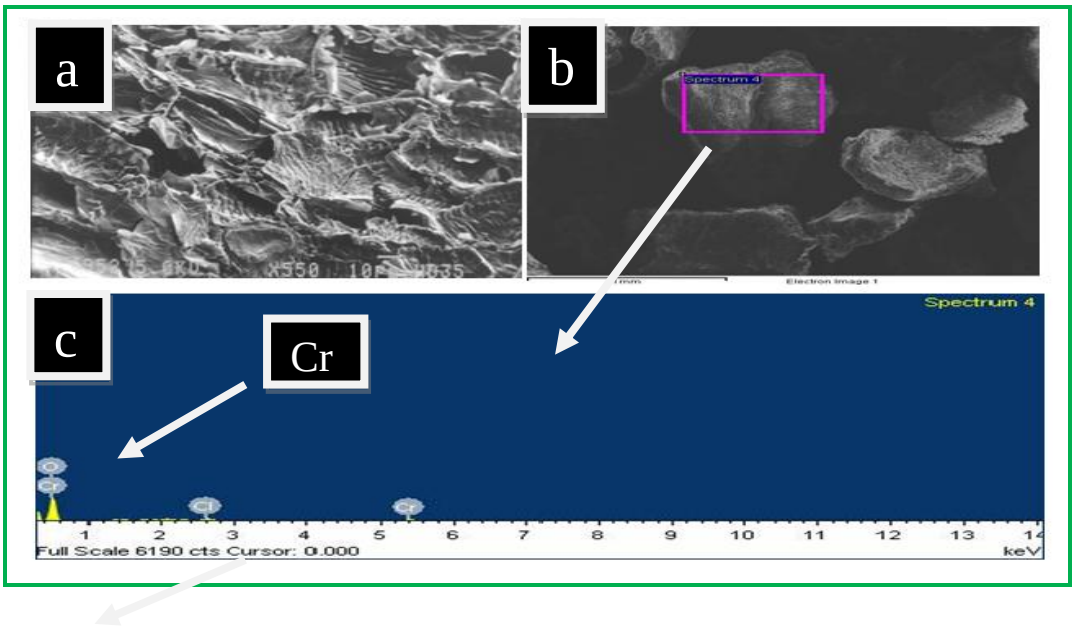

Figure 2: The SEM images of AAHSP (a) before (b) after the chromium biosorption and (c) EDX analysis of AAHSP after chromium biosorption.

3.3.2 Batch biosorption studies

3.3.2.1 Effect of pH

The pH of the medium is one of the most important parameter that could alter the binding properties of the biosorbent. Chromium exists in different oxidation states and the stability of these forms depends upon the pH of the system (Sharma and Foster, 1994; Hamadi *et al*., 2001). At pH 1.0, the chromium ions exist in the form of H_2CrO_4, while in the pH range of 1.0–6.0 different form of chromium ions such as $Cr_2O_7^-$, $HCrO_4^-$, $Cr_3O_{10}^{2-}$, $Cr_4O_{13}^{2-}$ coexist of which $HCrO_4^-$ predominates. As pH increases this form shifts to CrO_4^{2-} and $Cr_2O_7^{2-}$. The equilibrium that exists between different ionic species of chromium is as follows:

$$H_2CrO_4 \rightleftharpoons H^+ + HCrO_4^- \quad (1)$$

$$HCrO_4^{2-} \rightleftharpoons +CrO_4^- \quad (2)$$

$$2HCrO_4^- \rightleftharpoons Cr_2O_7^{2-} + H_2O \quad (3)$$

The effect of the pH (1.0 to 8.0) on the biosorption of Cr(VI) ions on the AAHSP was evaluated by taking 100 mg L^{-1} of Cr(VI) initial concentrations with biosorbent dose of 0.25 g/0.1 L. The mixtures so obtained were agitated in orbital shaker for 720 min at agitation speed of 225 rpm at 25 $^{\circ}$C. It was observed (Figure 3) that the maximum percentage removal of Cr(VI) occurred at pH 2.0 and there was significantly decrease in percentage removal with increase in pH values up to 8.0.

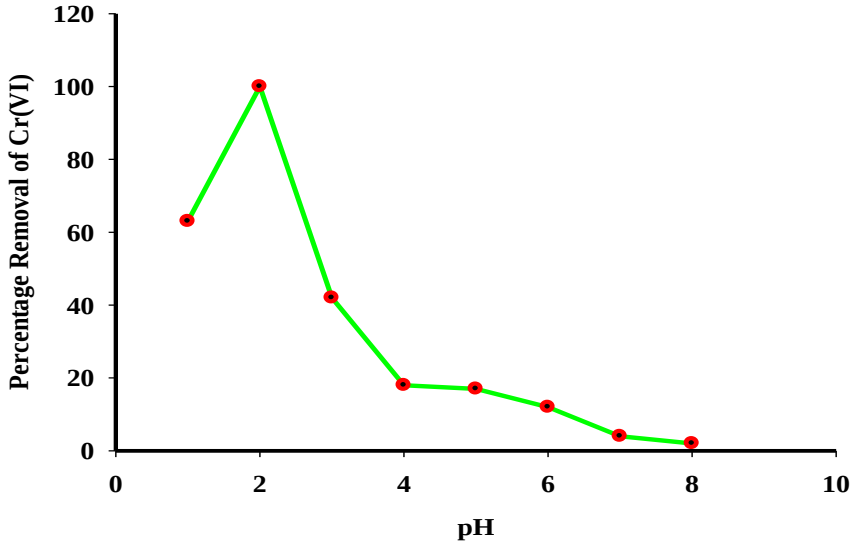

Figure 3: Effect of pH on Cr(VI) biosorption.

Maximum biosorption in acidic pH (pH=2.0) indicates that at low pH an increase in H^+ ions on the biosorbent surface occurs which results in strong electrostatic attraction between positively charged AASHP surface and $HCrO_4^-$ (hydrogen chromate) ions. However, at pH less than 2.0 a decrease in biosorption was observed due to the chromium being present predominantly as H_2CrO_4 (chromic acid). Biosorption of Cr(VI) was not significant in alkaline pH due to the dual competition between CrO_4^{2-} (chromate ion) and OH^- to be biosorbed on AAHSP. Since, maximum biosorption occurs at pH 2.0, all further experiments were conducted at this pH only.

Further the final concentration of total chromium, hexavalent chromium and trivalent chromium in a pH range 1 to 8 were also analyzed. The percentage removal of Cr(VI) and reduction to Cr(III) as a function of pH is shown in Table 1. The results indicated that in acidic pH a combined effect of Cr(VI) biosorption and reduction to Cr^{3+} was found. The maximum 44.25% Cr(VI) was reduced to chromium Cr^{3+} at pH 2.0. As pH increases the percent removal of Cr(VI) and reduction to Cr(III) decrease gradually, thus the mechanism involved in biosorption of Cr(VI) may be biosorption along with reduction (Vinodhini and Das, 2010).

Table 1: Percentage removal and reduction efficiency of Cr(VI) at different pH values

pH	% Removal of Cr(VI)	% Reduction of Cr(VI) to Cr(III)
1	65	12.22
2	99	44.25
3	53	12.5
4	15	4.5
5	10	1.5
6	8	0
7	6	0
8	4	0

3.3.2.2 Effect of contact time and kinetics of biosorption

The effect of contact time on Cr(VI) biosorption onto AAHSP was studied in the time range 1-720 min by using 100 mg L^{-1} of Cr(VI) solutions at pH 2.0 with 0.25 g/0.1 L of the AAHSP. The samples were collected at regular intervals, filtered and analyzed for Cr(VI) concentration by UV visible spectrophotometer. As shown in Figure 4a, more than 60 % biosorption of Cr(VI) took place in first 60 min and then it continued to increase until 100 % biosorption was achieved after

720 min of contact time. Based on these results, a contact time of 720 min was assumed to be suitable for subsequent biosorption experiments.

The kinetics of the AAHSP-Cr(VI) interactions was tested using pseudo-first-order and pseudo-second-order kinetic models as mentioned in chapter 2. The fitting of the obtained data according to pseudo-first-order do not fall on straight line, indicating that this model is not suitable for the biosorption of Cr(VI) on AAHSP. The pseudo-first-order rate constant k_1, the value of q_e and the correlation coefficient were calculated from the model and are presented in Table 2. The value of the correlation coefficient was found to be 0.1106 and was indicative of a poor correlation. The plot of t/q_t versus t of pseudo-second-order gave a straight line as shown in Figure 4b and the rate constant k_2 and q_e were determined from slope and intercept of the plot respectively.

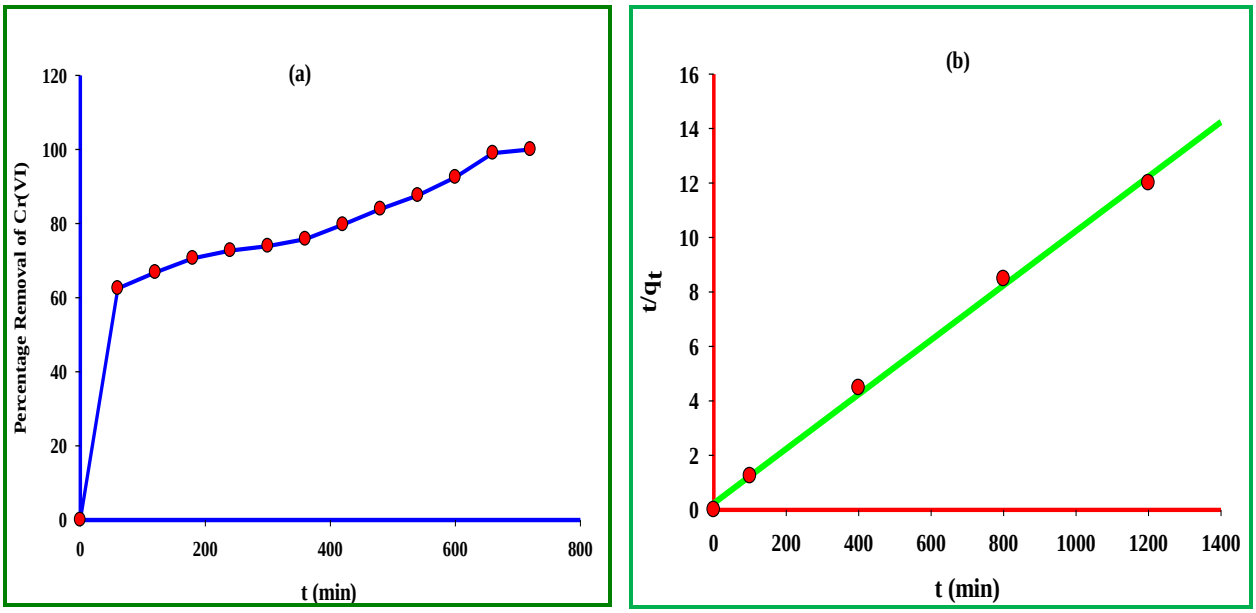

Figure 4: a) Effect of contact time and b) the pseudo-second-order kinetic model for Cr(VI) biosorption.

The value of the correlation coefficient was found to be 0.99 (Table 2). This implies that the data tends to follow pseudo-second-order kinetics for Cr(VI) on to AAHSP very well; hence the rate-limiting step may be chemisorptions. Similar results have been observed in the biosorption of Cr(VI) using neem saw dust (Vinodhini and Das, 2010) and activated carbons derived from agricultural waste materials.

Table 2: Parameters of pseudo-first-order and pseudo-second-order kinetic models

pseudo-first-order			pseudo-second-order		
k_1 ($g\ mg^{-1}min^{-1}$)	q_e ($mg\ g^{-1}$)	R^2	k_2 ($g\ mg^{-1}min^{-1}$)	q_e ($mg\ g^{-1}$)	R^2
-3.6×10^{-3}	1.875	0.11	4.16×10^{-3}	100.0	0.997

3.3.2.3 Effect of biosorbent dose

The effect of the biosorbent dose on biosorption process was studied by varying the biosorbent doses in the range of 0.050 – 0.750 g for 0.1 L Cr(VI) solution with 100.0 mg L^{-1} concentration at pH 2.0. It was observed from Figure 5 that the percentage removal of Cr(VI) increased with increase of biosorbent dose, reaching a maximum (99.0 %) at around 0.25 g.

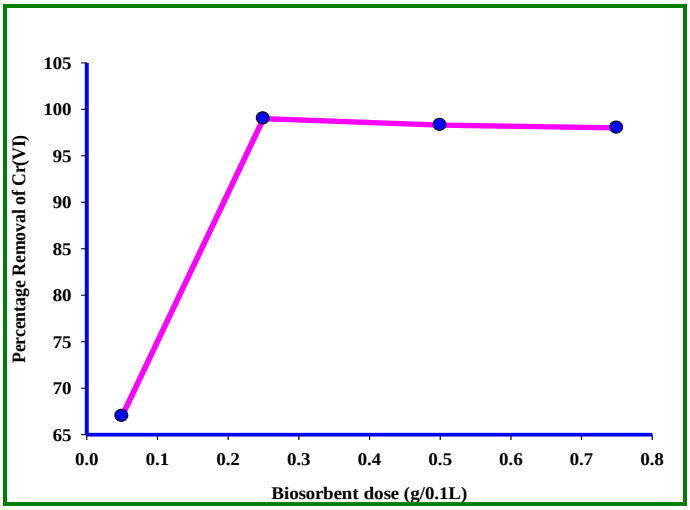

Figure 5: Effect of biosorbent dose on Cr(VI) biosorption.

It may be due to the availability of more biosorption sites with increase in the biosorbent dose. Further increase in biosorbent dose did not significantly change the percentage removal of Cr(VI). This could be due to the overlapping of the biosorption sites as a result of overcrowding of the biosorbent particles when the biosorbent dosage was increased above 0.25 g/0.1 L. Moreover, the high biosorbent dosage could impose a screening effect on the dense outer layer of the cells, thereby shielding the binding sites from metals as explained by Garg *et al*. (2003),

Babel and Kurniawan (2004). Thus 0.25 g/0.1 L of the biosorbent dose was selected for further studies.

3.3.2.4 Effect of initial metal ion concentration and isotherm modeling

The consequence of change of initial Cr(VI) concentration on the biosorption process was evaluated by agitation 0.25 g/0.1 L of the AAHSP with varying concentrations (50.0 to 300.0 mg L^{-1}) of Cr(VI) at pH 2.0. Metal biosorption ability of AAHSP was found to increase with the increase in initial metal ion concentration until it reached the maximum capacity of 99% with 100 mg L^{-1} but the biosorption of the Cr(VI) was found to decrease with further increase in Cr(VI). It may be due to the saturation of the binding sites of the biosorbent at high metal concentration or the increase in the number of Cr(VI) ions competing for available binding sites of the biosorbent.

Both Langmuir and Freundlich isotherm models (as mentioned by equation 8 and 11 respectively in chapter 2) were used to study the relationship between the amount of metal ions adsorbed on biosorbent and its equilibrium concentration in aqueous solution. The plots of C_e/q_e versus C_e and $ln\ q_e$ versus $ln\ C_e$ as shown in Figure 6 were found to be linear indicating the applicability of both the isotherm model to the experimental data obtained.

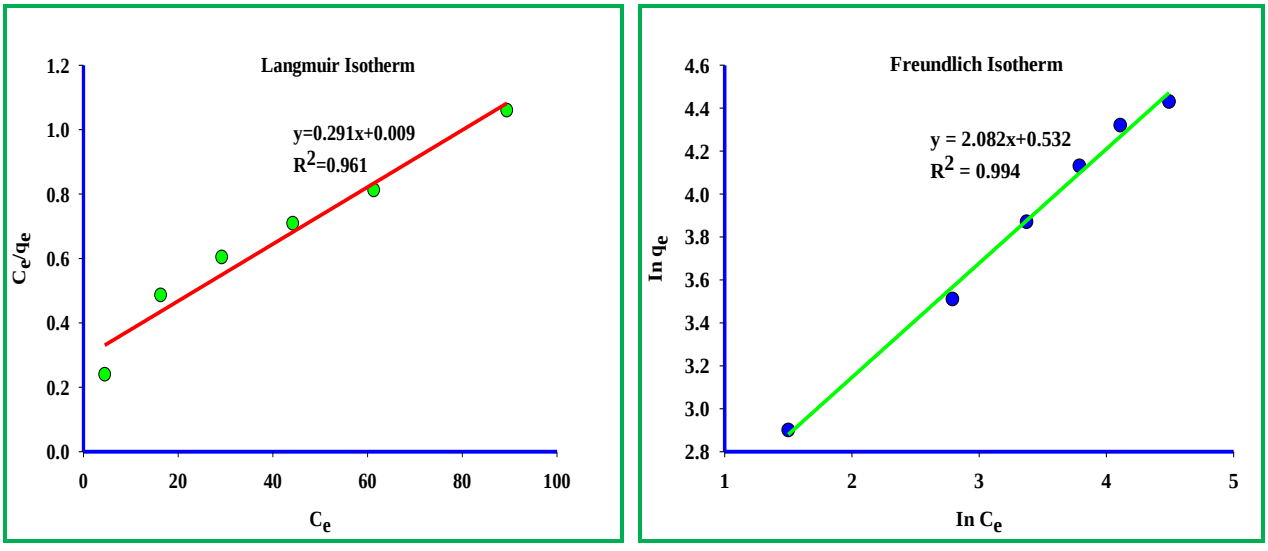

Figure 6: The Langmuir and Freundlich biosorption isotherms for Cr(VI) biosorption on AAHSP.

The Langmuir and Freundlich constants q_{max}, K_F were determined from the intercepts and b, $1/n$ from the slopes of the linear plots, respectively and are given in Table 3. The values of the correlation coefficients were found to be extremely high indicating both homogeneous and heterogeneous distribution of active sites on the surface of the AAHSP (Gundogdu *et al.*, 2009). The values of $1/n$ were smaller than 1 again proving that the biosorption process was favorable under studied conditions. Also the values of R_L (calculated using equation 9 as mentioned in chapter 2) for the Cr(VI) concentration in the range of 50–300 mg L^{-1} and were found to be between 0.4–0.1 at fixed AAHSP mass of 0.250 g/0.1 L. This result also sustains the fact that the biosorption of Cr(VI) on AAHSP was a favorable process.

Table 3: Langmuir and Freundlich isotherm constants and correlation coefficients for the biosorption of Cr(VI) on AAHSP

Wt. of AAHSP (g)	Langmuir isotherm constants			Freundlich isotherm constants		
	q_{max} (mg g^{-1})	b (L mg^{-1})	R^2	K_F (L g^{-1})	n	R^2
0.250	111.11	0.030	0.99	2.08	1.87	0.96

3.3.2.5 Biosorption thermodynamics

The biosorption of Cr(VI) was studied at different temperatures, ranging from 15 to 30 °C with fixed Cr(VI) concentration of 100 mg L^{-1} and biosorbent dose of 0.25 g/0.1 L at pH 2.0. The biosorption capacity of the AAHSP for Cr(VI) ion was maximum at 25 °C and was nearly same at 30 °C (Table 4). This could be attributed due to the increase in molecular diffusion or due to the availability of more active sites on the surface of the AAHSP by expansion of the pores at the same temperature (Karthikeyan *et al*., 2005). The spontaneity of the biosorption process was decided by several thermodynamic parameters viz., Gibb's free energy change (ΔG°), enthalpy change (ΔH°) and entropy change (ΔS°). The values of the ΔH° and ΔS° were obtained from slope and intercept of a plot of $ln\ K_d$ versus $1/T$ (Figure 7) respectively. The negative values of ΔG° (calculated using Equation 12 as given in chapter 2) supported the spontaneity of the biosorption process (Namasivayam and Yamuna, 1995). An increase in magnitude of ΔG° with temperature indicates that biosorption was most favorable between 25 to 30 °C.

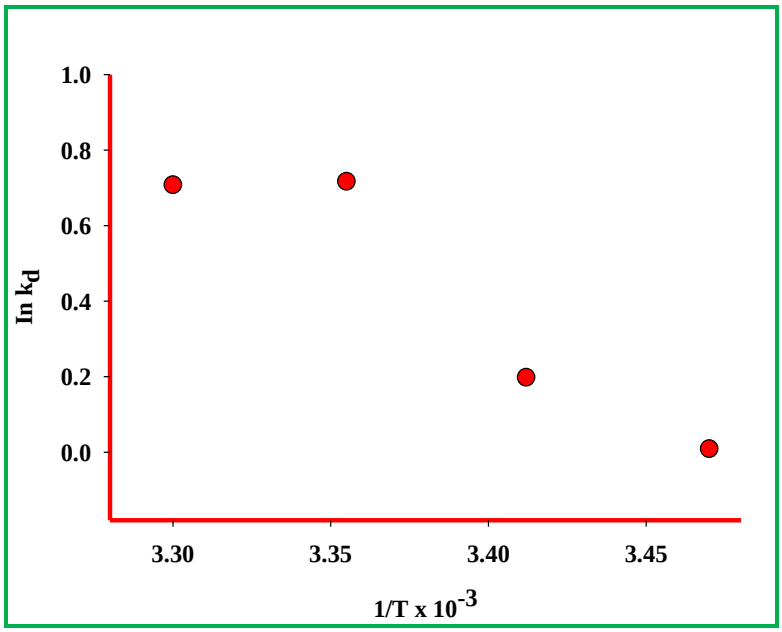

Figure 7: Plot of *In* K_d versus *1/T* for the biosorption of Cr(VI) on AAHSP

The values of ΔH° was positive, indicating the endothermic nature of the biosorption of Cr(VI) on AAHSP while the positive value of ΔS° (Table 4) stated that randomness at the solid/liquid interface increases during the biosorption of Cr(VI) ions on the AAHSP (Namasivayam and Yamuna, 1995).

Table 4: Thermodynamic parameters for Cr(VI) biosorption on the AAHSP at different temperatures

T (°C)	C_e (mg L^{-1})	q_e (mg g^{-1})	K_d	ΔG° (kJ mol^{-1})	ΔS° (kJ $mol^{-1}K^{-1}$)[a]	ΔH° (kJ mol^{-1})[a]
15	28.2	28.72	1.01	-0.021		
20	24.7	30.12	1.22	-0.482		
25	16.3	33.48	2.05	-1.776	0.134	0.038
30	16.41	33.44	2.03	-1.783		

[a] Measured between 15 to 30°C

3.3.2.6 Desorption of Cr(VI) and regeneration of exhausted AAHSP

The results obtained using different desorbing agents indicated that desorption of Cr(VI) with acids was marginal (Figure 8). Maximum desorption of Cr(VI) was achieved using NaOH as desorbing medium. Further experiments were conducted with different concentration of NaOH (0.1M, 0.2M, 0.3M, 0.4M) and it was noticed that the percentage desorption of Cr(VI) increased with increase in concentration of the desorbing agent up to 0.4 M, and, a further increase in NaOH concentration (> 0.5M) was found to deteriorate the biosorbent.

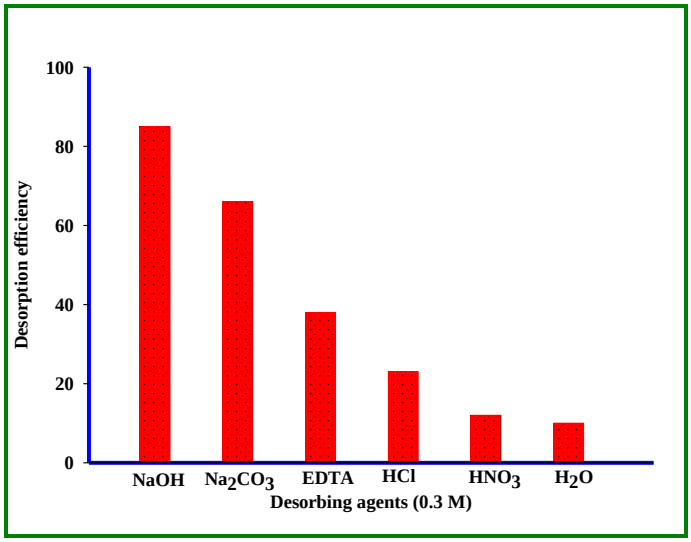

Figure 8: Desorption of Cr(VI) by different desorbing agents

3.3.3 Column studies

3.3.3.1 Effect of bed depth

The biosorption of the metal ions in fixed bed column studies were found to be dependent on the quantity of biosorbent in the column. The continuous biosorption experiments were performed, at three different bed depths of 13.0, 17.0 and 20.0 cm, by taking 6.5, 8.5 and 10.0 g, respectively, of AAHSP in the column. The flow rate and initial Cr(VI) concentration were kept constant at 2.0 ml min^{-1} and 50 mg L^{-1} respectively during the experiments.

As shown in Figure 9, the shapes and gradient of the breakthrough curves changes with the increase in bed depth from 13.0 to 20.0 cm. The metal ion concentration in the effluent was found to increase as the breakthrough time was reached and same was indicated by the sharp increase of the slope in each curve. The breakthrough was observed in 18 h when the column of

low bed depth of 13.0 cm was used. This observation could be explained by considering the fact that with low bed depth (less biosorbent), all the metal ions were not biosorbed and most of them escaped throw the column giving early breakthrough. Whereas on increasing the bed depth, (as well as increase in the mass of the biosorbent) the breakthrough time was found to increase from 18 to 65 h. This may be due to two reasons (i) increase in the residence time of the Cr(VI) (due to longer bed length) with the biosorbent and (ii) availability of more sites for the Cr(VI) biosorption due to the higher amount of the biosorbent used while increasing the column height (Vinodhini and Dass, 2010).

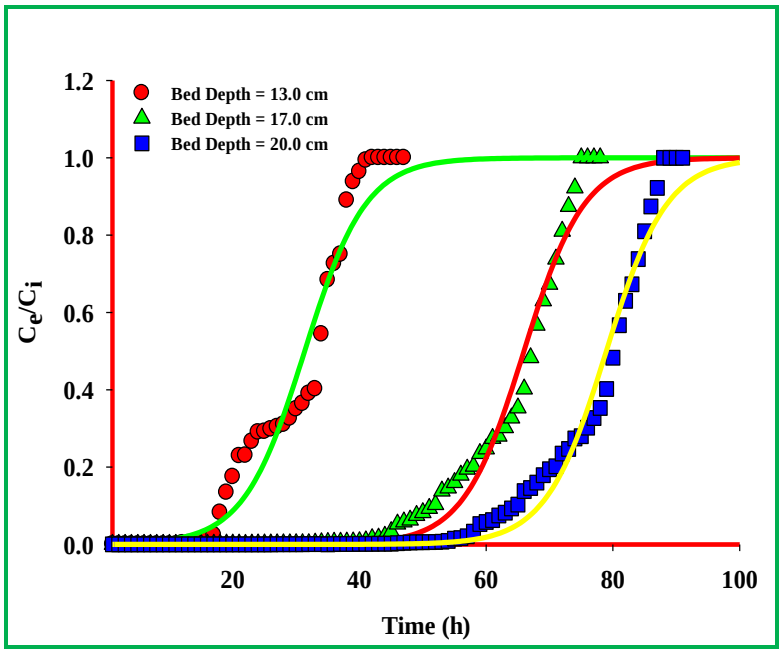

Figure 9: Effect of bed depth on biosorption of Cr(VI) at pH 2.0 by AAHSP packed column.

The BDST model (given by equation 16 in chapter 2) was applied to the data obtained. A plot of t_b versus Z at flow rate of 2.0 mL $min^{-1}$was linear (R^2= 0.9713) as shown in Figure 10, indicating the validity of BDST model for the present system.

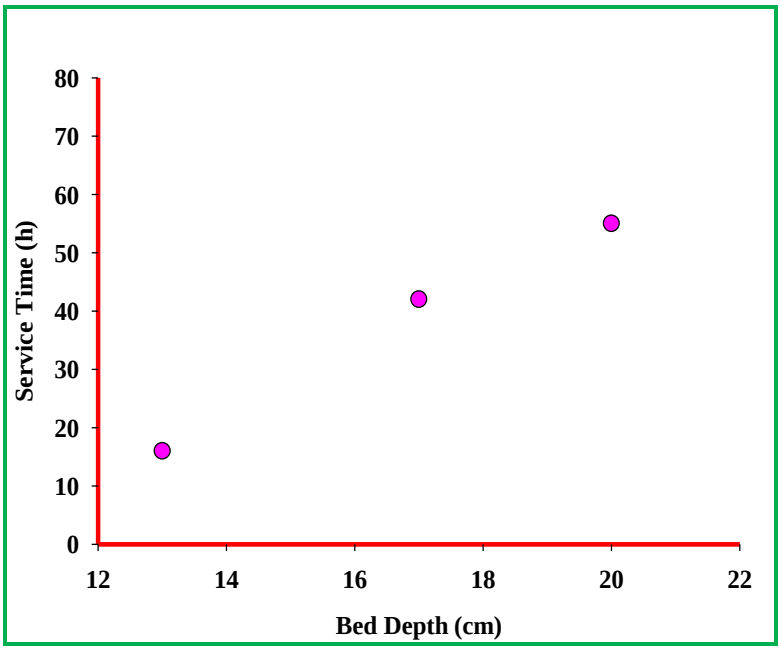

Figure 10: Plot between bed-depth service time and bed depth of AAHSP for Cr(VI) biosorption.

The values of biosorption capacity N_o and rate constant K_a were evaluated from the slope and intercept, respectively and are given in Table 5. The value of K_a characterized the rate of solute transfer from the solution to the biosorbent. In general if the value of K_a is small (< 1.0) (Vinodhini and Dass, 2010), even the high bed depth column cannot prevent the breakthrough, but with high K_a value lower bed depth can prevent breakthrough. The BDST model parameters could be helpful in scaling the column studies for other bed depths without further experiments.

Table 5: BDST model parameters analyzed for Cr(VI) biosorption by AAHSP in column studies.

Slope	Intercept	N_o (mg L^{-1})	K_a (L mg^{-1} h^{-1})	R^2
6.8108	-68.5135	681.08	0.0003	0.9713

3.3.3.2 Effect of effluent flow rate

Flow rate of the column could alter the residence time of the metal solution in the column and hence is an important parameter that could influence the sorption capacity of the biosorbent in

fixed bed operations. To explore the effect of flow rate on Cr(VI) biosorption, the influent of fixed 50 mg L^{-1} Cr(VI) concentration was passed through the column with fixed bed depth of 13.0 cm at pH 2.0 with different flow rates of 2.0, 4.2 and 5.4 mL min^{-1}. As shown in Figure 11, the column performance was found to be better at lower flow rate. An earlier breakthrough and column exhaustion times were achieved, when the flow rate was increased from 2.0 to 5.4 mL min^{-1}. This behavior could be due to the decrease in the residence time, which restricted the contact of metal solution to the biosorbent. In addition, at higher flow rates the metals ions did not have enough time to diffuse into the biosorbent and they leave the column before equilibrium occurred resulting in low metal uptake and earlier breakthrough curves. At lower flow rates the residence time of the metal solution in the column was increased and hence metal ions have enough time to bind the biosorbent effectively giving late breakthrough curves.

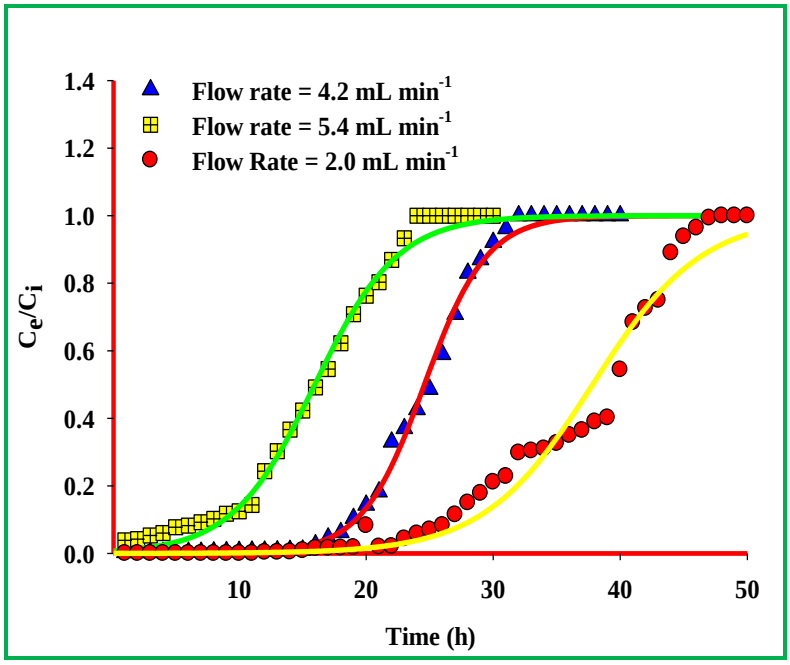

Figure 11: Effect of flow rates on Cr(VI) biosorption by AAHSP packed column at pH 2.0.

To predict the biosorption behavior of Cr(VI) onto the AAHSP packed columns, the data obtained were analyzed by Thomas model (Thomas, 1944). The Thomas model gave a good fit with high value of correlation coefficients (0.98) using the experimental data performed with different flow rates as given in Table 6. At lower flow rate of 2.0 mL min^{-1} a little deviation of

the experimental data from Thomas model was observed could be due to the dominance of intra particle diffusion mechanism. The value of metal uptake capacity (q_e) decreases (145.44 mg g^{-1} to 61.33 mg g^{-1}) with increasing flow rate with bed depth of 13.0 cm (Table 6). This is due to the less residence time of the metal solution in the column which results in lower solute diffusion from the mobile phase into the solid matrix of the biosorbent as mentioned above.

Table 6: Thomas model parameters for biosorption of Cr(VI) by AAHSP at different bed depth and flow rates.

C_i (mg L^{-1})	R (mL min^{-1})	S (cm)	k_{Th} (mL min^{-1} mg^{-1})	q_e (mg g^{-1})	R^2
50	2.0	13.0	0.0047	145.44	0.9798
50	2.0	17.0	0.0042	193.98	0.9820
50	2.0	20.0	0.0042	197.38	0.9814
50	4.2	13.0	0.0081	94.54	0.9974
50	5.4	13.0	0.0062	61.33	0.9933

3.3.4 Comparison of AAHSP with other biosorbents of agricultural origin

Table 7 shows the comparison of biosorption capacities of different biosorbents used for Cr(VI) biosorption in literature. The maximum biosorption capacity of AAHSP was found to be 111.11 mg for Cr(VI) when one gram of AAHSP was used at pH 2.0 and this value is relatively better than most of the earlier reported results as shown in Table 7. Further additional advantages of AAHSP are its easy availability and cost effectiveness, which make it better biosorbent for the removal of Cr(VI) from aqueous systems.

Table 7: Comparison of maximum biosorption capacity of AAHSP with other agricultural residues for Cr(VI) biosorption

Different biosorbents	pH	Isotherm models	Biosorption capacity (mg g^{-1})	Reference
Pine needles	2.0	Langmuir	21.50	Dakiky *et al*., 2003.
Maple sawdust	6.0	Langmuir	5.10	Yu *et al*., 2003.
Raw rice bran	5.0	Freundlich	0.07	Oliveira *et al*., 2005.
Ground nut shell	4.0	Langmuir	5.90	Agarwal *et al*., 2006.
Walnut shell	4.0	Langmuir	18.40	Agarwal *et al*., 2006.
Almond shell	4.0	Langmuir	22.0	Agarwal *et al*., 2006.
Coniferous leaves	3.0	Freundlich	6.30	Aoyama *et al*., 1999.
Larch bark	3.0	Langmuir	31.30	Aoyama *et al*., 2001.
Sugar beet pulp	2.0	Langmuir	17.20	Sharma and Forster, 1994.
Maize cob	1.5	Langmuir	13.80	Sharma and Forster, 1994.
Sugarcane bagasse	2.0	Langmuir	13.40	Sharma and Forster, 1994.
Sawdust	2.0	Langmuir	39.70	Sharma and Forster, 1994.
AAHSP	2.0	Langmuir	111.11	Present work.

3.3.5 Removal of Cr(VI) from electroplating chrome wastewater

To evaluate the effectiveness of AAHSP shell powder for the treatment of the industrial effluent, electroplating chrome wastewater was collected from the electroplating unit located at Roorke, Uttarakhand, India. Collected water sample was analyzed for few physicochemical parameters as given in Table 8. The same chrome effluent was passed through the column of AAHSP with fixed bed depth of 20.0 cm at pH 2.0 and flow rates of 2.0 mL min^{-1}.

Table 8: Different parameters of the electroplating chrome wastewater and AAHSP treated wastewater

Parameters Analyzed	Electroplating Wastewater	Treated wastewater with AAHSP
pH	2.04	2.0
Temperature (°C)	25	25
Dissolved solids (mg L^{-1})	1085.01	402.02
Suspended solids (mg L^{-1})	45.65	06.04
Total solids (mg L^{-1})	1130.66	408.06
Total Hardness (mg L^{-1})	643.11	247.02
Biological oxygen demand (BOD), (mg L^{-1})	125.61	124.55
Chemical oxygen demand (COD), (mg L^{-1})	132.06	131.02
Chromium (mg L^{-1})	89.03	0.01
Chloride (mg L^{-1})	245.74	241.35
Sulphates (mg L^{-1})	38.25	17.23
Turbidity (NTU)	9.07	0.03

Three sorption-desorption cycles with electroplating chrome wastewater were completed in a continuous way (Figure 12) and the regeneration of the exhausted columns were done using 0.4 M NaOH after each cycle.

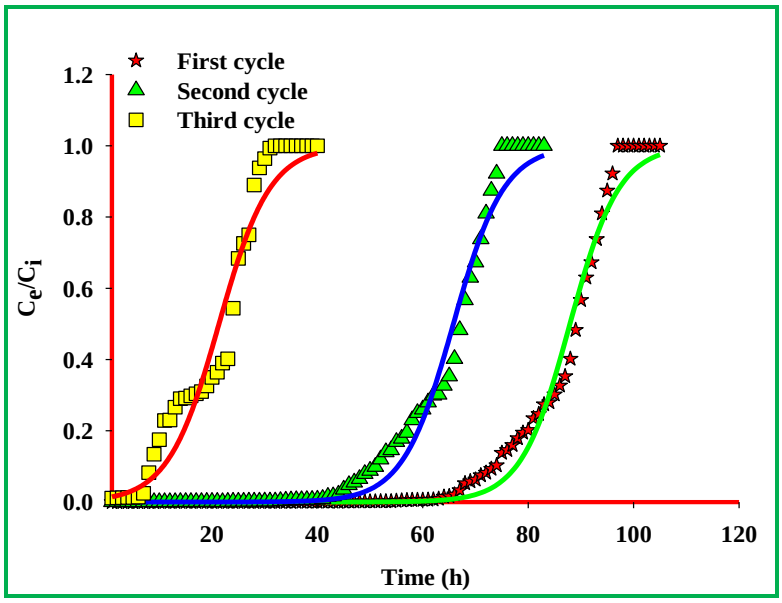

Figure 12: Breakthrough curves for Cr(VI) biosorption from electroplating chrome wastewater by AAHSP packed column.

The Thomas rate constant k_{TH} and chromium uptake capacity q_e for all three cycles are summarized in Table 9. The metal uptake capacity was found to be maximum (q_e = 298.45 mg g^{-1}) in the first cycle and found to decrease in the successive cycles. This could be ascribed due to the gradual deterioration of the biosorbent by basic elution and moreover desorption of Cr(VI) from the biosorbent was not achieved 100 % after every recycle.

Table 9: Thomas model parameters for biosorption of Cr(VI) by AAHSP from electroplating chrome wastewater.

Biosorption of Cr(VI) from Chrome effluent	**k_{Th} (mL min^{-1} mg^{-1})**	**q_e (mg g^{-1})**	**R^2**
1st Cycle	0.0032	298.45	0.96
2nd Cycle	0.0031	183.98	0.96
3rd Cycle	0.0035	166.10	0.95

3.3.6 Cost estimation of AAHSP

In India, the easily available low cost variety of commercially available carbon costs approximately $ 15-30/100 kg (Kan Carbon Pvt. Ltd., India). *Arachis hypogea* shells are available for $ 2/100 kg, and considering the cost of transport, chemicals, electrical energy etc., used in activation process, the finished product would cost approximately $ 8/100 kg. Hence, the developed biosorbent would be a good replacement for commercial available carbon based on its comparatively low cost, availability and efficiency.

3.4 Conclusions

In light of the experimental results obtained and their evaluation, AAHSP, an agro based waste material, has considerable potential for the biosorption of Cr(VI) from synthetic and industrial effluents. The biosorption of Cr(VI) by AAHSP was found to be spontaneous at pH 2.0 with the maximum biosorption capacity of 111.11 mg g^{-1} at 25°C in batch studies. The comparison of the literature reported biosorbents with AAHSP revealed that later had better Cr(VI) biosorption capacity. The batch studies of Cr(VI) biosorption were found to follow the pseudo-second-order kinetics and equilibrium data obtained was best fitted with Langmuir isotherm model. The probable mechanism involved in biosorption of Cr(VI) may be biosorption coupled reduction. The column breakthrough curves were analyzed at different flow rates and bed depths, and best results were obtained by following both Thomas and BDST models. The same biosorbent (AAHSP) in column mode was used for the biosorption of Cr(VI) from the chromium electroplating wastewater. The column was run successfully for three successive sorption desorption cycles with ~ 100% Cr(VI) removal in the first cycle. In summary, the present study suggests that AAHSP is a potential biosorbent for the removal of Cr(VI) from synthetic and electroplating wastewater.

References

Ali, I.; Asim, M. and Khan, T.A.; Low cost adsorbents for the removal of organic pollutants from wastewater; *Journal of Environmental Management;* **2012**, 113, 170–183.

Agarwal, G.S.; Bhuptawat, H.K. and Chaudhari, S.; Biosorption of aqueous chromium(VI) by tamarindus indica seeds; *Bioresour. Technol*.; **2006,** 97 (7), 949–956.

Aksu, Z.; G¨onen, F. and Demircan, Z.; Biosorption of chromium (VI) ions by mowital B30H resin immobilized activated sludge in a packed bed: comparison with granular activated carbon; *Process Biochem*.; **2002,** 38, 175–186.

Aoyama, M.; Sugiyama, T.; Doi, S.; Cho, N. S. and Kim, H.E.; Removal of hexavalent chromium from dilute aqueous solution by coniferous leaves; *Holzforschung;* **1999,** 53, 365–368.

Aoyama, M. and Tsuda, M.; Removal of Cr(VI) from aqueous solutions by larch bark; *Wood Sci. Technol*; **2001,** 35 (5), 425–432.

Ashkenazy, R.; Gottlieb, L.; and Yannai, S.; Characterization of acetone-washed yeast biomass functional groups involved in lead biosorption; *Biotechnol. Bioeng*.; **1997,** 55, 1–10.

CPCB; Pollution Control Acts, Rules, and Notification issued hereunder; Central Pollution Control Board; Ministry of Environment and Forests; New Delhi; **1998,** 501, 311–312.

Babel, S. and Kurniawan, T. A.; Cr(VI) removal from synthetic wastewater using coconut shell charcoal and commercial activated carbon modified with oxidizing agents and/or chitosan; *Chemosphere;* **2004,** 54 (7), 951–967.

Dakiky, M.; Khamis, M.; Manassra, A. and Mer'eb, M.; Selective biosorption of chromium(VI) in industrial wastewater using low-cost abundantly available biosorbent; *Adv. Environ. Res*; **2002,** 6 (4), 533–540.

Feng, N.; Guo, X. and Liang, S.; Biosorption study of copper(II) by chemically modified orange peel; *J. Hazard. Mater*.; **2009,** 164(2–3), 1286–1292.

Garg, V. K.; Gupta, R.; Yadav, A. B. and Kumar, R. D., Dye removal from aqueous solution by biosorption on treated sawdust; *Bioresour. Tech.,* **2003**, 89 (2), 121–124.

Gundogdu, A.; Ozdes, D.; Duran, C.; Bulut, V.N.; Soylak, M. and Senturk, H.B.; Biosorption of Pb(II) ions from aqueous solution by pine bark (*Pinus brutia Ten*.); *Chem. Eng. J;* **2009**, 153, 62–69.

Hamadi, N.K.; Chen, X.D.; Farid, M.M. and Lu, M.G.Q.; Biosorption kinetics for the removal of chromium (VI) from aqueous solution by biosorbents derived from used tyres and sawdust; *Chem. Eng. J.;* **2001**, 84, 95–105.

Jacques, R.A.; Lima, E.C.; Dias, S.L.P.; Mazzocato, A.C. and Pavan, F.A. Yellow passion fruit shell as biosorbent to remove Cr(III) and Pb(II) from aqueous solution; *Sep. Purif. Technol.;* **2007**, 57, 193–198.

Jain, M.; Garg, V.K. and Kadirvelu, K.; Chromium Removal from Aqueous System and Industrial Wastewater by Agricultural Wastes; *Bioremediation Journal;* **2013**,17 (1), 30–39.

Karthikeyan, T. ; Rajgopal, S. and Miranda L.R.; Chromium(VI) biosorption from aqueous solution by *Hevea Brasilinesis* sawdust activated carbon; *J. Hazard. Mater.;* **2005,** B124, 192–199.

Kan Carbon Pvt. Ltd.; Delhi road; Sampla; Haryana; India; 124501.

Mohan, D.; Singh, K.P.; Singh, V.K.; Removal of hexavalent chromium from aqueous solution using low-cost activated carbons derived from agricultural waste materials and activated carbon fabric cloth; *Ind. Eng. Chem. Res*.; **2005,** 44, 1027–1042.

Namasivayam, C. and Yamuna, R.T.; Biosorption of chromium(VI) by a low-cost biosorbent: biogas residual slurry; *Chemosphere*; **1995**, 30, 561–578.

Oliveira, E. A.; Montanher, S. F.; Andrade, A. D.; Nóbrega, J. A.; Rollemberg, M. C., Equilubrium studies for the sorption of chromium and nickel from aqueous solutions using raw rice bran; *Proc. Biochem.*; **2005,** 40, 3485–3490.

Pavan, F.A.; Lima, I.S.; Lima, E.C.; Airoldi, C. and Gushikem, Y.; Use of ponkan mandarin peels as biosorbent for toxic metals uptake from aqueous solutions; *J. Hazard. Mater*.; **2006**, 137, 527–533.

Perez Marin, A.B; Aguilar, M.I.; Meseguer, V.F.; Ortuno, J.F.; Saez, J. and Llorens, M.; Biosorption of chromium(III) by orange (*Citrus cinensis*) waste: Batch and continuous studies; *Chem. Eng.*; **2009,** 155, 199–206.

Sharma, D.C. and Forster, C.F.; A preliminary examination into the biosorption of hexavalent chromium using low-cost biosorbents; *Bioresour. Technol*; **1994**, 47 (3), 257–264.

Thomas, H.C.; Heterogeneous ion exchange in a flowing system; *J Am. Chem. Soc.*; **1944**, 66, 1446-1664**.**

Vaghetti, Julio C.P.; Lima, Eder C.; Royer, B.; da Cunha, B. M.; Cardoso, N. F.; Brasil, J. L. and Dias, S.L.P.; Pecan nutshell as adsorbent to remove Cu(II), Mn(II) and Pb(II) from aqueous solutions; *, J. Hazard. Mater.*; **2009,** 162, 270–280.

Vinodhini, V. and Dass, N.; Packed bed column studies on Cr(VI) removal from tannery wastewater by neem sawdust; *Desalination*; **2010, 264**, 9–14.

Visa, M.; Isac, L. and Duta, A.; Fly ash adsorbents for multi-cation wastewater treatment; *Applied Surface Science;* **2012**, 258, 6345– 6352.

Yu, L. J.; Shukla, S.S.; Dorris, K.L.; Shukla, A. and Margrave, J.L.; Biosorption of chromium from aqueous solutions by maple sawdust; *J. Hazard. Mater.*; **2003,** 100 (1–3), 53–63.

Chapter 4

Insight into the Mechanism of Pb^{2+} Biosorption from Synthetic and Lead Acid Batteries Wastewater

Contents

Abstract

This chapter explores the ability of five different combinations of two adsorbents (*Arachis hypogea* shell powder and *Eucalyptus sp*. saw dust) to remove Pb^{2+} from synthetic and lead acid batteries wastewater through batch and column mode. The effects of solution pH, adsorbent dose, initial Pb^{2+} concentration and contact time were investigated with synthetic solutions in batch mode. The FTIR study revealed that carboxyl and hydroxyl functional groups were mostly responsible for the removal of Pb^{2+} ions from test solutions. The kinetic data was found to follow pseudo-second-order model with correlation coefficient of 0.99. Among Freundlich and Langmuir adsorption models, the Langmuir model provided the best fit to the equilibrium data with maximum adsorption capacity of 270.2 mg g^{-1}. Column studies were carried out using lead acid batteries wastewater at different flow rates and bed depths. Two kinetic models viz., Thomas and Bed depth service time model were applied to study the breakthrough curves and breakthrough service time. The Pb^{2+} uptake capacity (q_e = 540.41 mg g^{-1}) was obtained using bed depth of 35.0 cm and a flow rate of 1.0 mL min^{-1} at 6.0 pH. The results from this study showed that adsorption capacity of agricultural residues in different combinations is much better than reported by other authors, authenticating that the prepared biosorbents has potential in remediation of lead contaminated waters.

Keywords: Lead acid batteries wastewater, point of zero charge, hydroxyl groups, Thomas model, and breakthrough service time.

4.1 Introduction

Industrial activities are principally responsible for generating large volume of effluents containing hazardous species (Gupta and Bhattacharyya, 2006). Among these hazardous species, the heavy metals ions are most toxic and are non biodegradable (Leyva-Ramos *et al.*, 2012). One of the heavy metals that have been a major focus in wastewater treatment is lead. It is quite toxic to humans as it interacts with the sulfhydryl group of proteins, resulting in disruption of the metabolism and biological activities of different proteins in the body. It impairs hemoglobin synthesis, cause damage to liver and kidneys as well as lead to neurological disorders (Markowitz, 2000). Hence the elimination of lead from wastewater in economic and proficient way is the need of the day.

In the present chapter, the biosorption of Pb^{2+} from synthetic and lead acid batteries wastewater was carried out through batch and column mode using five different combinations of *Eucalyptus sp.* saw dust and *Arachis hypogea* shell powder. The influence of pH, adsorbent dose, initial metal ions concentration and contact time on biosorption of Pb^{2+} was performed in batch experiments. The ion exchange capacity and blocking of the functional groups of the biosorbent were done in order to study the mechanism of biosorption. In fixed bed column operations, lead acid batteries wastewater was treated using one of the five combinations and the data was analyzed using Thomas and Bed depth service time models.

4.2 Experimental section

4.2.1 Preparation of different combinations of the biosorbents

The *Eucalyptus sp.* saw dust (ESD) was mixed with *Arachis hypogea* shell powder (AHSP) in different wt % as mentioned in Table 1 to prepare the combinations (A to E). The combinations were prepared intentionally to enhance the biosorption capacity of the biosorbents for multi metal ion solutions, where the single biosorbent fails to biosorb all the metal ions up to an excellent (> 90) extent.

Table 1: Different combinations of *Eucalyptus sp.* saw dust (ESD) and *Arachis hypogea* shell powder (AHSP).

Combinations	Agricultural Residues (wt %)
A	ESD (10) + AHSP (90)
B	ESD (30) + AHSP (70)
C	ESD (50) + AHSP (50)
D	ESD (70) + AHSP (30)
E	ESD (90) + AHSP (10)

4.2.2 Batch studies

Batch trials for Pb^{2+} biosorption from synthetic solutions were carried out at different pH values viz., 1.0 to 8.0 by agitating 2.0 g/0.1 L of biosorbent dose of all the five combinations (A to E) with 200 mg L^{-1} initial Pb^{2+} concentration in 250 mL screw-cap conical flasks. The mixtures so obtained were agitated in orbital shaker at 225 rpm agitation speed for 300 min at 30 $^{\circ}$C. After every 30 min of agitation, 2.0 mL of the suspensions were filtered through Whatman no. 40 filter paper and the filtrates were analyzed using AAS. Under optimized pH, rpm and temperature the effect of biosorbent dose (0.5 g to 3.0 g), initial metal ion concentration (50 to 250 mg L^{-1}) and contact time (1 to 300 min) were studied. The percent of Pb^{2+} removal (*R%*) and the metal uptake capacities were calculated for each experiment using equation 1 and 2 as mentioned in chapter 2.

4.2.3 Characterization of lead acid batteries wastewater

Lead acid batteries wastewater was collected from Singh batteries manufacturer, Yamuna Nagar, Haryana, India. Analysis of the same is given in Table 2.

Table 2: Characteristics of the wastewater collected from lead acid battery manufacturer.

Concentration of heavy metal (mg L^{-1}) and anions					
Pb^{2+}	Fe^{2+}	Zn^{2+}	Cl^{-}	SO_4^{2-}	NO_3^{-}
645.15	88.20	5.23	175.85	105.42	496.28

pH = 2.5

4.2.4 Column studies using lead acid batteries effluent

Continuous flow experiments were conducted in glass columns having 50.0 cm length and 1.5 cm internal diameter. The packed columns were held vertically with the help of stands and clamps. To stabilize the process, before each run, 2.0 L deionized water adjusted to pH 6.0 was circulated through the columns for 12 h at a flow rate of 0.5 mL min^{-1} using peristaltic pump. The lead acid batteries wastewater containing Pb^{2+}, Fe^{2+} and Zn^{2+} metal ions with adjusted pH 6.0 was passed through the columns with different flow rates (1.0, 2.0 and 5.0 mL min^{-1}) till the concentration of all the metal ions reached to satisfy the Central pollution control board standards (CPCB, 1998). To measure the concentrations of the metal ions in the effluents of each column, 5.0 mL samples of the effluents were intermittently collected and analyzed using AAS. The percolation of the wastewater into each column was stopped as soon as the breakthrough point (BTP) in that particular column was achieved. The columns were recharged using 0.5 M HCl. Further the effect of different bed depths on the breakthrough curves was also investigated.

4.3 Results and Discussion

4.3.1 Characterization of the biosorbent (combination B)

4.3.1.1 FTIR analysis

In order to determine the main functional groups responsible for the biosorption of Pb^{2+} from the lead battery wastewater in column studies, the combination B was recovered from the column, dried and subjected to the FTIR studies. The recorder spectra have been compared as shown in Figure 1. The broad and intense peak at 3421 cm^{-1} was assigned to the presence of free or hydrogen bonded O–H groups (from carboxylic acids or alcohols) on the surface of the biosorbent. The band at 2929 cm^{-1} indicates symmetric or asymmetric C–H stretching vibration of aliphatic acids. Peak observed at 1639 cm^{-1} is the stretching vibration of C=O functional group and may be assigned to carboxylic acids that exists in with intermolecular hydrogen bond (Vaghetti *et al.,* 2009; Jacques *et al.,* 2007; Pavan *et al.,* 2006). The peak observed at 1524 cm^{-1} is assigned to C=C ring stretch of aromatic rings. Numerous bands ranging from 1315 to 1057 cm^{-1} refer to C–O bonding of phenols (Jacques et al., 2007). FTIR spectra of Pb^{2+} sorbed on combination B showed that the peaks expected at 3421, 2929, 1639,1524,1315 and 1057 cm^{-1} had shifted respectively to 3392, 2919, 1649,1510, 1281 and 1042 cm^{-1} respectively, due to Pb^{2+}

biosorption. These groups may function as proton donors, hence deprotonated hydroxyl and carbonyl groups may be involved in coordination with metal ions (Ashkenazy *et al.*, 1997).

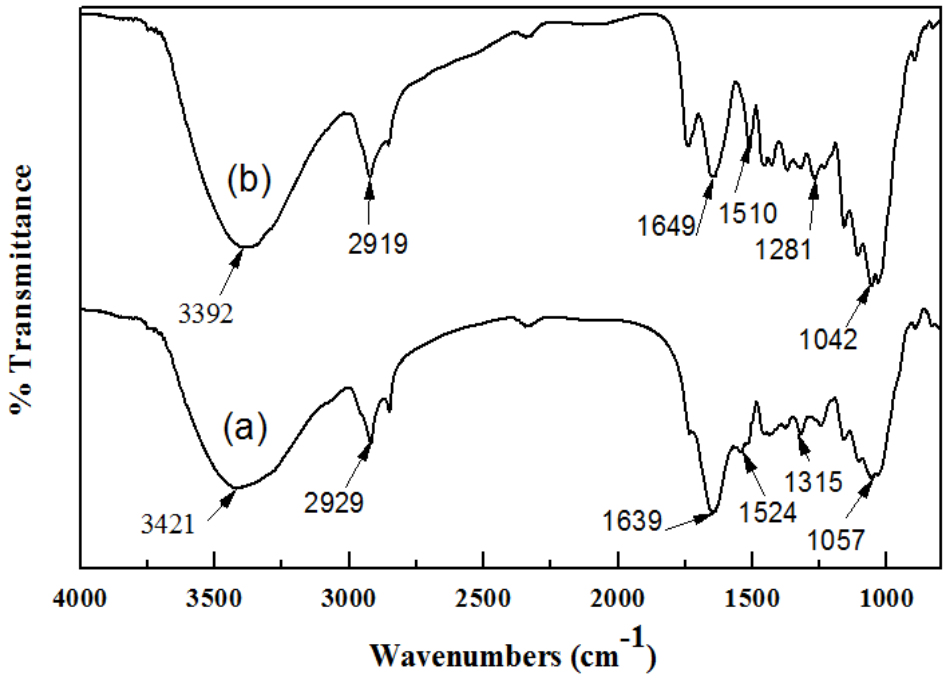

Figure 1: FTIR spectra: (a) before biosorption of Pb^{2+} and (b) after biosorption of Pb^{2+} on combination B.

4.3.1.2 SEM and EDX analysis

SEM along with EDX analysis was done for the characterization of the biosorbent as well as for the elucidation of the probable mechanism of biosorption. SEM images and EDX spectra obtained from fresh combination B and lead loaded combination B are shown in Figure 2. SEM images of fresh combination B (Figure 2a) revealed the nature of the biomass such as rough, uneven, porous with lots of ups and down and thus making possible for the biosorption of lead ions in different parts of the biomass. Lead loaded combination B, SEM image (Figure 2c), was comparably bit smoother, it may be due to the presence of lead on it. EDX analysis provides the elemental analysis of fresh combination B and lead loaded combination B. Figure 2b indicated the presence of C and O in blank biomass. EDX spectra Figure 2d revealed the additional signal of lead, which confirmed the binding of the metal ions to the surface of the biomass.

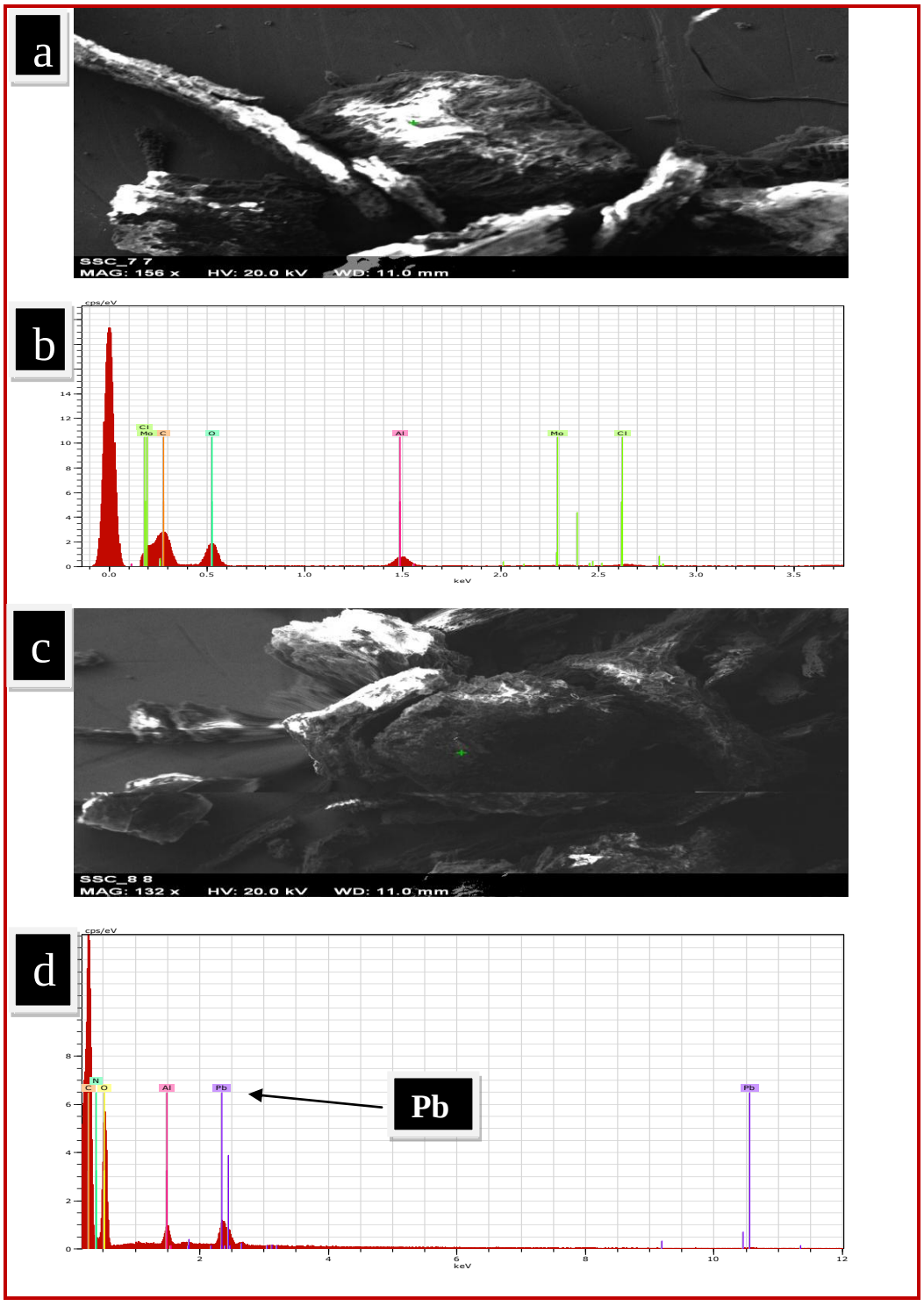

Figure 2: SEM and EDX images of combination B before (a, b) and after (c, d) biosorption of Pb^{2+}, respectively.

4.3.2 Batch studies

4.3.2.1 Effect of pH

The pH of the solution has a significant impact on the uptake of metal ions, since it determines the surface charge of the biosorbent, the degree of ionization and speciation of the metal ions (Kobya *et al.*, 2005; Boudrahem *et al.*, 2009; Machida *et al.*, 2005). In order to study the effect of pH on the biosorption of Pb^{2+} by all five combinations i.e. A to E, the batch equilibrium studies were carried out in the pH range of 1.0 to 8.0 as shown in Figure 3.

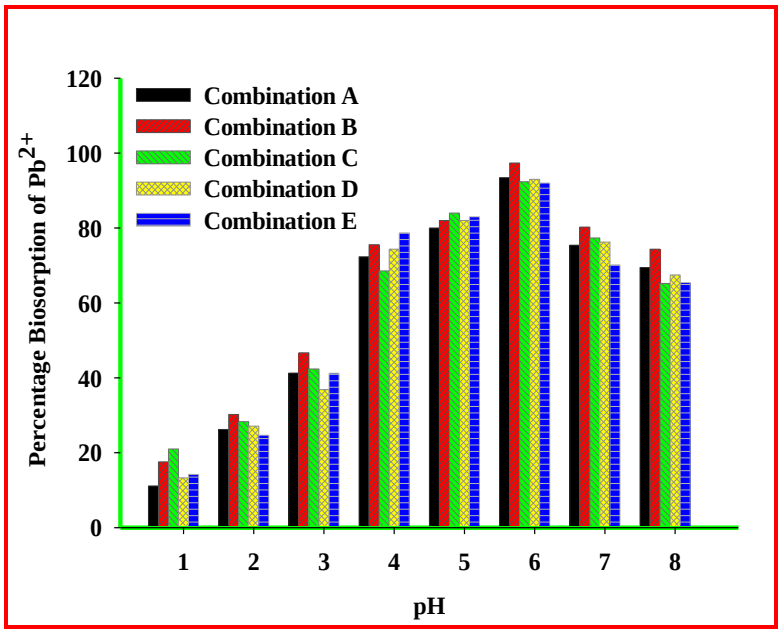

Figure 3: Effect of pH on biosorption Pb^{2+} on to different combinations A to E

This pH range was chosen to avoid metal solid hydroxide precipitation. The maximum biosorption of Pb^{2+} by all the combinations used were obtained at pH 6.0 and a significant decrease or increase in biosorption capacity was observed at pH values lower or higher than 6.0. This could be explained with the help of point of zero charge (pH_{PZC}) of the biosorbent. The point of zero charge (pH_{PZC}) is the pH value, at which the solid surface of the biosorbent has the net zero charge. The points of zero charges (pH_{PZC}) of all the five combinations (A to E) were experimentally found to be at pH 5.1, 4.9, 4.5, 5.3 and 5.5 respectively (Figure 4) according to the procedure mentioned in chapter 2.

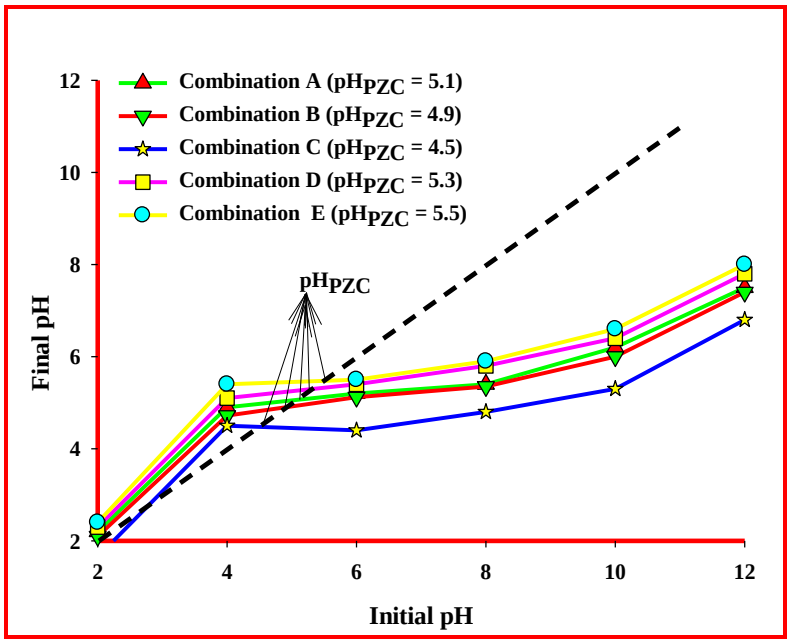

Figure 4: Determination of point zero charge (pH_{PZC}) of all the combinations A to E.

Further, at pH> pH_{PZC}, the combinations became negatively charged and the metal species were positively charged. Under such circumstances, the electrostatic attraction between the positively charged metal ions and the negatively charged biosorbent (combinations A to E) surface increased resulting enhanced biosorption of the metal ions from the solution. On the other hand, at pH< pH_{PZC}, the surface of the biosorbent became positively charged resulting in a decrease in the metal ions biosorption apparently due to the higher concentration of H^+ ions in the solution that were challenging the positively charged metal for the active sites. The minimal biosorption was seen at pH >6.0. It was due to the metal (Pb^{2+}) hydrolysis and precipitation, so the subsequent studies were conducted at pH 6.0.

4.3.2.2 Effect of contact time and biosorption kinetics

The effect of contact time on biosorption of lead on different combinations were studied in the time range of 1-300 min by using 200.0 mg L^{-1} of Pb^{2+} solutions at pH 6.0 with 2.0 g/0.1 L of the biosorbent. The mixtures were agitated at 30°C with 225 rpm and the samples were taken after every 20 min, filtered and analyzed by AAS. As shown in Figure 5, about 80 % biosorption

of Pb^{2+} took place in first 60 min and then it continued to increase at a lower rate until greater than 92 %, biosorption was achieved for all the five combinations after 300 min of contact time.

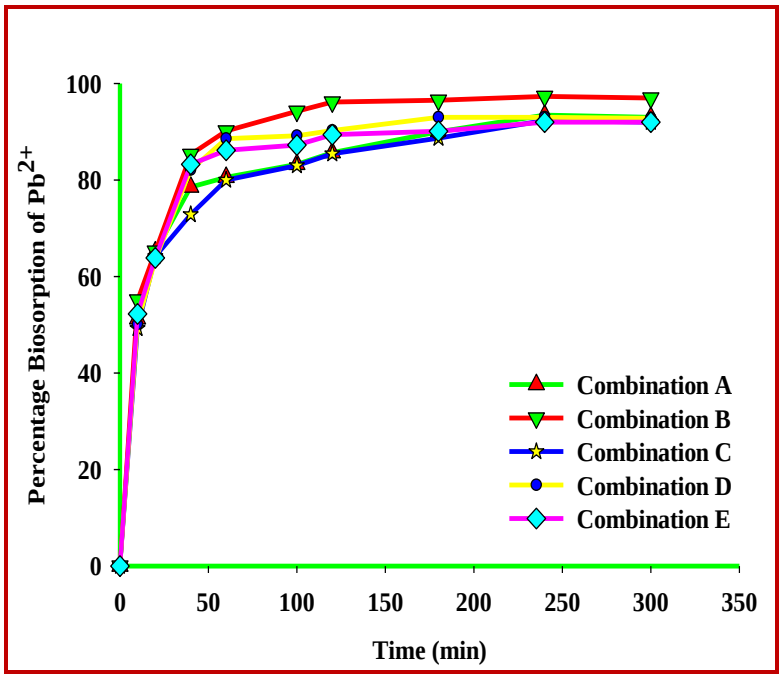

Figure 5: Effect of contact time on biosorption Pb^{2+} onto different combinations A to E.

The rate of percent metal removal was higher in the beginning due to the availability of the vacant specific sites for metal ion binding. It could be mentioned here that the two stage biosorption mechanism was operating which involved a very rapid biosorption for shorter duration in initial stage followed by slow one for longer duration (Boudrahem *et al*., 2009). Based on these results, a contact time of 300 min was assumed to be suitable for the subsequent biosorption experiments.

The biosorption kinetics of Pb^{2+} by all five combinations was studied using the pseudo first and pseudo-second-order kinetic models as mentioned in chapter 2. The straight line in the graph of $ln\ (q_e - q_t)$ versus t and t/q_t versus t suggests the applicability of both the kinetic models. The value of kinetic constants and regression coefficient are presented in Table 3. Among the two kinetic models used, the best fittings of the experimental values were obtained (R^2 = 0.99) by following the pseudo-second-order kinetic model. This implies that the reaction is due to

chemical sorption involving valency forces through sharing or exchange of electrons between biosorbent and biosorbate (Ho, 2006).

Table 3: The pseudo-first-order and second-order-kinetic model for Pb^{2+} biosorption on different combination (A–E) at pH 6.0.

Different combinations	pseudo-first-order			pseudo-second-order		
	k_1	q_e	R^2	k_2	q_e	R^2
A	0.010	4.19	0.93	0.058	192.30	0.99
B	0.046	5.17	0.94	0.024	192.30	0.99
C	0.008	4.20	0.93	0.058	192.30	0.99
D	0.009	3.79	0.76	0.039	192.30	0.99
E	0.007	3.81	0.77	0.039	188.67	0.99

4.3.2.3 Effect of biosorbent dose, initial Pb^{2+} concentration and isotherm modeling

The influence of the biosorbent dose and initial Pb^{2+} concentrations on the present biosorption process was studied by employing Pb^{2+} solutions with initial concentrations in the range of 50–250 mg L^{-1}, and biosorbent dose in the range of 0.5–3.0 g/0.1 L at pH 6.0. Concentrations of Pb^{2+} from each batch were measured at equilibrium. Both Langmuir and Freundlich isotherms were applied to the data obtained and it was seen that increase in biosorbent dose from 0.5–3.0 g/0.1 L resulted in a rapid increase in the uptake of Pb^{2+} ions. But no significant increase in biosorption was found beyond 2.0 g/0.1 L. It could be due to the presence of excess/surplus metal binding sites on the combination B than the available Pb^{2+} ions. Or in other words decrease in biosorption capacity could be due to the overlapping of the biosorption sites as a result of overcrowding of the biosorbent particles when the biosorbent dosage is increased above 2.0 g/0.1 L. This imposed a screening effect on the dense outer layer of the biosorbent, thereby shielding the binding sites from metals as explained by Garg *et al*., (2003), Babel and Kurniawan, (2004). However, when the initial concentration of Pb^{2+} was continuously increased from 50.0 to 250 mg L^{-1} using the fixed amount of the biosorbent dose (2.0 g/0.1 L), the biosorption of the Pb^{2+} was found to decrease due to the early saturation of the binding sites of the biosorbent at high Pb^{2+} concentration. This may also be due to the increase in the number of Pb^{2+} ions competing for available binding sites of the biosorbent.

The Langmuir and Freundlich constants and their correlation coefficients (R^2) evaluated from these isotherms for Pb^{2+} are given in Table 4.

Table 4: Langmuir and Freundlich isotherm constants and correlation coefficients for the biosorption of Pb^{2+} on combination B at pH 6.0

Wt. of combination B (g)	Langmuir			Freundlich		
	q_{max} (mg g^{-1})	b (L mg^{-1})	R^2	n (L g^{-1})	K_F	R^2
0.5	222.2	0.123	0.97	3.92	4.13	0.98
1.0	238.1	0.143	0.96	4.83	4.42	0.93
1.5	250.0	0.286	0.99	4.61	4.55	0.99
2.0	270.2	0.840	0.99	4.86	4.73	0.84
2.5	263.2	1.15	0.94	2.58	4.01	0.92
3.0	222.2	1.28	0.99	2.71	3.99	0.92

The sorption characteristics of Pb^{2+} on the combination B followed more closely the Langmuir isotherm model with q_{max}=270.2 mg L^{-1} than the Freundlich isotherm model. It suggests that sorption of metal ions occurs uniformly by mono-layer adsorption on a homogenous surface, with no interaction between the adsorbed ions (Freundlich, 1906). This observation is further supported by the assessment of the respective correlation coefficients values which are a measure of how well the theoretical values match with the experimental data. Also the values of R_L were calculated with Pb^{2+} concentrations in the range of 50.0–250.0 mg L^{-1} and were found to fall between zero and one (Singh *et al*., 2008; Vinodhini and Das, 2010) which is again an indication of the favorable biosorption for Pb^{2+} on the all the five combinations used. The value of *n*, which is related to the distribution of bonded ions on biosorbent surface, represents beneficial biosorption if it is between 1 and 10 (Kadirvelu and Namasivayan, 2000). The value of n was between 1 and 10, indicating that the biosorption of Pb^{2+} was beneficial under studied conditions.

4.3.2.4 Combination B as the better biosorbent

The biosorption capacities of various biosorbents used for Pb^{2+} biosorption are given in Table 5. The comparison between the present study and with that of the literature reported one showed

that agricultural residues used in combination in the current study exhibit very good sorption efficiency.

Table 5: Comparison of biosorption capacities of Pb^{2+} on different biosorbents

Biosorbents	Mass of biosorbent (g L^{-1})	pH	Biosorption capacity (mg g^{-1})	References
Barely	6.25	6.0	23.20	Pehlivan *et al*., 2009.
Snowberry	4.0	5.5	62.16	Akara *et al.*, 2009.
Rice husk	3.0	6.0	58.1	Krishnani *et al.*, 2008.
Hazelnut shell	10.0	6.0	28.18	Pehlivan *et al*., 2009.
Pecan nutshell	4.0	5.5	211.7	Vaghetti *et al.*, 2009.
Macro fungus	4.0	5.0	38.4	Sari and Tuzen, 2009.
Sawdust	7.5	5.0	88.49	Naiya *et al.*, 2008.
Pinus silvestris sawdust	1.0	5.0	22.22	Taty Costodes *et al.*, 2003.
Combination B	2.0	6.0	270.2	Present work.

The maximum biosorption capacity (q_{max}) was found to be 270.2 mg for Pb^{2+} when 2.0/.01 L of the combination B was used at pH 6.0 and this value is relatively better than most of the earlier reported results as given in Table 5.

4.3.2.5 The ion exchange capacity of the combination B

Among all the five combinations studied, combination B showed maximum removal of lead metal ions in the batch studies and the ion exchange capacity of the same was evaluated. 1.0 g of the combination B was mixed with 100 mL Pb^{2+} solution in a conical flask with 200 mg L^{-1} initial concentration at pH 6.0. The mixture so obtained was agitated in orbital shaker at 225 rpm speed for 300 min. After 300 min the mixture was centrifuged at 5000 rpm for 10 min and analyzed for the release of Na^{+}, K^{+}, Ca^{2+} and Mg^{2+} and unabsorbed Pb^{2+} ions in the solution.

It was observed (Table 6) that 91 % removal of Pb^{2+} was due to the ion exchange process involving Na^{+}, K^{+}, Ca^{2+} and Mg^{2+}. The remaining 9 % biosorption of the same could be due to its ion exchange with protons, as pH of the supernatant was found to decrease at equilibrium. Hence, it may be concluded that the sorption process for Pb^{2+} on combination B occurs primarily through ion exchange mechanism involving the replacement of alkali and alkaline earth metals. The protons bound to native carboxylate groups are also involved in ion exchange

process but to the lesser extent. Similar type of ion exchange mechanism was reported and dicussed for other agrowaste materials (Naiya *et al.*, 2008; Iqbal *et al.*, 2009).

Table 6: Release of Na^+, K^+, Mg^{2+}, Ca^{2+} and H^+ after sorption of Pb^{2+} by the combination B.

Metal ion	Total metal biosorbed (mg g^{-1})	Total cations and protons released in mg g^{-1} (%)				
		Na^+	K^+	Mg^{2+}	Ca^{2+}	H^+
Pb^{2+}	138.4	26.2 (18.9)	28.5 (20.6)	22.5 (16.2)	49.3 (35.6)	12.0 (8.7)

4.3.2.6 Blocking of functional groups and computation of their role in metal biosorption

To study the role of carboxyl (–COOH) and hydroxyl (–OH) groups in metal biosorption, they were blocked in combination B. Carboxyl group was protected by treating combination B with methanol (Gardea-Torresdey *et al.,* 1990) as given in equation 1.

$$RCOOH + CH_3OH \rightarrow RCOOCH_3 + H_2O \quad (1)$$

To block the carboxylic group, 9.0 g of the combination B was treated with CH_3OH (633 mL) in presence of 5.4 mL HCl (5.0 M), with continuous stirring on magnetic stirrer at 225 rpm for 6 h. The combination B residue was then separated by centrifugation and washed thrice with deionised water to remove excess CH_3OH and HCl. The final biomass obtained was dried in hot air oven at 105 $^{\circ}$C for 12 h and stored in for further use.

Hydroxyl group of the biosorbent was protected by treating combination B with formaldehyde (Chen and Yang, 2006) as given in equation 2.

$$2R-OH + HCHO \rightarrow (R-O)_2CH_2 + H_2O \quad (2)$$

In a typical experiment, 5.0 g of the combination B was treated with HCHO (100 mL) under agitation on magnetic stirrer at 225 rpm for 6 h. The residual biomass was then separated and further processed and stored following the same method as mentioned for the carboxylic group protection.

The carboxyl (–COOH) and hydroxyl (–OH) groups blocked combination B was further tested for Pb^{2+} biosorption. It was observed that the metal removal capacity was badly inhibited when carboxyl groups were blocked and a decrease of 70.5% in the biosorption of Pb^{2+} was observed.

It clearly indicates that the carboxyl groups have the major role in the process of biosorption. On the other hand 29.5% of Pb^{2+} was removed by combination B, even after the blockage of carboxyl groups, indicating that other functional groups were also involved in biosorption of metal ions. To support the presence of other functional groups on the biosorbent, sorption of Pb^{2+} by combination B was carried out after blocking the hydroxyl groups. The biosorption capacity of the hydroxyl group blocked biosorbent B, was found to decrease 32.8% for the removal of Pb^{2+}. Further, the total metal uptake capacity of carboxyl and hydroxyl group blocked biosorbent together was found to be almost equal to the total metal ions uptake by unblocked biosorbent as shown in Table 7.

Table 7: Biosorption of Pb^{2+} with and without blocked functional groups on the combination B

Metal ion	Biosorption on UCB* mg g^{-1}	Biosorption on CGBCB** mg g^{-1} (%)	Decrease in metal sorption (%)	Biosorption on HGBCB*** mg g^{-1} (%)	Decrease in metal sorption (%)
Pb^{2+}	138.40	40.83 (29.5)	70.5	93.0 (67.2)	32.8

**Unblocked combination B, **Carboxyl groups blocked combination B,*

**** Hydroxyl groups blocked combination B*

These results along with the functional groups study of biosorbent by the FTIR technique (Figure 2) supported that carboxyl and hydroxyl groups are mainly responsible for uptake of Pb^{2+} by combination B.

4.3.2.7 Desorption studies

The 15.0 g of the combination B loaded with Pb^{2+} was collected and dried in an electric hot air oven at 105 $^{\circ}$C for 12 h. 1.0 g of it was mixed with each 100 ml of HCl with varying concentration (0.1 to 0.5 M) in 250 mL screw cap conical flasks. The mixtures so obtained were agitated in orbital shaker at 225 rpm speed for 300 min at 30 $^{\circ}$C. After 300 min of agitation, the suspensions were filtered through Whatman no. 40 filter paper and the filtrates were analyzed for Pb^{2+} using AAS. Same procedure was repeated with H_2SO_4, HNO_3 and deionised water. It was observed that the desorption efficiency increased with increase in the concentration from 0.1 M

to 0.5 M of the desorption agents (HCl, H_2SO_4 and HNO_3) but the biosorbent started deteriorating at higher concentrations of the same. Furthermore it was noticed that HCl gave maximum desorption (99%) as compared to H_2SO_4 (83%), HNO_3 (74%) and H_2O (10%) as mentioned in Figure 6.

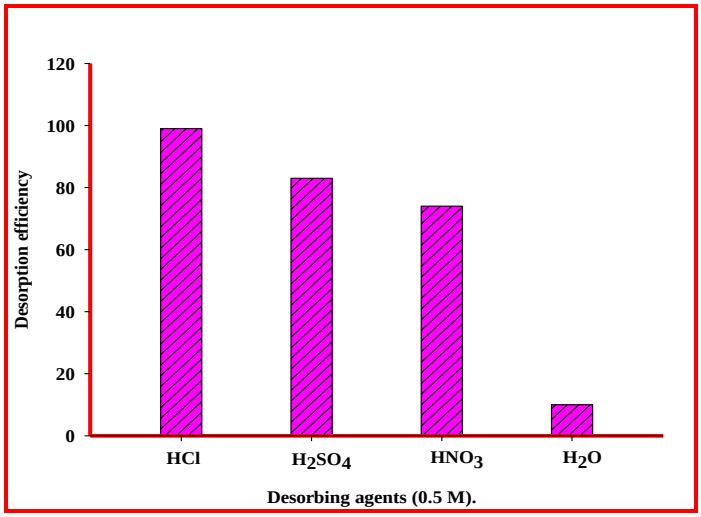

Figure 6: Desorption of Pb^{2+} by different desorbing agents.

The reusability of the combination B was tested in three consecutive biosorption-desorption cycles in batch mode and the results suggested that the combination B has the potential to be used repeatedly in Pb^{2+} biosorption studies without much significant loss in total biosorption capacity.

4.3.3 Column studies

4.3.3.1 Effect of flow rate

To explore the effect of flow rate on Pb^{2+} biosorption, the lead acid batteries wastewater (containing Pb^{2+}, Fe^{2+} and Zn^{2+}) was passed through the column with fixed bed depth of 25.0 cm (combination B) at pH 6.0 with different flow rates of 1.0, 2.0 and 5.0 mL min^{-1}.

As anticipated, an increase in flow rate from 1.0 to 5.0 mL min^{-1} (Figure 7) causes a diminution in breakthrough point and column exhaustion times, and as a result, the curves became steeper with shorter mass transfer zone (Vinodhini and Das, 2010).

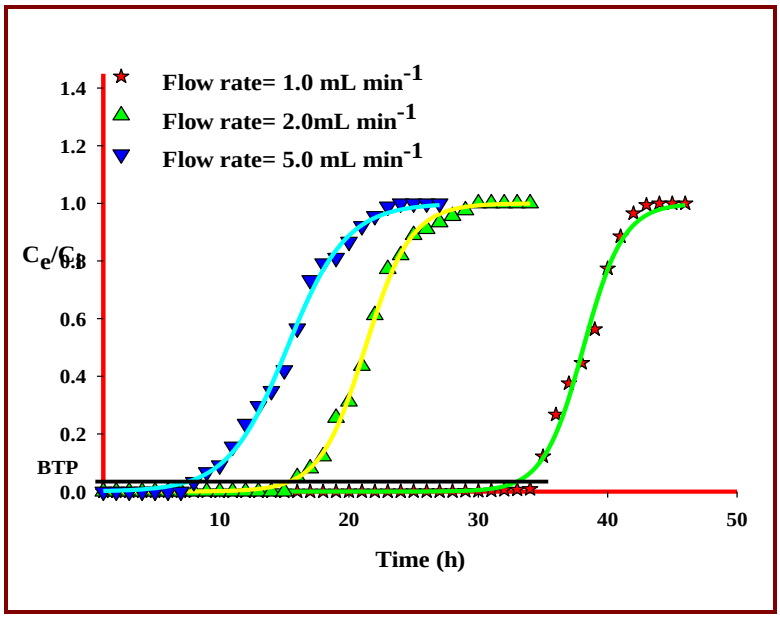

Figure 7: Effect of flow rates on metal biosorption from lead acid batteries wastewater on combination B packed column at pH 6.0.

This behavior could be due to insufficient residence time of metal solution which restricted the contact of the same to the biosorbent. Along with this, at higher flow rates the metals ions did not have enough time to diffuse into the biosorbent and they depart the column before equilibrium occurred resulting in low metal uptake, hence earlier breakthrough curves. On the other hand, at lower flow rates the residence time of the metal solution in the column was increased and as a consequence metal ions have enough time to diffuse into the biosorbent through intra-particle diffusion giving the late breakthrough curves.

Thomas model was applied to the data obtained and the value of k_{TH} and q_e were determined from the plot of C_e/C_i against time t. The value of the regression coefficient (R^2>0.99) as given in Table 8.0 indicated that the model describes the column performance data very well for the biosorption of Pb^{2+}, Fe^{2+} and Zn^{2+} in all three sorption cycles. It was also found that the experimental and model predicted normalized values at experimental conditions were very close. Further the metal uptake capacity found to decrease (q_e= 512.45 to 204.74 mg g^{-1}) in the successive cycles where as Thomas rate constant did not change significantly. This behavior was primarily attributed to gradual deterioration and depletion of binding sites caused by the acidic elution (Vinodhini and Das, 2010) and continuous usage or it might be due to blocking of the

active sites for solute uptake by the organic moieties present in the lead batteries effluents (Singh *et al*., 2008; Vinodhini and Das, 2010). The effluent from first cycle showed complete biosorption of all three metals ions satisfying the CPCB standards and making that water fit for reuse.

Table 8: Thomas model parameters for metal biosorption from lead acid batteries wastewater on combination B at different flow rates

R (mL min^{-1})	S (g)	k_{Th} (mL $min^{-1}mg^{-1}$)	q_e (mg g^{-1})	R^2	*BTP (h)*
1.0	12.0	0.001	512.45	0.99	33.0
2.0	12.0	0.009	285.76	0.99	15.0
5.0	12.0	0.007	204.74	0.99	8.0

4.3.3.2 Effect of bed depth

The effect of bed depth in continuous biosorption experiments were performed, at three different bed depths of 25.0, 30.0 and 35.0 cm, achieved by taking 12.0, 14.0 and 16.0 g of the combination B. The flow rate of the lead acid batteries wastewater was kept constant at 1.0 mL min^{-1}. As shown in Figure 8, the shapes and gradient of the breakthrough curves changes with the decrease in bed depth from 35.0 to 25.0 cm. The metal ion concentration in the effluent was found to increase as the breakthrough time was reached and same was indicated by the sharp increase of the slope in each of the curves. The breakthrough time of 35.0 h was observed when the column of low bed depth of 25.0 cm was used for the biosorption study of metal ions (Pb^{2+}, Fe^{2+} and Zn^{2+}) from wastewater. This observation could be explained by considering the fact that with low bed depth, less biosorbent surface area, the metal ions do not have enough binding sites to bind, resulting the earlier breakthrough time. On increasing the bed depth from 25.0 to 35.0 cm the breakthrough time was found to increase from 35.0 to 47.0 h and metal uptake capacity q_e from 512.45 to 540.41 mg g^{-1} (Table 9).

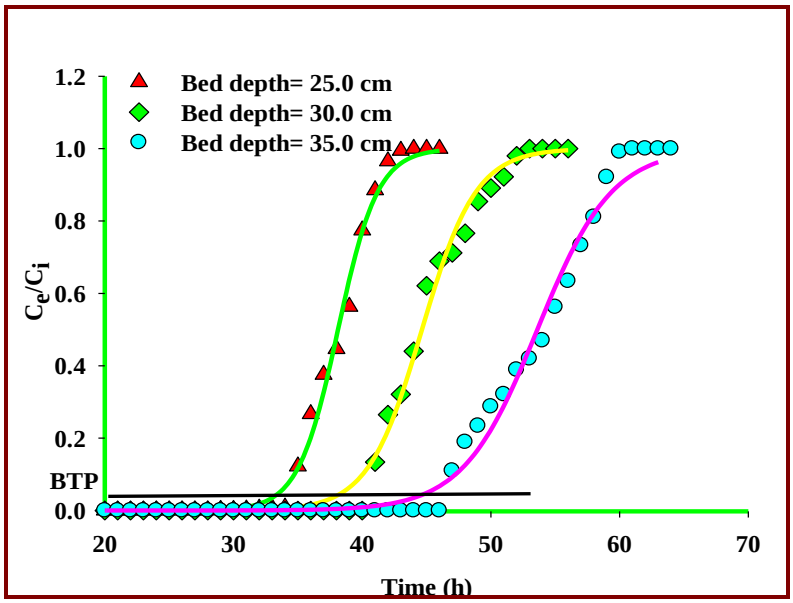

Figure 8: Effect of bed depths on metal biosorption from lead acid batteries wastewater on combination B packed column at pH 6.0.

This may be due to increase in the biosorbent surface area, enhancing the number of binding sites with increase in bed depth of the column, giving higher values of the breakthrough time and metal up take capacity.

Table 9: Thomas model parameters for metal biosorption from lead acid batteries wastewater on combination B at different bed depths.

R (mL min^{-1})	S (g)	k_{Th} (mL $min^{-1}mg^{-1}$)	q_e (mg g^{-1})	R^2	*BTP*
1.0	12.0	0.001	512.45	0.99	35.0
1.0	14.0	0.007	514.37	0.99	41.0
1.0	16.0	0.005	540.41	0.99	47.0

The Bed depth service time model was applied to the data obtained using different bed depths to study the relationship between bed depth (Z) and breakthrough service time (t_b).

A plot of t_b versus Z at flow rate of 1.0 mL.min^{-1}was linear (R^2= 1.0) as shown in Figure 9, indicating the validity of BDST model for the present system.

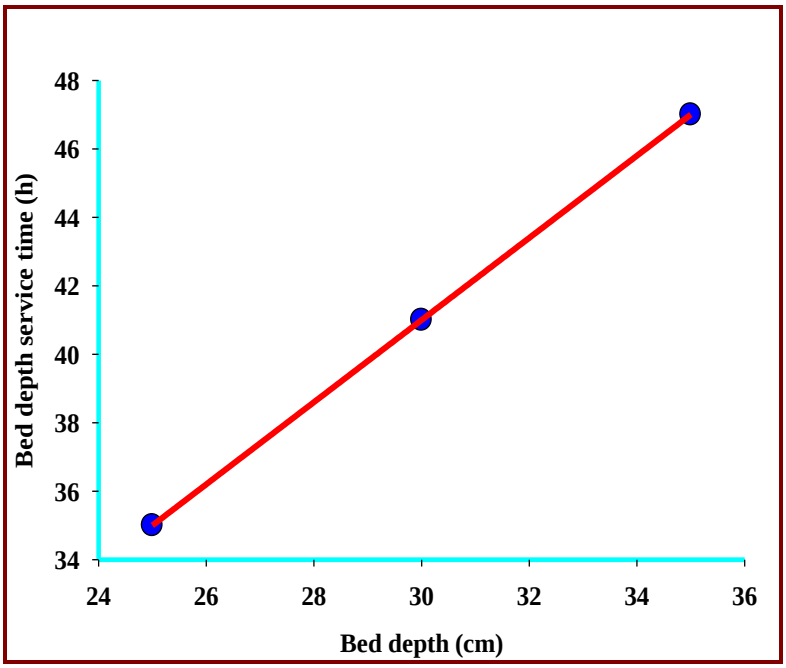

Figure 9: Plot between bed depth service time and bed depth of combination B for biosorption of metal ions from lead acid batteries wastewater.

The values of biosorption capacity N_o and rate constant K_a were evaluated from the slope and intercept of the plot respectively and are given in Table 9.

Table 9: Bed depth service time model parameters for biosorption of metal ions from lead acid batteries wastewater.

Slope	Intercept	N_o (mg L^{-1})	K_a (L mg^{-1} h^{-1})	R^2
1.200	5.00	774.18	0.0006	1.0

The value of K_a could be used to describe the biosorption capacity of the column. A large value of K_a indicates that even a short bed could avoid the breakthrough, but as K_a decreases a longer bed is required (Singh and Ali, 2012) for maximum biosorption of the metal ions. In present study, the low value of K_a indicated that the columns with longer bed depth are required for maximum biosorption of metal ions from industrial wastewater.

4.4 Conclusions

The chapter has demonstrated that agricultural residues viz *Arachis hypogea* shell powder and *Eucalyptus sp.* saw dust used in five different combinations have shown excellent potential for the biosorption of Pb^{2+} from synthetic and lead acid batteries effluent. The biosorption process was a function of pH, biosorbent dose, initial metal ion concentration and contact time. The effective pH for Pb^{2+} removal was found to be 6.0. Biosorption kinetics was found to follow pseudo-second-order kinetic model and the equilibrium sorption data are satisfactorily fitted to Langmuir isotherm. Among the five different combinations used, combination B showed maximum biosorption capacity (q_{max} = 270.2 mg g^{-1}) in batch mode. FTIR spectra analysis of the same showed that the carboxyl and hydroxyl groups were the principal functional groups responsible for sorption of Pb^{2+} ions. The chemical blocking of the carboxyl and hydroxyl groups verified their participation in the metal sorption process. Further the discharge of nearly equal amount of Na^{+}, K^{+}, Ca^{2+}, Mg^{2+} and H^{+} during the uptake Pb^{2+} ions showed that the biosorption process was entirely ion exchange.

The combination B was further used in column studies for treating lead acid batteries effluent. Thomas and BDST models were applied to the data obtained in column studies and the biosorption behavior and biosorption capacity was evaluated. The metal uptake capacity was found to be maximum (q_e = 540.4 mg g^{-1}) at flow rate of 1.0 mL min^{-1} with 35.0 cm bed depth. Further increase in flow rate and decrease in bed depth resulted decrease in metal uptake capacity. Present study reveals that the biosorbents used in combinations are quite effective for the removal of different metal ions from the lead acid batteries wastewater in continuous flow studies.

References

Ashkenazy, R.; Gottlieb, L.; and Yannai, S.; Characterization of acetone-washed yeast biomass functional groups involved in lead biosorption; *Biotechnol. Bioeng.*; **1997**, 55, 1–10.

Akara, S.T.; Gorgulu, A.; Anilan, B.; Kaynak, Z. and Akara, T., Investigation of the biosorption characteristics of lead(II) ions onto Symphoricarpus albus batch and dynamic flow studies; *J. Hazard. Mater.*; **2009**,165, 126–133.

Babel, S. and Kurniawan, T. A.; Cr(VI) removal from synthetic wastewater using coconut shell charcoal and commercial activated carbon modified with oxidizing agents and/or chitosan; *Chemosphere;* **2004**, 54 (7), 951–967.

Boudrahem, F.; Aissani-Benissad F. and Aı¨t-Amar, H.; Batch sorption dynamics an equilibrium for the removal of lead ions from aqueous phase using activated carbon developed from coffee residue activated with zinc chloride; *Journal of Environmental Management;* **2009**, 90, 3031–3039.

Chen, J.P. and Yang, L., Study of a heavy metal biosorption onto raw and chemically modified Sargassum sp. via spectroscopic and modeling analysis; *Langmuir;* **2006**, 22, 8906–8914.

CPCB; Pollution Control Acts, Rules, and Notification issued hereunder; Central Pollution Control Board; Ministry of Environment and Forests; New Delhi; **1998,** 501, 311–312.

Freundlich, H.M.F; Over the biosorption in solution; *J. Phys. Chem.*; **1906**, 57, 385–470

Gardea-Torresdey, J.; Becker-Hapak, M.K.; Hosea, J.M. and Darnall, D.W.; Effect of chemical modification of algal carboxyl groups on metal ion binding; *Environ. Sci. Technol.*; **1990,** 24, 1372–1378.

Garg, V. K.; Gupta, R.; Yadav, A. B. and Kumar, R. D.; Dye removal from aqueous solution by biosorption on treated sawdust; *Bioresour. Tech.;* **2003**, 89 (2), 121–124.

Gnanasambandam, R. and Protor, A.; Determination of pectin degree of esterification by diffuse reflectance Fourier transform infrared spectroscopy; *Food Chem.;* 2000, 68, 327–332.

Guibaud, G.; Tixier, N.; Bouju, A. and Baudu, M.; Relation between extracellular polymers composition and its ability to complex Cd, Cu and Pb; *Chemosphere;* **2003**, 52, 1701–1710.

Gupta, S.S and Bhattacharyya , K.G; Removal of Cd(II) from aqueous solution by kaolinite, montmorillonite and their poly(oxo zirconium) and tetrabutylammonium derivatives; *J. of Hazard. Mater.;* **2006**, B128, 247–257.

Ho, Y-S.; Review of second-order models for adsorption systems; *J. of Hazard. Mater.;* **2006**, B136, 681–689.

Hutchins, R.A.; New method simplifies design of activated carbon system; *Chem. Eng.*; **1973**, 80, 133–135.

Iqbal, M.; Saeed, A. and Zafar, S.I; FTIR spectrophotometry, kinetics and adsorption isotherms modeling, ion exchange, and EDX analysis for understanding the mechanism of Cd^{2+} and Pb^{2+} removal by mango peel waste; *J. Hazard. Mater*.; **2009**, 164, 161–171.

Jacques, R.A.; Lima, E.C.; Dias, S.L.P.; Mazzocato, A.C. and Pavan, F.A.; Yellow passion fruit shell as biosorbent to remove Cr(III) and Pb(II) from aqueous solution; *Sep Purif Technol*.; **2007** 57: 193–198.

Kadirvelu, K. and Namasivayan, C.; Agricultural by-products as metal biosorbents: sorption of lead(II) from aqueous solutions onto coir-pith carbon; *Environ. Technol.;* **2000**, 21 (10), 1091–1097.

Kobya, M.; Demirbas, E.; Senturk, E. and Ince. M.; Biosorption of heavy metal ions from aqueous solutions by activated carbon prepared from apricot stone; *Bioresour. Technol.;* **2005,** 96, 1518–1521.

Krishnani, K.K.; Meng, X.; Christodoulatos, C. and Boddu, V.M.; Biosorption mechanism of nine different heavy metals onto biomatrix from rice husk.; *J. Hazard. Mater.;* **2008**, 153, 1222–1234.

Leyva-Ramos, R.; Landin-Rodriguez, L.E.; Leyva-Ramos, S. and Medellin-Castillo N.A.; Modification of corncob with citric acid to enhance its capacity for adsorbing cadmium(II) from water solution; *Chemical Engineering Journal***; 2012**, 180, 113– 120.

Li, F.T.; Yang, H.; Zhao, Y. and Xu, R.; Novel modified pectin for heavy metal biosorption; *Chin. Chem. Lett;* **2007**, 18, 325–328.

Machida, M.; Yamazaki, R.; Aikawa, M. and Tatsumoto. H., Role of minerals in carbonaceous biosorbents for removal of Pb(II) ions from aqueous solution; *Separ. Purif. Technol.;* **2005**, 46, 88–94.

Markowitz, M.; Lead poisoning; *Pediatr Rev*.; **2000**, 10:327–335.

Naiya, T.K.; Bhattacharya, A.K. and Das, S.K.; Biosorption of Pb(II) by sawdust and neem bark from aqueous solutions; *Environ. Prog.*, **2008**, 27, 313–328.

Pavan, F.A.; Lima, I.S.; Lima, E.C.; Airoldi, C. and Gushikem, Y.; Use of ponkan mandarin peels as biosorbent for toxic metals uptake from aqueous solutions; *J. Hazard. Mater*.; **2006**,137: 527–533.

Pehlivan, E.; Altun, T. and Parlayıcı, S.; Utilization of barley straws as biosorbents for Cu^{2+} and Pb^{2+} ions; *J. Hazard. Mater*.; **2009**, 164, 982–986.

Sari, A. and Tuzen, M.; Kinetic and equilibrium studies of biosorption of Pb(II) and Cd(II) from aqueous solution by macrofungus (Amanita rubescens) biomass; *J. Hazard. Mater.;* **2009,**164, 1004–1011.

Singh, C.K.; Sahu, J.N.; Mahalik, K.K.; Mohanty, C.R.; Raj Mohan, B. and Meikap. B.C.; Studies on the removal of Pb(II) from wastewater by activated carbon developed from Tamarind wood activated with sulphuric acid; *J. Hazard. Mater*.; **2008,** 153, 221–228.

Singh, J. and Ali. A.; Kinetics, Thermodynamics and Breakthrough Studies of Biosorption of Cr(VI) Using Arachis hypogea Shell Powder; *Res. J. Chem. Environ*.; **2012**, 16 (1), 69–79.

Taty-Costodes, V.C.; Fauduet, H.; Porte, C. and Delacroix, A.; Removal of Cd(II) and Pb(II) ions; from aqueous solution by adsorption onto sawdust of Pinus sylvestris; *J. Hazard. Mater*.; **2003,** B105, 121–142.

Thomas, H.C.; Heterogeneous ion exchange in a flowing system; *J Am. Chem. Soc*.; **1944**, 66, 1446–1664.

Vaghetti, J.C.P.; Lima, E.C.; Royer, B.; da Cunha, B.M.; Cardoso, N.F.; Brasil, J.L. and Dias, S.L.P.; Pecan nutshell as biosorbent to remove Cu(II), Mn(II) and Pb(II) from aqueous solutions; *J. Hazard. Mater.*; **2009,** 162, 270–280.

Vinodhini, V. and Das. N.; Packed bed column studies on Cr(VI) removal from tannery wastewater by neem sawdust; *Desalination*; **2010**, 264, 9–14.

Chapter 5

Biosorption of Ni^{2+}, Cu^{2+} and Zn^{2+} Using Different Combinations of Agricultural Residues: Kinetics, Isotherm modeling and Mechanism *via* Chemical blocking

Abstract

In the previous chapter, we studied the removal of Pb^{2+} from synthetic solutions and lead acid batteries wastewater by using two biosorbents in different combinations. In this chapter we used three biosorbents viz., *Trifolium alexandrnium* biomass powder, *Arachis hypogea* shell powder and *Eucalyptus sp.* saw dust in four different combinations, for the removal of three metal ions (Ni^{2+}, Cu^{2+} and Zn^{2+}) from synthetic solutions and electroplating unit wastewater.

Batch biosorption experiments were conducted to study the effect of pH, contact time and initial metal concentration of Ni^{2+}, Cu^{2+} and Zn^{2+} for maximum biosorption. The biosorption kinetics of all the three metals were relatively fast attaining the equilibrium within 300 min and were best described by pseudo-second order kinetics. The biosorption equilibrium followed Freundlich and Langmuir biosorption isotherm models. The release of Na^{+}, K^{+}, Mg^{2+} Ca^{2+}, and H^{+} from the combination A with the equivalent uptake of Ni^{2+}, Cu^{2+} and Zn^{2+} supported ion exchange as the foremost mechanism of biosorption.

The column studies were carried out with electroplating wastewater containing Ni^{2+}, Cu^{2+} and Zn^{2+}. Thomas model was applied to evaluate the metal uptake capacity for Ni^{2+}, Cu^{2+} and Zn^{2+} and at the breakthrough points, the columns were recharged using 0.1 M HCl for three successive sorption-desorption cycles without much loss in the initial sorption capacity of the combination used.

Keywords: *Trifolium alexandrnium, Arachis hypogea, Eucalyptus sp.* saw dust, chemical blocking, ion exchange mechanism, successive sorption-desorption cycles.

5.1 Introduction

Heavy metals discharged from various industries such as metal plating, mining, tanneries, painting and car radiator manufacturing are the major cause of water contamination (Visa *et al*., 2012; Leyva-Ramos *et al*., 2012). Utmost attention is being paid to the health hazards presented by the existence of Ni, Cu, Zn, Pb, Cd and Hg. Most of them are extremely harmful to humans, animals and plants mainly due to their accumulation in the body (Jain *et al*., 2013; Qi and Aldrich, 2008). Moreover unlike organic pollutants, the majority of which are liable to biological degradation (Ali *et al*., 2012), metal ions do not degrade into harmless end products making them more dangerous. The removal of heavy metal in an effective manner from water and wastewater is, thus, ecologically very important.

In present chapter, the biosorption of Ni^{2+}, Cu^{2+} and Zn^{2+} from synthetic solution was done in batch mode using four different combinations, obtained by mixing *Trifolium alexandrnium* biomass powder, *Eucalyptus sp.* saw dust and *Arachis hypogea* shell powder. The influence of pH, initial metal ion concentration and contact time were studied and the experimental data obtained were evaluated and fitted using equilibrium isotherms and kinetic models. Mechanistic aspect of metal adsorption were investigated using different experimental approaches such as FTIR studies, chemical blocking of the functional groups and the release of alkali and alkaline earth metals during adsorption of the metal ions in an ion exchange process. Under optimized conditions, column studies were conducted using the electroplating industrial wastewater containing Ni^{2+}, Cu^{2+} and Zn^{2+} and metal uptake capacity was evaluated using Thomas model.

5.2 Experimental section

5.2.1 Preparation of different combinations

The dried *Trifolium alexandrnium* biomass powder (TABP), *Eucalyptus sp.* saw dust (ESD) and *Arachis hypogea* shell powder (AHSP) were mixed in different wt % as mentioned in Table 1 to prepare the various combinations (A to D).

Table 1: Different combinations of TABP, ESD and AHSP

Combinations	Agricultural residues (wt %)
A	TABP (30) + ESD (35) + AHSP (35)
B	AHSP (50) + ESD (50)
C	TABP (50) + AHSP (50)
D	ESD (50) + TABP (50)

5.2.2 Batch Studies

Batch experiments for Ni^{2+}, Cu^{2+} and Zn^{2+} biosorption from synthetic solutions were carried out at different pH values viz., 2.0 to 7.0 for all the metal ions by agitating 1.0 g each of the four different combinations (A to D) in 250 mL screw-cap conical flasks with 100.0 mL of metal ion solutions respectively. The mixtures so obtained were agitated in orbital shaker at 225 agitation speed for 300 min at 30 $^{\circ}$C. After every 20 min of agitation, 2.0 mL of the suspensions were centrifuged at 5000 rpm for 10 min and analyzed using AAS. Under optimized conditions, the effect of initial metal ion concentration from 25 – 200 mg L^{-1} and contact time from 1– 300 min was studied.

The percent of the metal removal (*R %)* was calculated for each experiment using equation 1and 2 as mentioned in chapter 2.

5.2.3 Column studies using electroplating industrial wastewater

Three glass columns (1, 2 and 3) having 50.0 cm length and 2.5 cm internal diameter were packed with bed depth of 12.0 cm by taking 10.0 gm of the combination A. The schematic diagram of the experimental set-up is shown in Figure 1. The process was operated in down-flow mode at room temperature (30 $^{\circ}$C). To stabilize the process, before each run, 1.0 L deionized water adjusted to pH 6.0, 5.0 and 4.0 was circulated through the columns 1, 2 and 3 respectively for 12.0 h at a flow rate of 2.5 mL min^{-1} using peristaltic pump. Then the electroplating wastewater containing Ni^{2+}, Cu^{2+} and Zn^{2+} with pH 6.0 was passed through the column 1 at the same flow rate. To measure the concentrations of the metal ions in the effluents of each column, 5.0 mL samples of the effluents were intermittently collected after 20 min and analyzed using AAS. The percolation of the wastewater into column 1 was stopped as soon as the breakthrough

point (BTP) in that particular column was achieved. Effluent of the column 1 was readjusted to pH 5.0 using a 0.1 M HCl solution and then passed through the column 2. On achieving the breakthrough point in column 2, finally the effluent pH was changed to 4.0 and was passed through the column 3.

The columns were regenerated using 0.1 M HCl. The wastewater was treated till the concentration of all the metal ions reached to satisfy the Central pollution control board standards (CPCB, 1998).

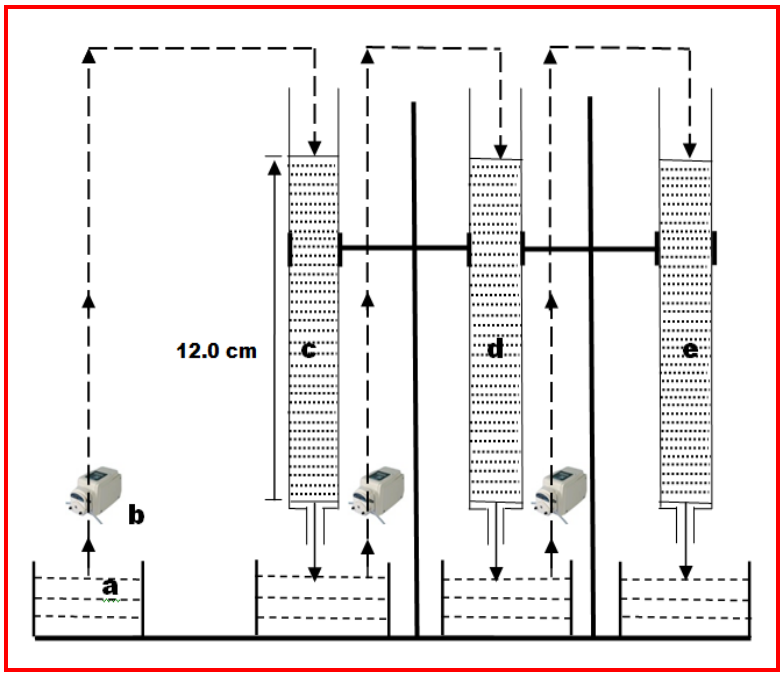

Figure 1: Schematic diagram of column experimental set-up for the removal of Ni^{2+}, Cu^{2+} and Zn^{2+} from electroplating wastewater (a = Electroplating wastewater containing Ni^{2+}, Cu^{2+} and Zn^{2+}, b = Peristaltic pump, c, d, e = column 1, 2 and 3 respectively).

5.2.4 Column regeneration studies

For desorption of Ni^{2+}, Cu^{2+} and Zn^{2+} bound on the biomass, 1.0 L of 0.1 M HCl solution was circulated through each column at flow rate of 2.5 mL min^{-1} for 12 h at the breakthrough point (BTP). Three cycles of sorption followed by desorption were carried out to assess the reusability potential of the biosorbents.

5.3 Result and Discussions

5.3.1 Characterization of the combination A by FTIR analysis

To study the main functional groups accountable for the biosorption of Ni^{2+}, Cu^{2+} and Zn^{2+} from the industrial wastewater in column studies, the combination A was recovered separately from the all three columns, dried and subjected to the FTIR studies. The recorded spectra were compared as shown in Figure 2.

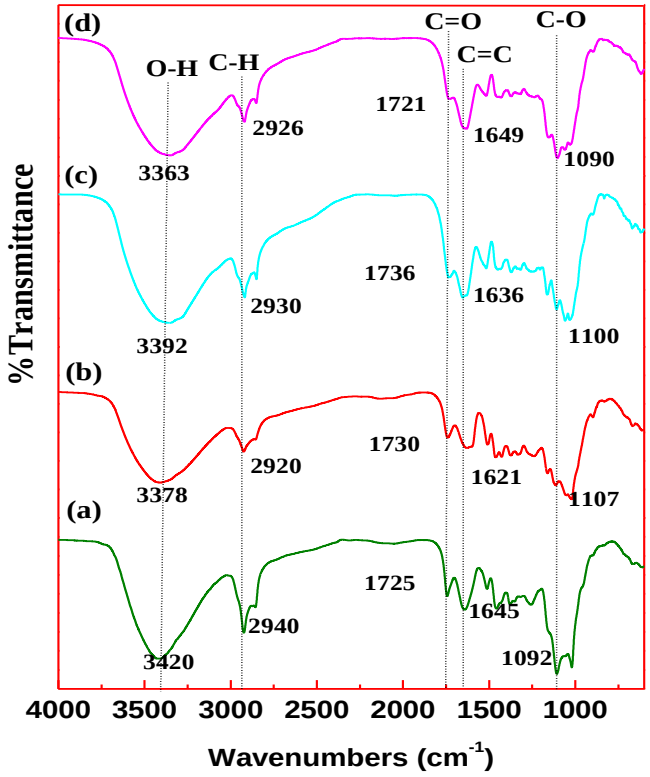

Figure 2: FTIR spectra of combination A (a) before biosorption (b) after Ni^{2+} biosorption and (c) after Cu^{2+} biosorption (d) after Zn^{2+} biosorption.

In the spectra 2a, the broad and intense peak around 3420 cm^{-1} was assigned to the presence of free or hydrogen bonded O–H groups (from carboxylic acids or alcohols) on the surface of the biosorbent (Gnanasambandam and Protor, 2000). The band at 2940 cm^{-1} indicates symmetric or asymmetric C–H stretching vibration of aliphatic acids (Li *et al*., 2007). Peak observed at 1725 cm^{-1} is the stretching vibration of C=O functional group and may be assigned to carboxylic acids and their esters (Guibaud *et al*., 2003). The peaks at 1645 cm^{-1} may be assigned to C=C

stretching vibrations of aromatic rings (Farinella *et al*., 2007). The peak at 1092 cm^{-1} can be assigned to stretching vibration of C–OH of alcoholic groups and carboxylic acids. Hence the FTIR study confirms the presence of carboxylic and hydroxyl functional group in combination A.

The peaks expected at 3420, 2940, 1725,1645 and 1092 cm^{-1} in spectra 2a were shifted to 3378, 2920, 1730, 1621and 1107 cm^{-1} respectively in spectra 2b. Similar was the case in spectra 2c and 2d. These shifts in the position of peaks may be due to biosorption Ni^{2+}, $Cu^{2+}$and Zn^{2+} on combination A. Hence it could be concluded that carbonyl and hydroxyl groups are primarily responsible for the metal biosorption from aqueous solutions (Ashkenazy *et al*., 1997).

5.3.2 Batch studies

5.3.2.1 Effect of pH

The pH of the solution is one of the most important factors governing the biosorption of metal ions by the biosorbent (Ravindran *et al*., 1999). The interaction of the different metal ions in solution with the biosorbent may be illustrated by the equation 1.

$$M^{n+} + AH_n \rightarrow AM + nH^+ \qquad (1)$$

where M represent the metal, n its charge and A the active biosorption sites of the adsorbent. The competition between the metal and H^+ ions for the active sorption sites (Li *et al*., 2007) on the biosorbent took place under different pH values of the solution. The pH affects both the solubility of the metal ions in the solution as well as the ionization states of the functional groups on the adsorbents. To study the effect of pH on metal ion biosorption on all the combination A to D, batch equilibrium studies were conducted at different pH values in the range of 2.0 to 7.0 for all the three metal ions as shown in Figure 3.

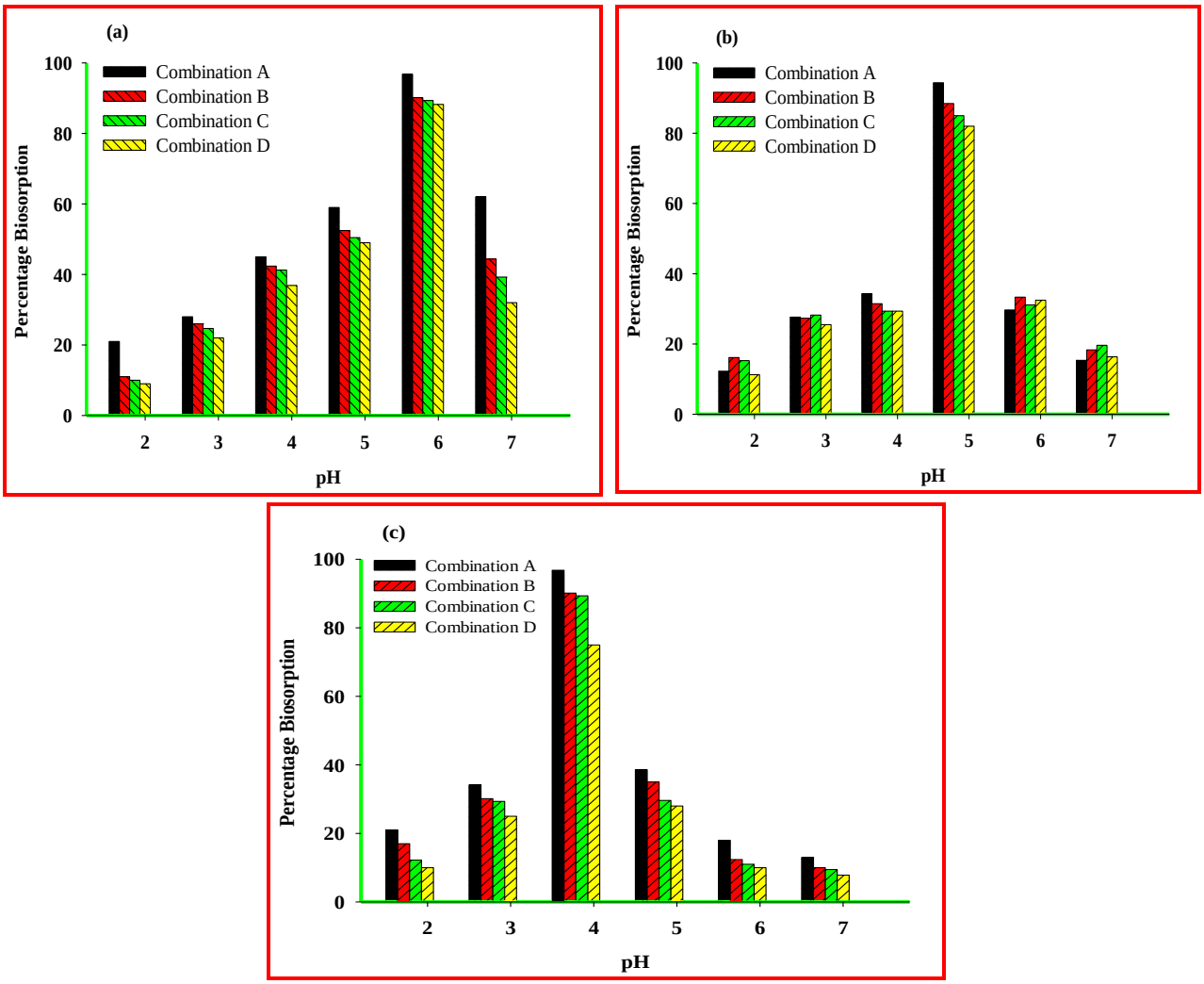

Figure 3: Effect of pH on (a) Ni^{2+}, (b) Cu^{2+} and (c) Zn^{2+} percentage biosorption onto different combinations A to D.

The maximum biosorption of Ni^{2+}, Cu^{2+} and Zn^{2+}, by all the combinations used, were obtained at pH 6.0, 5.0 and 4.0 respectively, and a significant decreased in biosorption capacity was observed at lower pH values. According to Low *et al*. (1993) little biosorption at lower pH could be ascribed to the hydrogen ions competing with metal ions for sorption sites. This means that at higher H^+ concentration, the biosorbent surface becomes more positively charged, thus, reducing the attraction between biosorbent and metal ions. In contrast as the pH increases, biosorbent surface become more negatively charged thus, facilitating greater metal uptake (Chang *et al*.,

1997). Hence, the optimum pH for the maximum biosorption for Ni^{2+}, Cu^{2+} and Zn^{2+} were found to be 6.0, 5.0 and 4.0 respectively and further column studies were carried out at the same pH.

5.3.2.2 Effect of biosorbent dose

The effect of the biosorbent dose on sorption process was studied by varying the biosorbent dose in the range of 0.200 – 1.200 g/0.1 L with 150.0 mg L^{-1} initial metal ion concentration of Ni^{2+}, Cu^{2+} and Zn^{2+}. The results are presented in Figure 4.

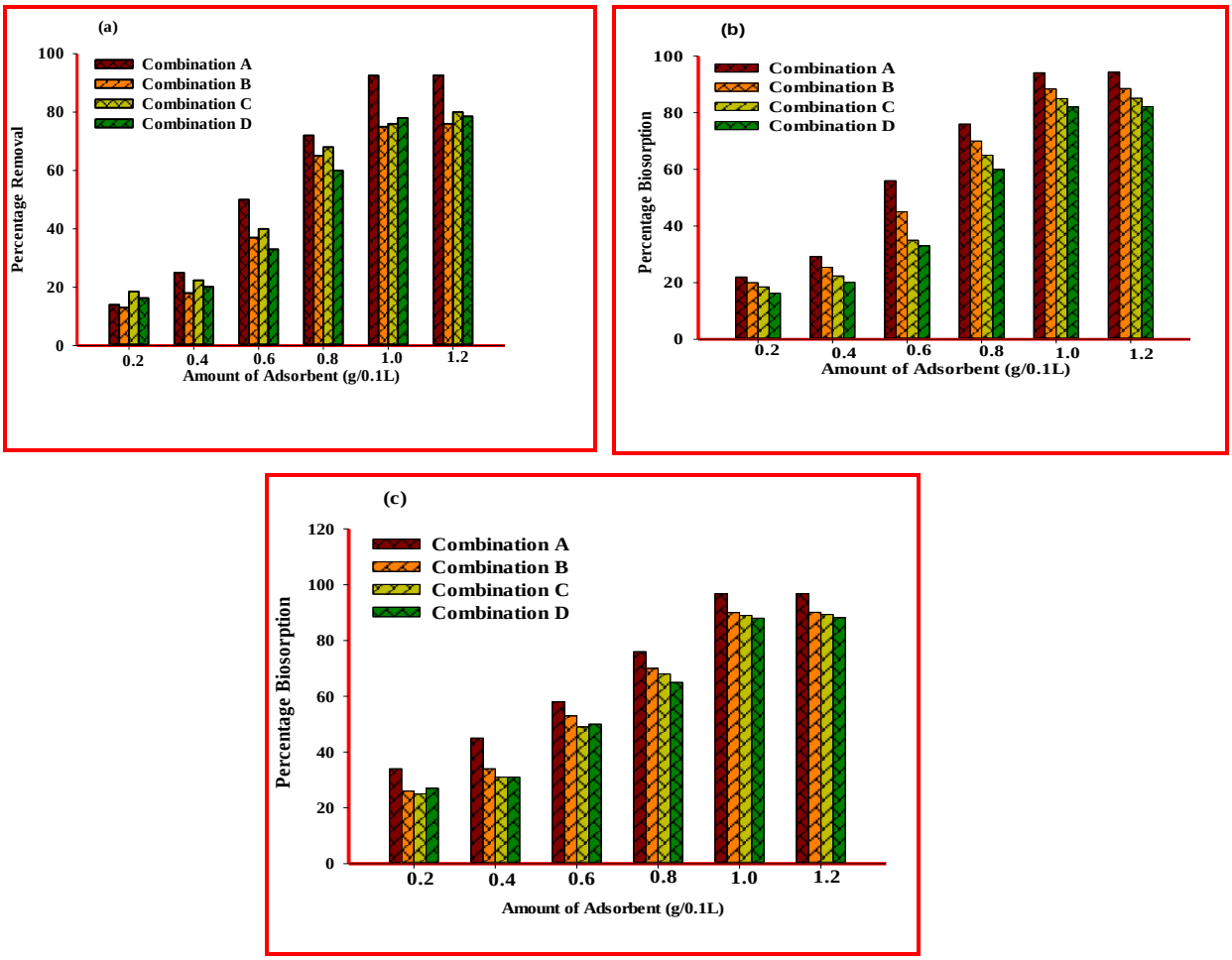

Figure 4: Effect of biosorbent dose on (a) Ni^{2+}, (b) Cu^{2+} and (c) Zn^{2+} percentage biosorption at pH 6.0, 5.0 and 4.0 respectively onto different combinations A to D.

Increase in biosorbent dose from 0.200 – 1.200 g/0.1 L resulted in a rapid increase in the uptake of all the three metal ions. But there was no noticeable change in biosorption was found beyond 1.0g/0.1L. It could be attributed to the presence of excess metal–binding sites on all the four combinations than the available Ni^{2+}, Cu^{2+} and Zn^{2+} ions in solution at the fixed concentration of 150.0 mg L^{-1}. Thus 1.0g/0.1 L biosorbent dose was selected for further studies. These interpretations are already reported in the literature for the biosorption of metals ions by different agricultural residues (Xuan *et al*., 2006)

5.3.2.3 Effect of contact time and biosorption kinetics

The effect of contact time on biosorption of metal ions on different combinations were studied in the time range of 1–300 min by using 150.0 mg L^{-1} of Ni^{2+}, Cu^{2+} and Zn^{2+} solutions at pH 6.0, 5.0 and 4.0 respectively with 1.0g/0.1 L of the biosorbent. The mixture was agitated on 225 rpm at 30°C and the samples were taken after every 20 min, filtered and analyzed by AAS.

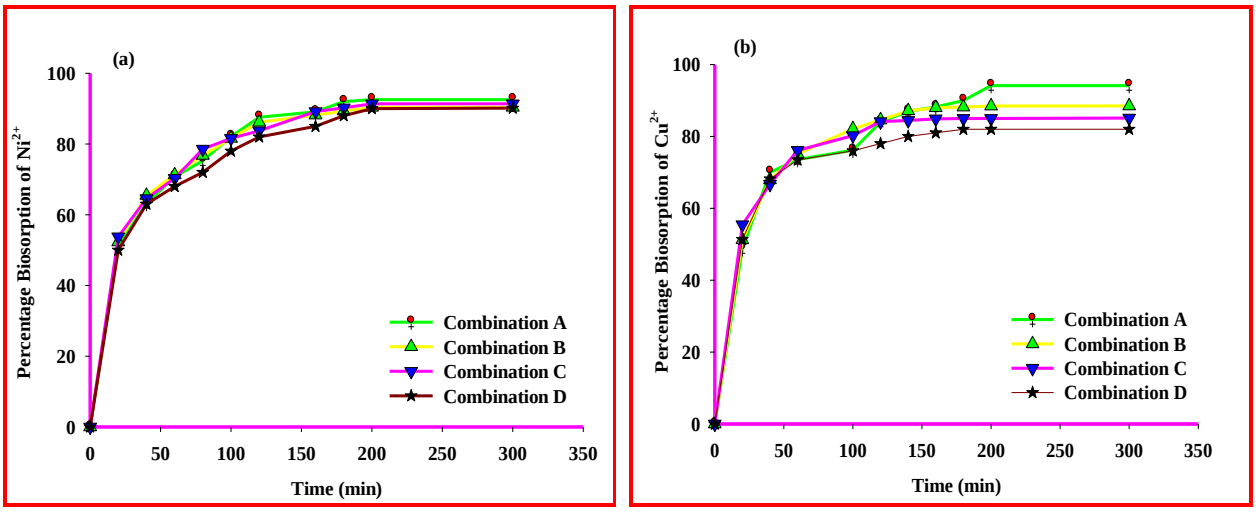

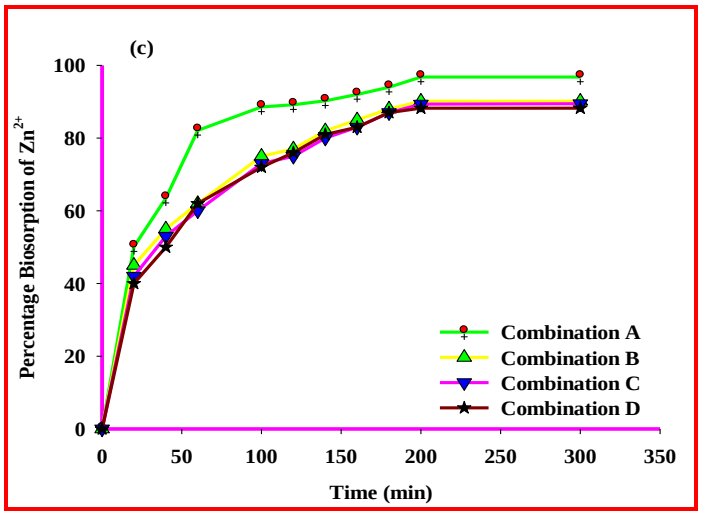

Figure 5: Effect of contact time on (a) Ni^{2+}, (b) Cu^{2+} and (c) Zn^{2+} percentage biosorption at pH = 6.0, 5.0 and 4.0 respectively onto different combinations A to D.

As shown in Figure 5, above 70 % biosorption of all the three metal ions took place in first 60 min and then it continued to increase at a lower rate until ~ 92.52%, 94.12% and 96.75 % biosorption was achieved for Ni^{2+}, Cu^{2+} and Zn^{2+} respectively, after 300 min of contact time. The rate of percent metal biosorption is higher in the beginning due to the availability of empty specific sites for metal ion binding. The two stage biosorption mechanism (Saeed *et al.*, 2005) is followed, as mentioned in previous chapters, which involves a very rapid biosorption for shorter duration in the first step followed by slow one for longer duration. Based on these results, a contact time of 300 min was assumed to be suitable for the subsequent biosorption experiments.

In order to analyze the biosorption kinetics of Ni^{2+}, Cu^{2+} and Zn^{2+} by all four combinations, the pseudo-first-order and pseudo-second-order kinetic models were applied to the experimental data obtained. The plot of $ln\ (q_e - q_t)$ versus t and t/q_t versus t gave straight lines, and the values of rate constant k_1, k_2 and q_e were determined from slope and intercept of the plot respectively, and are presented in Table-3. Better fittings of the experimental values were obtained (R^2 = 0.99) by following the pseudo-second-order kinetic model as given in Table 3.

Table 3: The pseudo-first-order and second-order-kinetic model for Ni^{2+}, Cu^{2+} and Zn^{2+} biosorption at pH 6.0, 5.0 and 4.0 respectively on different combination A to D

Different combinations	pseudo-first-order-kinetic constants		pseudo-second-order kinetic constants	
	k_1	R^2	k_2	R^2
		Ni		
A	0.005	0.97	0.028	0.99
B	0.006	0.99	0.025	0.99
C	0.007	0.95	0.023	0.99
D	0.005	0.97	0.020	0.99
		Cu		
A	0.009	0.92	0.034	0.99
B	0.005	0.92	0.027	0.99
C	0.007	0.96	0.033	0.99
D	0.006	0.94	0.033	0.99
		Zn		
A	0.009	0.89	0.040	0.99
B	0.008	0.92	0.032	0.99
C	0.005	0.87	0.053	0.99
D	0.008	0.89	0.039	0.99

This implies that the data confirms the pseudo-second-order reaction i.e. the biosorption took place in two steps, the first step very quick with maximum biosorption, and the second one slower with minor biosorption of the metal ions. It has been reported that the fast reaction is due to chemisorptions (Volesky and Holan, 1995) involving valence forces through sharing or exchange of electrons between biosorbent and biosorbate and slow one is by diffusion of ions into cell structure.

5.3.2.4 Metal sorption capacity and isotherm modeling

The maximum metal biosorption capacity of all the combinations (A to D), were evaluated by shaking 1.0 g/0.1L of the all the four combinations with varying concentrations (25.0 to 200.0 mg L^{-1}) of Ni^{2+}, Cu^{2+} and Zn^{2+} at pH 6.0, 5.0 and 4.0 respectively. Metal biosorption ability of all the combinations (A to D), was found to increase with the increase in initial metal ion concentration until it reached the maximum capacity of 92.52, 94.12 and 96.75 mg g^{-1} for Ni^{2+}, Cu^{2+} and Zn^{2+} respectively as shown in Figure 6.

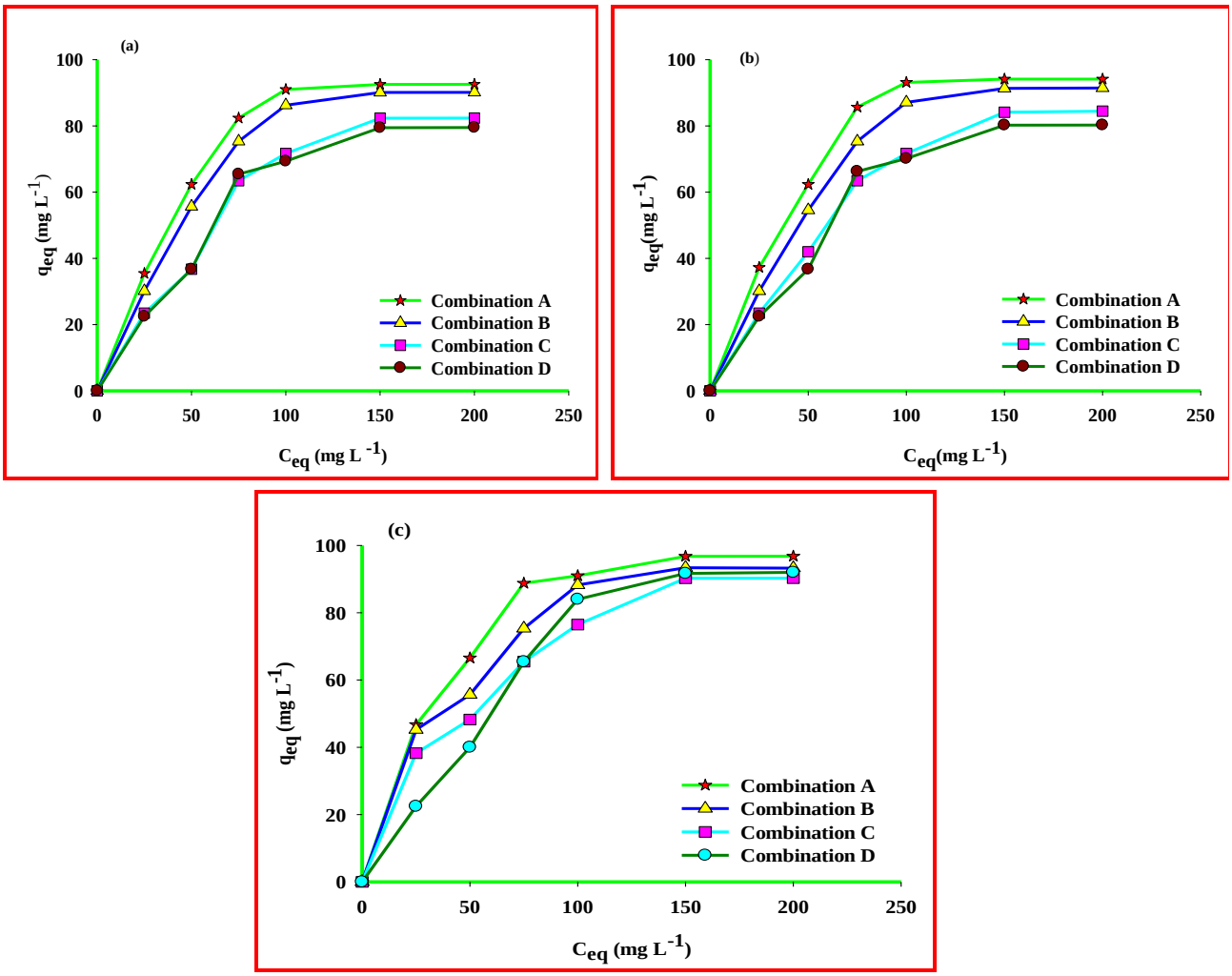

Figure 6: Effect of initial metal ion concentration on (a) Ni^{2+}, (b) Cu^{2+} and (c) Zn^{2+} percentage biosorption at pH 6.0, 5.0 and 4.0 respectively onto different combinations A to D

The Langmuir and Freundlich constants and their correlation coefficients (R^2) evaluated from these isotherms for Ni^{2+}, Cu^{2+} and $Zn^{2+}$are given in Table 4.

Table 4: Langmuir and Freundlich isotherm constants and correlation coefficients for the biosorption of Ni^{2+}, Cu^{2+} and Zn^{2+} at pH 6.0, 5.0 and 4.0 respectively on different combination A to D

Different combinations	Langmuir isotherm constants			Freundlich isotherm constants		
	q_{max}	B	R^2	n	K_F	R^2
			Ni			
A	90.18	0.13	0.99	2.54	0.59	0.98
B	90.10	0.11	0.99	2.19	0.41	0.98
C	89.41	0.14	0.99	2.39	0.51	0.99
D	87.13	0.17	0.98	2.66	0.77	0.93
			Cu			
A	93.25	0.09	0.99	2.18	0.37	0.97
B	88.84	0.13	0.99	2.39	0.54	0.96
C	89.01	0.14	0.99	2.43	0.61	0.96
D	87.94	0.10	0.99	2.28	0.40	0.94
			Zn			
A	94.87	0.12	0.99	2.26	0.50	0.99
B	90.40	0.39	0.96	4.04	1.18	0.97
C	91.80	0.10	0.99	2.22	0.35	0.97
D	88.98	0.12	0.99	2.33	0.48	0.97

The sorption characteristics of Ni^{2+}, Cu^{2+} and Zn^{2+} on all the combinations followed more closely the Langmuir isotherm model than the Freundlich isotherm model. The theoretical maximum biosorption capacity (q_{max}) of Ni^{2+}, Cu^{2+} and $Zn^{2+}$was calculated as 90.18, 93.25 and 94.87 mg g^{-1} respectively. It was maximum and was given by combination A, proving it to be the best combination for desalinating multimetal ion solutions. The theoratical value of q_{max} was quite close to the value found experimentally 92.52, 94.12 and 96.75 mg g^{-1} for Ni^{2+}, Cu^{2+} and Zn^{2+}

respectively. The maximum metal uptake capacity of combination A for Ni^{2+}, Cu^{2+} and Zn^{2+} was significantly higher than the metal sorption capacity of other agricultural residues reported in the literature (Hall *et al.*, 2001; Sag *et al.*, 2002 Toles and Marshall, 2002; Babel and Kurniawan, 2003). Further the values of 1/*n* were smaller than 1 indicating that the biosorption process was favorable under studied conditions.

5.3.2.5 Total cationic contents of the combination A

Among the four combinations used, the combination A showed maximum removal for all three metal ions. Combination A is the mixture of three biosorbents (TABP (30) + ESD (35) + AHSP (35)) which enhances its metal sorption capacity as compared to other combinations. For this reason it was further used to study the total cationic content release. Combination A (1.0 g) was treated with 100 ml, 0.1 M HCl solution in consecutively three wash and with deionized water as control. As given in Table 5 the total amount of cations released by the combination A was 84.55 mg g^{-1} which comprised of 12.50, 20.26, 39.10 and 12.69 mg g^{-1} of and Na^+, K^+, Ca^{2+} and Mg^{2+}, respectively. The total amount of cations released can gives an idea about the approximate cation exchange capacity of combination A.

Table 5: Major cations released by 1.0 g of combination A on acidification with 0.1 M HCl

Wash medium/number of washings	Cations released (mg g^{-1})				
	Na^+	K^+	Mg^{2+}	Ca^{2+}	Total cations released
Washing with 0.1 M HCl (100 ml/wash)					
First	12.50	19.24	13.62	38.58	83.94
Second	3.24	6.11	4.34	8.12	21.81
Third	0.0	0.0	1.5	2.45	3.95
Sum of three washings (a)	15.74	25.35	19.46	49.15	109.7
Washing with deionized water (100 ml/wash)					
First	3.24	3.21	4.62	5.34	16.41
Second	0.0	1.88	2.15	3.21	7.24
Third	0.0	0.0	0.0	1.50	1.50
Sum of three washings (b)	3.24	5.09	6.77	10.05	25.15
Total cations released on acidification (a – b)	12.50	20.26	12.69	39.10	84.55

5.3.2.6 Biosorption mechanism

Among the different mechanisms proposed in the literature, the ion exchange process has been suggested to be involved in biosorption process. Exchange occurs between light metal ions and protons present on the biomass and heavy metal ions present in aqueous solution (Sud *et al*., 2008).

To understand the mechanism involved in the biosorption of Ni^{2+}, Cu^{2+} and Zn^{2+} onto different combination used, 1.0 g of the combination A was mixed with 100 ml of Ni^{2+}, Cu^{2+} and Zn^{2+} solution in three different flasks with 150 mg L^{-1} initial concentration at pH 6.0, 5.0 and 4.0 respectively. The mixtures so obtained were agitated in orbital shaker at 225 rpm speed for 300 min. After 300 min the mixtures were centrifuged at 5000 rpm for 10 min and analyzed by AAS for the release of Na^{+}, K^{+}, Ca^{2+} and Mg^{2+} and unabsorbed metal ion in the solution. The results given in Table 6 supported that ~ 93 % Ni^{2+} removal is due to the ion exchange process involving Na^{+}, K^{+}, Ca^{2+} and Mg^{2+}. The remaining 7 % Ni^{2+} biosorption could be due to its ion exchange with protons, as pH of the supernatant was found to decrease at equilibrium. Similarly ~ 93.48% and 95.20% removal for Cu^{2+} and Zn^{2+} respectively, was due to ion exchange with Na^{+}, K^{+}, Ca^{2+} and Mg^{2+} and the rest 6.52% and 4.96 % may be due to proton release. Hence, it may be concluded that the biosorption of Ni^{2+}, Cu^{2+} and Zn^{2+} on combination A occurs primarily through ion exchange mechanism involving the replacement of alkali and alkaline earth metals. The protons bound bound to native carboxylate groups (Garg *et al*., 2008) are also involved in ion exchange process but to the lesser extent.

Table 6: Release of Na^{+}, K^{+}, Mg^{2+}, Ca^{2+} and H^{+} after sorption of Ni^{2+}, Cu^{2+} and Zn^{2+} by the combination A

Metal ions	Total metal sorbed (mg g^{-1})	Total cations and protons released in mg g^{-1} (%)				
		Na^{+}	K^{+}	Mg^{2+}	Ca^{2+}	H^{+}
Ni^{2+}	92.52	13.5 (14.6)	19.2 (20.8)	14.6 (15.8)	38.5 (41.7)	6.6 (7.2)
Cu^{2+}	94.12	10.2 (10.7)	22.4 (23.8)	18.2 (19.3)	37.1 (39.4)	6.1 (6.5)
Zn^{2+}	96.75	12.6 (13.0)	23.0 (23.8)	17.5 (18.1)	38.9 (40.2)	4.8 (5.0)

5.3.2.7 Blocking of functional groups and computation of their role in metal sorption

To confirm and compute the role of carboxyl and hydroxyl groups in the removal of Ni^{2+}, Cu^{2+} and Zn^{2+}, both the groups of the combination A were individually blocked in two separate experiments as mentioned in chapter 4 (Chen and Yang, 2006) and the results obtained after blocking them are given Table 7. It was observed that the metal removal capacity was badly inhibited when carbonyl groups were blocked and a decrease of 74.7%, 71.7% and 70.9% in the biosorption of Ni^{2+}, Cu^{2+} and Zn^{2+}respectively, was observed. It clearly indicates that the carboxyl groups have the major role in the process of biosorption. On the other hand 25.3%, 28.3% and 29.1% of Ni^{2+}, Cu^{2+} and Zn^{2+} were removed by combination A, even after the blockage of carboxyl groups, indicating that other functional groups are also involved in biosorption of metal ions.

Table 7: Biosorption of Ni^{2+}, Cu^{2+} and Zn^{2+} with and without blocked functional groups on the combination A

Metal ion	Biosorption on Unblocked Combination A mg g^{-1}	Biosorption on carboxyl groups blocked Combination A mg g^{-1} (%)	Decrease in Metal sorption (%)	Biosorption on hydroxyl groups blocked Combination A mg g^{-1} (%)	Decrease in Metal sorption (%)
Ni^{2+}	92.52	23.42 (25.3)	74.7	63.92 (73.2)	26.8
Cu^{2+}	94.12	26.60 (28.3)	71.7	66.58 (70.7)	29.3
Zn^{2+}	96.75	28.12 (29.1)	70.9	69.00 (71.3)	28.7

To support the presence of other functional groups on the biosorbent, sorption of Ni^{2+}, Cu^{2+} and Zn^{2+} by combination A was carried out after blocking the hydroxyl groups. The biosorption capacity of the hydroxyl group blocked biosorbent A, was found to decrease 26.8%, 29.3% and 28.7 % for the removal of Ni^{2+}, Cu^{2+} and Zn^{2+}, respectively. Further, the total metal uptake capacity of carboxylic and hydroxyl group blocked biosorbent together was found to be almost equal to the total metal ions uptake by unblocked biosorbent as shown in Table 7. These results supported that carboxyl and hydroxyl groups are chiefly responsible for uptake of Ni^{2+}, Cu^{2+} and Zn^{2+} by combination A.

5.3.2.8 Characterization of electroplating industrial wastewater

Electroplating industrial wastewater was collected from the electroplating unit situated in Karnal, Haryana (India) and analyzed for Ni^{2+}, Cu^{2+} and Zn^{2+} as given in Table 8. The collected wastewater was desalinated using combination A in column studies in a pilot experiment and same could be enlarged even at industrial level.

Table 8: Concentration of heavy metal and anions (mg L^{-1}) in electroplating industrial wastewater

Concentration of heavy metal and anions (mg L^{-1})					
Ni^{2+}	Cu^{2+}	Zn^{2+}	Cl^-	SO_4^{2-}	NO_3^-
119.15	137.35	105.23	166.78	208.22	98.78

pH = 6.0, turbidity (NTU) = 36.32

5.3.3 Column studies

The potential shown by combination A (among the four combination studied) for the removal Ni^{2+}, Cu^{2+} and Zn^{2+} in the batch studies were further tested in fixed bed column operations using electroplating industrial wastewater for the removal of the same metal ions. The data obtained in fixed bed column studies were analyzed by Thomas model (Thomas, 1944) as mentioned in chapter 2. The plot of C_e/C_i against time t (Figure 8) using non linear regression analysis clearly indicated that the predicted curves proposed by Thomas model were in good agreement with the experimental curves. The value of k_{TH}, q_e and R^2 obtained from the plot are given in Table 8. The metal uptake capacity (q_e) found to decrease in the successive cycles in all three columns where as Thomas rate constant did not change significantly. This behavior was primarily credited to gradual deterioration and diminution of the binding sites caused by the acidic washing during regeneration (Gupta *et al*., 2009; Debnath *et al*., 2010) or it may be due to nonstop usage of the biosorbent. Moreover there might be organic substances present in the electroplating effluent which leads to blocking of the active sites on the biosorbent (Debnath *et al*., 2010).

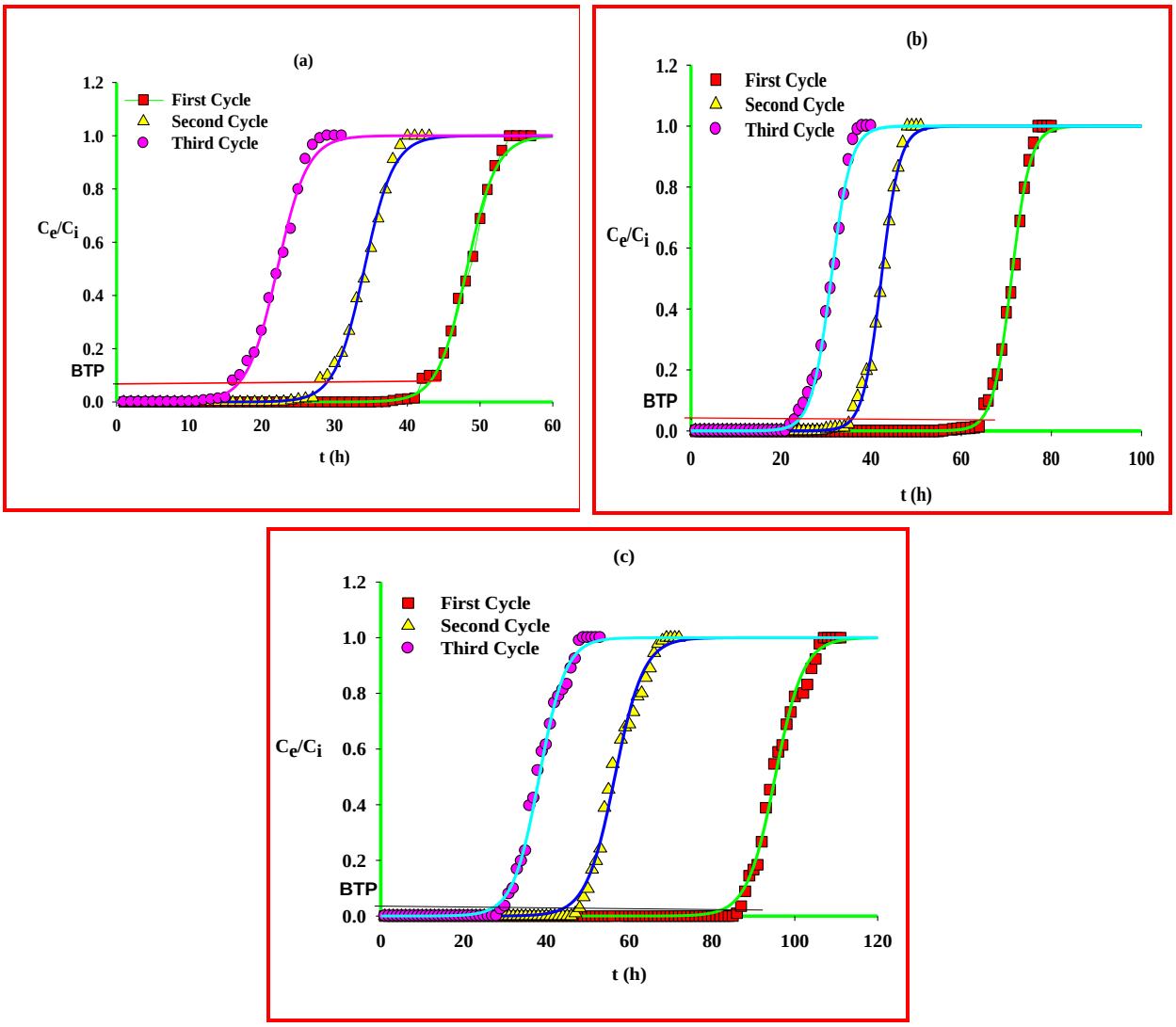

Figure 8: Breakthrough curves for (a) Ni^{2+} (b) Cu^{2+} and (c) Zn^{2+} during three sorption desorption cycles at pH 6.0, 5.0 and 4.0 respectively with electroplating industrial wastewater on combination A.

Further the effluents from the first cycle in all three columns showed complete biosorption of Ni^{2+} in column 1, Cu^{2+} in column 2 and Zn^{2+} in column 3 satisfying the Central pollution control board standards and making that water fit for reuse.

Table 8: Thomas model parameters for the Ni^{2+}, Cu^{2+} and Zn^{2+} during sorption desorption cycles with electroplating effluents on combination A.

Cycles	Columns	k_{Th} (mLmin^{-1} mg)	q_e (mg g^{-1})	R^2	% Removal of Ni^{2+}	% Removal of Cu^{2+}	% Removal of Zn^{2+}
Column 1 [Ni^{2+}]	1st Cycle	0.0041	157.40	0.99	100.0	26.0	32.0
(Influent pH=6.0)	2nd Cycle	0.0041	122.25	0.99	89.3	19.7	16.6
	3rd Cycle	0.0040	98.45	0.99	78.6	13.2	10.1
Column 2 [Cu^{2+}]	1st Cycle	0.0035	124.25	0.99	0.0	100.0	25.0
(Influent pH=5.0)	2nd Cycle	0.0036	88.65	0.99	18.5	88.4	13.2
	3rd Cycle	0.0033	96.45	0.99	16.5	77.8	6.5
Column 3 [Zn^{2+}]	1st Cycle	0.0028	101.55	0.99	0.0	0.0	100.0
(Influent pH=4.0)	2nd Cycle	0.0027	99.56	0.99	10.8	6.5	86.5
	3rd Cycle	0.0030	80.22	0.99	2.8	3.4	76.2

5.3.3.1 Column regeneration

The columns were regenerated thrice using 1.0 L of 0.1 M HCl. It can be seen form Figure 8, the breakthrough points (BTP) was achieved earlier in second and third cycles as compared to the first cycle in all the three columns used and recharged. This may be again due to the fact that the biosorbent started deteriorating in the second and third cycle and may be also due to depletion of binding sites caused by the acidic elution (Vinodhini and Das, 2010; Gupta *et al*., 2009; Debnath *et al*., 2010) as mentioned above.

5. 4 Conclusions

The present study reports the application of four different combinations, prepared by mixing various amounts of *Trifolium alexandrinum* biomass powder, *Arachis hypogea* shell powder and *Eucalyptus sp.* saw dust for the removal of Ni^{2+}, Cu^{2+} and Zn^{2+} from aqueous solutions. The main aspects examined for the purpose included biosorption kinetics, isotherms modeling, FTIR spectral analysis, chemical blocking of the functional groups and the discharge of Na^{+}, K^{+}, Ca^{2+}, Mg^{2+} and H^{+} by the biosorbent during the sorption of Ni^{2+}, Cu^{2+} and Zn^{2+}. The biosorption

kinetics was found to follow pseudo-second order kinetic model and the Langmuir isotherms provided best fit to the equilibrium sorption data obtained.

The column studies were fruitfully carried out for treating electroplating wastewater at fixed bed depth of 12.0 cm in three different columns for Ni^{2+}, Cu^{2+} and Zn^{2+}ions. The reusability of desorbed-biosorbent in columns were tested thrice in sorption–desorption cycles, showing more than 75% biosorption in the third cycle. Form the present study it can be concluded that the agricultural residues used in combinations are quite effective for removing different metal ions from the synthetic and industrial wastewater in batch as well as in column studies.

References

Ashkenazy, R.; Gottlieb, L.; and Yannai, S.; Characterization of acetone-washed yeast biomass functional groups involved in lead biosorption; *Biotechnol. Bioeng.*; **1997**, 55, 1–10.

Babel, S. and Kurniawan, T.A.; Low-cost adsorbents for heavy metals uptake from contaminated water: a review; *Hazard. Mater.*; **2003**, 97, 219–243.

Chang, J.; Law, R. and Chang, C.; Biosorption of lead, copper and cadmium by biomass of Pseudomonas aeruginosa PU21; *Water Res.*; **1997**, 31, 1651–1658.

Chen, J.P. and Yang, L.; Study of a heavy metal biosorption onto raw and chemically modified Sargassum sp. via spectroscopic and modeling analysis; *Langmuir;* **2006**, 22, 8906–8914.

Debnath, S.; Biswas, K. and Ghosh, U.C.; Removal of Ni(II) and Cr(VI) with Titanium(IV) Oxide Nanoparticle Agglomerates in Fixed-Bed Columns; *Ind. Eng. Chem. Res.;* **2010**, 49, 2031–2039.

Garg, U.; Kaur, M.P.; Jawa, G.K.; Sud, D. and Garg, V.K.; Removal of cadmium(II) from aqueous solution by biosorption on agriculturalwaste biomass; *J. Hazard. Mater.*; **2008**, 154, 1149–1157.

Gnanasambandam, R. and Protor, A.; Determination of pectin degree of esterification by diffuse reflectance Fourier transform infrared spectroscopy; *Food Chem.;* **2000**, 68, 327–332.

Gupta, B. S.; Curran, M.; Hasan S. and Ghosh, T.K.; Biosorption characteristics of Cu and Ni on Irish peat moss; *J. Environ. Manag*.; **2009,** 90, 954–960.

Guibaud, G.; Tixier, N.; Bouju, A. and Baudu, M.; Relation between extracellular polymers composition and its ability to complex Cd, Cu and Pb; *Chemosphere;* **2003**, 52, 1701**–**1710.

Hall, C.; Wales, D.S. and Keane, M.A.; Copper removal from aqueous systems: Biosorption by Pseudomonas Syringae*; Sep. Sci. Technol*.; **2001,** 36, 223–240.

Jain, M.; Garg, V.K. and Kadirvelu, K.; Chromium Removal from Aqueous System and Industrial Wastewater by Agricultural Wastes; *Bioremediation Journal;* **2013**,17 (1), 30–39

Leyva-Ramos, R.; Landin-Rodriguez, L.E.; Leyva-Ramos, S. and Medellin-Castillo, N.A.; Modification of corncob with citric acid to enhance its capacity for adsorbing cadmium(II) from water solution; *Chemical Engineering Journal;* **2012**; 180, 113–120.

Li, F.T.; Yang, H.; Zhao, Y. and Xu, R.; Novel modified pectin for heavy metal biosorption; *Chin. Chem. Lett;* **2007**, 18, 325–328.

Low, K.S.; Lee, C.K. and Lee, K.P.; Sorption of copper by dye-treated oil-palm fibres; *Bioresour. Technol*.; **1993**, 44, 109–112.

Qi, B.C. and Aldrich C.; Biosorption of heavy metals from aqueous solutions with tobacco dust; *Bioresource Technology*; **2008**; 99, 5595–5601.

Ravindran, V.; Stevens, M.R.; Badriyha, B.N. and Pirbazari, M.; Modeling the sorption of toxic metals on chelant-impregnated adsorbent; *AICHE J.;* **1999**, 45, 1135–1146.

Saeed, A.; Iqbal, M. and Akhtar, M.; Removal and recovery of heavy metals from aqueous solution using papaya wood as a new biosorbent ; *Sep. Purif. Technol*.; **2005**, 45, 25–31.

Sag, Y.; Akcael, B. and Kutsal, T.; Ternary biosorption equilibria of chromium(VI), copper(II), and cadmium(II) on Rhizopus arrhizus; *Sep. Sci. Technol*.; **2002**, 37, 279–309.

Sud, D.; Mahajan, G. and Kaur, M.P.; Agricultural waste material as potential biosorbentfor sequestering heavy metal ions from aqueous solutions; A review; *Bioresour. Technol*.; **2008**, 99 6017–6027.

Thomas, H.C; Heterogeneous ion exchange in a flowing system; *J Am. Chem. Soc*; **1944**, 66, 1446–1664**.**

Toles, C.A. and Marshall, W.E.; Copper ion removal by almond shell carbons and commercial carbons: batch and column studies; *Sep. Sci. Technol*.; **2002**, 37, 2369**–**2383.

Volesky, B. and Holan, Z.R.; Biosorption of Heavy Metals; *Biotechnol. Prog*.; **1995**,11, 235**–** 250.

Vinodhini, V. and Das. N.; Packed bed column studies on Cr(VI) removal from tannery wastewater by neem sawdust; *Desalination*; **2010**, 264, 9–14.

Visa, M.; Isac, L. and Duta, A.; Fly ash adsorbents for multi-cation wastewater treatment; *Applied Surface Science;* **2012**, 258, 6345– 6352.

Xuan, Z.X.; Tang, Y.R.; Li, X.M.; Liu, Y.H. and Luo, F.; Study on the equilibrium, kinetics and isotherm of biosorption of lead ions onto pretreated chemically modified orange peel; *Biochem. Eng. J*.; **2006**, 31, 160**–**164.

Chapter 6

Aspergillus niger Decomposed *Citrus limetta* Peel Powder as Biosorbent for Remediation of Heavy Metals from Paint Manufacturing Industrial Wastewater

Contents

Abstract

This chapter highlights the application of *Aspergillus niger* decomposed *Citrus limetta* peels powder for desalinating Cd^{2+} and Pb^{2+} from synthetic and paint manufacturing industrial wastewater. *Aspergillus niger* was grown on *Citrus limetta* peels powder for 20 days and the died biomass of the same was used in batch and column studies. The batch mode was studied to optimize the essential parameters viz., pH, contact time, adsorbent dose, initial metal concentration and temperature. The kinetics of the studies was best described with pseudo-second-order kinetic model. The sorption characteristics of Cd^{2+} and Pb^{2+} on the biomass followed more closely the Langmuir isotherm model with metal uptake capacity (q_{max}) of 370.4 and 286 mg L^{-1} respectively than the Freundlich isotherm model. The column studies were carried out with varying bed depth and flow rates with synthetic solutions in both down flow and up flow modes. The bed depth of 12.0 cm and flow rate of 1.0 mL min^{-1} gave the maximum removal of both Cd^{2+} and Pb^{2+}. With the same bed depth and flow rate paint manufacturing industrial waste water was treated in three sorption-desorption cycles. The metal uptake capacity was excellent in both the flows but it was higher in the case of up flow mode for both the metal ions.

Further the comparison of biosorption of Cd^{2+}in synthetic and paint manufacturing wastewater was studied and it was observed that the metal uptake capacity decreases in the case of industrial wastewater attributed to the competition of co-ions with Cd^{2+} for the biosorption sites on the biosorbent.

Keywords: *Aspergillus niger*, *Citrus limetta* peels powder, point of zero charge, up-flow column studies, acidic elution.

6.1 Introduction

Hasty industrializations have greatly increased the level of heavy metals (Ni, Zn, Pb, Cd, Hg) especially in aqueous systems. These metals are highly toxic and it is compulsory to treat the industrial wastewater to permissible limits before its disposal into normal water bodies.

The wastewater from paint manufacturing industry is rich in cadmium and lead. Both the metal ions are toxic, non biodegradable therefore tend to accumulate in the tissues of the human body and have potential to be toxic even at relatively minor levels of exposure. Therefore the removal of the same to an environmentally safe level in a cost effective and environment friendly manner is of greater significance. Biosorption seems to be an environment friendly technology to clean up contaminated water based on the utilization of dead biomass (Galun et al., 1987; Mullen et al., 1989).

Application of fungal species for metal removal from aqueous media has been reported by many groups (Huang and Huang, 1996; Zouboulis *et al.*, 2004). The use of dead cells for metal removal has received greater attention compared to living ones as former is non hazardous and do not demand the growth media (Awofolu *et al.*, 2006). The fungal biomass of *Penicillium* (Galun *et al.*, 1983), *Rhizopus arrhizus* (Tsezos and Velosky, 1982; Tobin *et al.*, 1984), *Rhizopus oryzae*, *Aspergillus oryzae* (Huang and Huang, 1996) and *Aspergillus niger* (Kapoor *et al.*, 1999; Park *et al.*, 2005; Awofolu *et al.*, 2006) have been used for the removal of metal ions from aqueous solutions. It has emerged as one of the most promising process, because of its high efficiency and favorable economics.

In this chapter, *Aspergillus niger* was grown on *Citrus limetta* peels powder and the dead biomass obtained was used for desalinating synthetic and paint manufacturing industrial wastewater containing Cd^{2+} and Pb^{2+} in batch mode and column studies. The batch mode was carried out to optimize the pH, adsorbent dose, contact time, metal ion concentration and temperature so that the same conditions can be used to carry out continuous column studies which is applicable at industrial level for water purification. The characterization of the dead biomass was done using FTIR, SEM and EDX analysis.

6.2 Experimental

6.2.1 Batch Studies

Batch studies were opted merely to optimize the parameters like pH, adsorbent dose, contact time, metal ion concentration, temperature etc. for maximum biosorption of Cd^{2+} and Pb^{2+} from synthetic aqueous solutions. The same parameters were utilized to carry out continuous column studies for actual applicability at industrial scale.

Batch experiments for Cd^{2+} and Pb^{2+} biosorption from synthetic solutions were carried out at different pH values (1.0 to 8.0) by agitating 2.0 g of ANDB (*Aspergillus niger* decomposed biomass) in 250 mL screw-cap conical flasks with 100.0 mL of metal ion solutions respectively. The mixtures so obtained were agitated in orbital shaker at 225 agitation speed for 300 min at 30 $^{\circ}$C. After every 20 min of agitation, 2.0 mL of the suspensions were centrifuged at 3000 rpm for 10 min and analyzed using AAS. Further, the effect of initial metal ion concentration (50 – 250 mg L^{-1}), adsorbent dose (0.5 g to 3.0 g/0.1 L), contact time (1– 300 min) and temperature (10 to 40 $^{\circ}$C) were studied. The percent of the metal removal (*R %)* was calculated for each experiment using equation 1 and 2 as mentioned in chapter 2.

6.2.2 Column studies

Column studies (both down flow and up flow) were conducted in glass columns (internal diameter = 3.0 cm and height 25.0 cm) at room temperature (around 30 $^{\circ}$C). They were packed with required bed depth of the ANDB over a sheet of glass wool. The pH of the columns were adjusted to pH 5.0 and 6.0 for Cd^{2+} and Pb^{2+} respectively by circulating 3.0 L deionized water adjusted to pH 5.0 and 6.0 for 12 h at a flow rate of 1.0 mL min^{-1} using peristaltic pump.

The effect of bed depth on the breakthrough curves was studied using bed depth of 8.0, 10.0 and 12.0 cm made by uniform packing of 15.40, 19.25 and 23.10 g, respectively, of ANDB. The feed solution having metal ion concentration of 200 mg L^{-1} for both metal ions in all the cases was circulated in down flow and up flow mode with 1.0 mL min^{-1} flow rate. The effect of effluent flow rate (1.0, 3.0 and 6.0 mL min^{-1}) on breakthrough was investigated using columns with a fixed bed depth of 12.0 cm.

6.2.2.1 Column studies with paint manufacturing industrial wastewater

Paint manufacturing industrial wastewater was collected from the paint manufacturing unit situated in Panipat, Haryana, India and the physico-chemical parameters (Table 1) of the same were analyzed. The concentration of heavy metals was analyzed using AAS.

Table 1: Different Parameters of the paint manufacturing industrial wastewater

Parameters analyzed	Results
pH	5.5
Temperature (°C)	30
Total Hardness (mg L^{-1})	870.5
Biological oxygen demand (BOD), (mg L^{-1})	350.25
Chemical oxygen demand (COD), (mg L^{-1})	420.6
Cadmium (mg L^{-1})	205.66
Lead (mg L^{-1})	197.60
Chloride (mg L^{-1})	288.20
Sulphates (mg L^{-1})	290.45
Nitrates (mg L^{-1})	305.42
Turbidity (NTU)	163.0

The paint manufacturing industrial wastewater was treated, first by passing through the column 1 (bed depth 12.0 cm) with pH adjusted to 5.0 at the flow rate of 1.0 mL min^{-1}. Samples were collected at column outlet at regular time intervals and analyzed for Cd^{2+} and Pb^{2+}. The percolation of the wastewater into the column 1 was stopped on achieving the breakthrough point (BTP). Effluent of the column 1 was readjusted to pH 6.0 using a 0.1 M NaOH solution and then passed through the column 2 up to the breakthrough point. The wastewater was treated till the concentration of both the metal ions was below detection limit.

The columns (1 and 2) used for treating paint manufacturing industrial wastewater were regenerated using 0.1 M HCl. A mean effluent flow rate of 1.0 mL min^{-1} was maintained and the effluents from both the columns were collected in 5.0 ml fractions and were analyzed for Cd^{2+} and Pb^{2+}. The columns were then washed with deionised water to make them acid free. Thereafter, the column 1 was treated with water adjusted to pH 5.0 and column 2 with water of

pH 6.0. The reactivated columns were then used again for another two cycles, for the treatment of the paint manufacturing industrial waste water.

6.2.2.2 Comparison of biosorption of Cd^{2+} from synthetic and paint manufacturing industrial wastewater

The comparison of biosorption of Cd^{2+} in synthetic solution (single metal ion system) and paint manufacturing wastewater (multi metal ion system) was studied in a columns (bed height 12.0 cm) fed with synthetic solution containing Cd^{2+}alone (C_i = 200.0 mg L^{-1}) and industrial waste water containing (Cd^{2+} and Pb^{2+}) at flow rate of 1.0 mL min^{-1} at pH 5.5.

6.3 Results and Discussion

6.3.1 Characterization of ANDB

6.3.1.1 FTIR analysis

The FTIR spectra were recorded before and after biosorption of Cd^{2+} and Pb^{2+} to find out the functional groups involed in metal binding during the metal biosoption. Changes in intensity and shift in position of the peaks were observed in the spectra after Cd^{2+} and Pb^{2+} biosorption on ANDB (Figure 1).

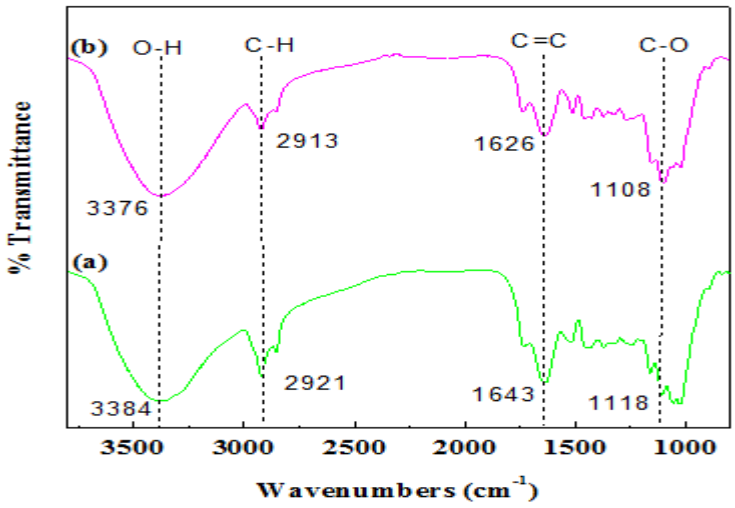

Figure 1: FTIR spectra: (a) before biosorption and (b) after biosorption of Cd^{2+} and Pb^{2+} on ANDB.

The broad and intense peak at 3384 cm^{-1} was assigned to the presence of free or hydrogen bonded O–H groups (from carboxylic acids or alcohols) on the surface of the biosorbent. The

band at 2921 cm^{-1} indicates symmetric or asymmetric C–H stretching vibration of aliphatic acids. Peak observed at 1643 cm^{-1} assigned to C=C stretching in aromatic ring. The peak observed at 1118 cm^{-1} represents C–O bonding of phenols (Jacques et al., 2007). FTIR spectra of Cd^{2+} and Pb^{2+} biosorbed ANDB showed the shift in peaks from 3384, 2921, 1643 and 1118 cm^{-1} to 3376, 2913, 1626 and 1108 cm^{-1} respectively. These observations confirmed the interaction of Cd^{2+} and Pb^{2+} with the biosorbent through –OH, –CH and –C–O– functional groups.

6.3.1.2 SEM and EDX analysis

SEM images and EDX spectra obtained before and after biosorption of Cd^{2+} and Pb^{2+} on to ANDB are shown in Figure 2. There was not much difference in the SEM images of ANDB before and after biosorption but the EDX spectra obtained after biosorption revealed the additional signals of Cd^{2+} and Pb^{2+}, which confirmed the binding of the metal ions to the surface of the biomass.

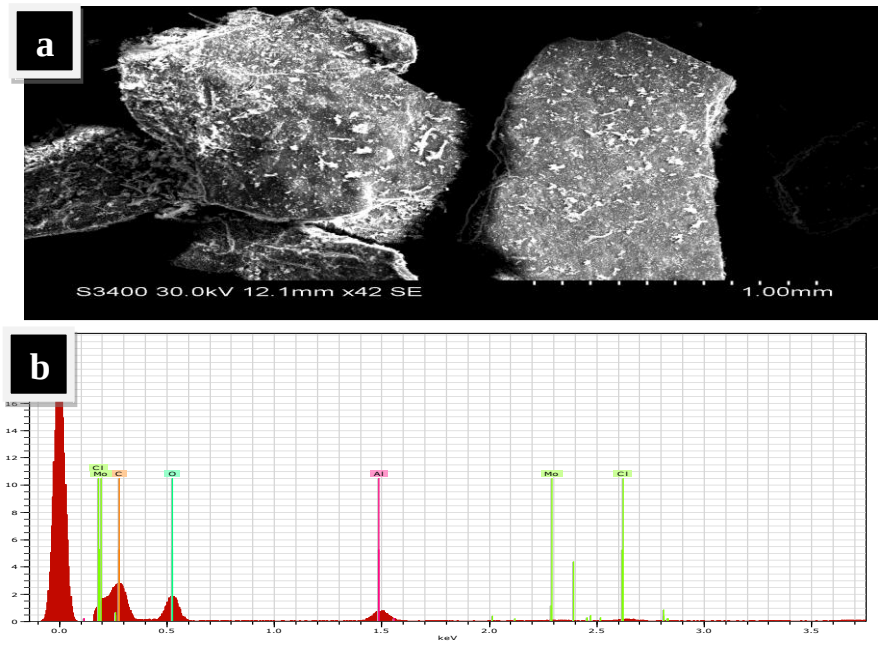

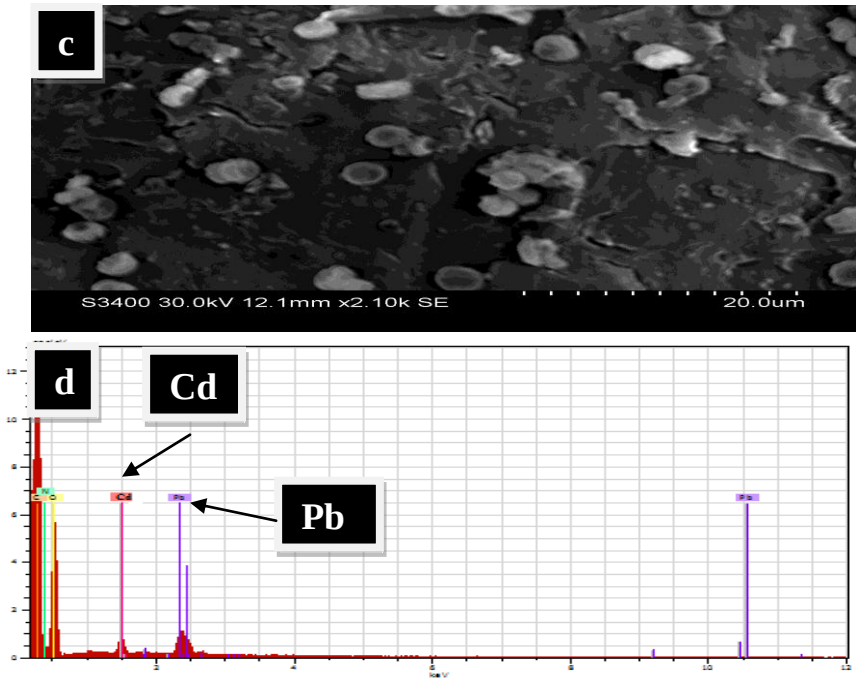

Figure 2: SEM and EDX images of ANDB before (a, b) after (c, d) biosorption of $Cd^{2+}$and Pb^{2+} respectively.

6.3.2 Batch studies

The maximum removal of Cd^{2+} and Pb^{2+} by ANDB, were obtained at pH 5.0 and 6.0 respectively as shown in Figure 3 and a significant decrease in biosorption capacity was observed at pH values other than 5.0 and 6.0. The point of zero charge (pH_{PZC}) of ANDB (Figure 3) was experimentally found to be 4.4 which supported that biosorption would be better at pH higher than 4.4 for both Cd^{2+} and Pb^{2+}. Further the negligible adsorption was seen at pH>7.0 for both the metal ions. It was due to the metal hydrolysis and precipitation, so the subsequent studies were conducted at pH 5.0 and 6.0 for $Cd^{2+}$and Pb^{2+} respectively.

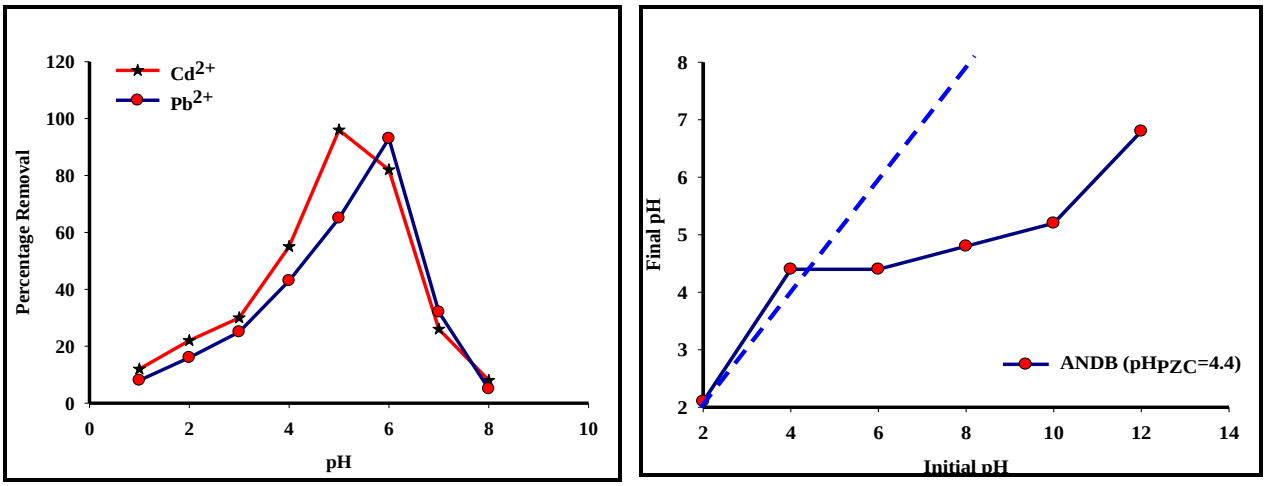

Figure 3: Effect of pH on $Cd^{2+}$and Pb^{2+} percentage removal and determination of point zero charge (pH_{PZC}) of ANDB.

The effect of contact time on biosorption of Cd^{2+} and Pb^{2+} on ANDB was studied in the time range of 1 to 300 min and it was observed that 65 % biosorption of Cd^{2+} and Pb^{2+} took place in first 60 min and then it continued to increase at a lower rate until 96% and 90% biosorption of Cd^{2+} and Pb^{2+} respectively was achieved after 300 min of contact time. The two stage biosorption mechanism was observed which involve the first rapid and quantitatively predominant, and the second slower and quantitatively irrelevant (Boudrahem *et al.* 2009). Hence it was concluded here that lower flow rate would be useful in column experiments.

The influence of the adsorbent dose and initial metal concentrations on the present biosorption process was studied and both Langmuir and Freundlich isotherms were applied to the data obtained. It was noticed that increase in adsorbent dose from 0.5 – 3.0 g/0.1 L resulted in a rapid increase in the uptake of Cd^{2+} and Pb^{2+}. But no considerable increase in biosorption was found beyond 2.0 g/0.1 L. The reason would be the same as mentioned in our previous chapters. The presence of additional biomass resulted in overlapping of the biosorption sites or overcrowding of the biosorbent particles when the biosorbent dosage was increased beyond 2.0 g/0.1 L. (Garg *et al.*, 2003; Babel and Kurniawan, 2004). However, when the initial concentration of Cd^{2+} and Pb^{2+} was continuously increased from 50.0 to 250 mg L^{-1} using the fixed amount of the adsorbent (2.0 g/0.1 L), the uptake of Cd^{2+} and Pb^{2+} was found to decrease due to the early saturation of the binding sites of the biosorbent at high metal concentration. This may also be accredited to the increase in the number of Cd^{2+} and Pb^{2+} competing for available binding sites of

the biosorbent. The sorption characteristics of Cd^{2+} and Pb^{2+} on ANDB followed more closely the Langmuir isotherm model with metal uptake capacity (q_{max}) of 370.4 and 286 mg L^{-1} respectively than the Freundlich isotherm model. The effect of temperature on the uptake of Cd^{2+} and Pb^{2+} on ANDB was studied at different temperatures, ranging from 10 to 40°C with fixed initial concentration of 200 mg L^{-1} and adsorbent dose 2.0 g/0.1 L at pH 5.0 and 6.0 respectively (Table 2).

Table 2: Thermodynamic parameters of Cd^{2+} and Pb^{2+} biosorption on ANDB at different temperatures with pH 5.0 and 6.0 respectively

Metal ion	T (°C)	K_d	ΔG° (kJ mol^{-1})	ΔS° (Jmol^{-1} K^{-1})*	ΔH° (kJ mol^{-1})*
Cd^{2+}	10	1.21	-2.26	245.52	0.69
	15	1.42	-0.84		
	20	1.58	-1.09		
	25	2.58	-2.33		
	30	24.96	-8.01		
	35	16.61	-7.26		
	40	16.61	-7.26		
Pb^{2+}	10	1.28	-0.57	218.49	0.62
	15	1.42	-0.84		
	20	1.56	-1.07		
	25	2.81	-2.55		
	30	9.96	-5.77		
	35	9.04	-5.67		
	40	9.04	-5.67		

*Measured between 10 and 40 °C

The biosorption capacity of Cd^{2+} and Pb^{2+} on ANDB was better at 30°C and this may possibly be attributed due to the increase in molecular diffusion or due to the availability of more active sites on the surface of the ANDB by expansion of the pores at the same temperature (Gundogdu *et al.*, 2009). The observed values of ΔH° and ΔG° as given in Table 2 supported the physical nature and spontaneity of the biosorption of Cd^{2+} and Pb^{2+} on ANDB.

Hence it was concluded from the batch studies that continuous biosorption experiments can be conducted using ANDB at specific pH (pH 5.0 and 6.0 for Cd^{2+} and Pb^{2+}, respectively) with lower flow rates (1.0 ml min^{-1}) with appropriate biosorbent dose at temperature around 30°C.

6.3.2.1 Comparison of ANDB with few literature reported biosorbents

On the basis of batch studies, the comparison was done between the biosorption capacity of ANDB and that of the literature reported biosorbents. It was observed that ANDB exhibit very good sorption efficiency for Cd^{2+} and Pb^{2+} (Table 3). The maximum biosorption capacity (q_{max}) was found to be 370.4 and 286 mg g^{-1} for Cd^{2+} and Pb^{2+} when 2.0/.01 L of ANDB was used at pH 5.0 and 6.0 respectively.

Table 3: Comparison of maximum biosorption capacity of Cd^{2+} and Pb^{2+} on different biosorbents

Adsorbents	Metal	Adsorption capacity (mg g^{-1})	References
Pleutrotus platypus	Cd	14.28	Vimala and Das, 2011.
Tea waste	Cd	46.0	Amarasinghe and Williams, 2007.
Granular activated carbon	Cd	19.0	Amarasinghe and Williams, 2007.
L. hyperborean	Cd	52.4	Yu *et al*., 1999.
Padina sp.	Cd	46.9	Sheng *et al*., 2004.
Sargassum siliquosum	Cd	49.4	Hashim and Chu, 2004.
ANDB	Cd	370.4	Present work.
Barely	Pb	23.20	Pehlivan *et al.*, 2009.
Snowberry	Pb	62.16	Akara *et al.*, 2009.
Rice husk	Pb	58.10	Krishnani *et al.*, 2008.
Hazelnut shell	Pb	28.18	Pehlivan *et al.*, 2009.
Pecan nutshell	Pb	211.7	Vaghetti *et al.*, 2009.
Macrofungus	Pb	38.40	Sari and Tuzen, 2009.
Sawdust	Pb	88.49	Naiya *et al.*, 2008.
ANDB	Pb	286.0	Present work.

6.3.3 Column studies

6.3.3.1 Effect of bed depth and flow rate

As noticed in previous chapters, the increase in bed depth and decrease in flow rate resulted increase in metal biosorption capacity with fixed initial metal ion concentration and specific pH. Identical results were obtained while studying the effect of bed depth and flow rate on the biosorption of Cd^{2+} and Pb^{2+} on to ANDB. The data obtained by varying the bed depth and flow rate in both down flow and up flow modes for Cd^{2+} and Pb^{2+} were analyzed using Thomas model. The Thomas model parameters are given in Table 4a and 4b for Cd^{2+} and Pb^{2+}

respectively. It was observed from Table 4a and 4b that the metal biosorption capacity, breakthrough point and volume of water treated increased with increase in bed depth and decreases with increase in flow rate of the ANDB columns in both the modes.

Table 4: a) Thomas model parameters for Cd^{2+} biosorption from synthetic solution in down flow/ up flow mode at pH 5.0 and C_i= 200 mg L^{-1}

Parameters varied	**Cd^{2+}**							
Bed depth (cm^{-1}) (g)	**q_e (mg g^{-1})**		**R^2**		**BTP (h)**		**VWT*** (mL)**	
	DF*	**UF****	**DF**	**UF**	**DF**	**UF**	**DF**	**UF**
8.0 (15.40)	520	575	0.99	0.99	28	32	1680	1920
10.0 (19.25)	565	605	0.99	0.99	35	39	2100	2340
12.0 (23.10)	588	633	0.99	0.99	45	47	2700	2820
Flow rate (mL min^{-1})								
1.0	588	633	0.99	0.99	45	47	2700	2820
3.0	358	412	0.99	0.99	12	13	2160	2340
6.0	213	261	0.99	0.99	5	6	1800	2160

* Down flow, ** Up Flow, *** Volume of water treated

The increase in metal biosorption capacity with increase in bed depth (increase in the biosorbent mass) is obvious as more biosorbent will provide more binding sites resulting higher metal uptake capacity. With increase in bed depth from 8.0 to 12.0 cm, the breakthrough point shifted from 28 to 45 h in down flow, 32 to 47 h in up flow for Cd^{2+} and 25 to 41 h in down flow, 29 to 44 h in up flow for Pb^{2+}. Thus, an increase in bed depth causes the solution to spend more time in the column, resulting maximum biosorption and late column exhaustion.

Table 4: b) Thomas model parameters for Pb^{2+} biosorption from synthetic solution in down flow/ up flow mode at pH 5.0 and C_i= 200 mg L^{-1}

Parameters varied	Pb^{2+}							
Bed depth (cm^{-1}) (g)	**q_e (mg g^{-1})**		**R^2**		**BTP (h)**		**VWT (mL)**	
	DF	**UF**	**DF**	**UF**	**DF**	**UF**	**DF**	**UF**
8.0 (15.40)	490	544	0.99	0.99	25	29	1500	1740
10.0 (19.25)	532	571	0.99	0.99	31	36	1860	2160
12.0 (23.10)	532	600	0.99	0.99	41	44	2460	2640
Flow rate (mL min^{-1})								
1.0	532	600	0.99	0.99	41	44	2460	2640
3.0	312	367	0.99	0.99	9	11	1620	1980
6.0	189	233	0.99	0.99	4	5	1440	1800

Further the volume of treated water and metal uptake capacity was higher in up flow mode as compared to down flow mode, signaling that the biosorption against gravitational force is more effective as the metal ions get comparably more time for binding to the active sites on the surface as well into the interior of the biosorbent. The value of R^2 for all the experiments was 0.99 which indicated that Thomas model described the column performance data very well for the biosorption of Cd^{2+} and Pb^{2+} in both the modes.

6.3.3.2 Removal of Cd^{2+} and Pb^{2+} from paint manufacturing industrial wastewater

Thomas model was also applied to the data obtained during three sorption desorption cycles for treating paint manufacturing industrial wastewater in two separate columns 1 and 2 maintained at pH 5.0 and pH 6.0 respectively. The breakthrough curves obtained for Cd^{2+} and Pb^{2+} biosorption in both down flow and up flow modes as shown in Figure 4.

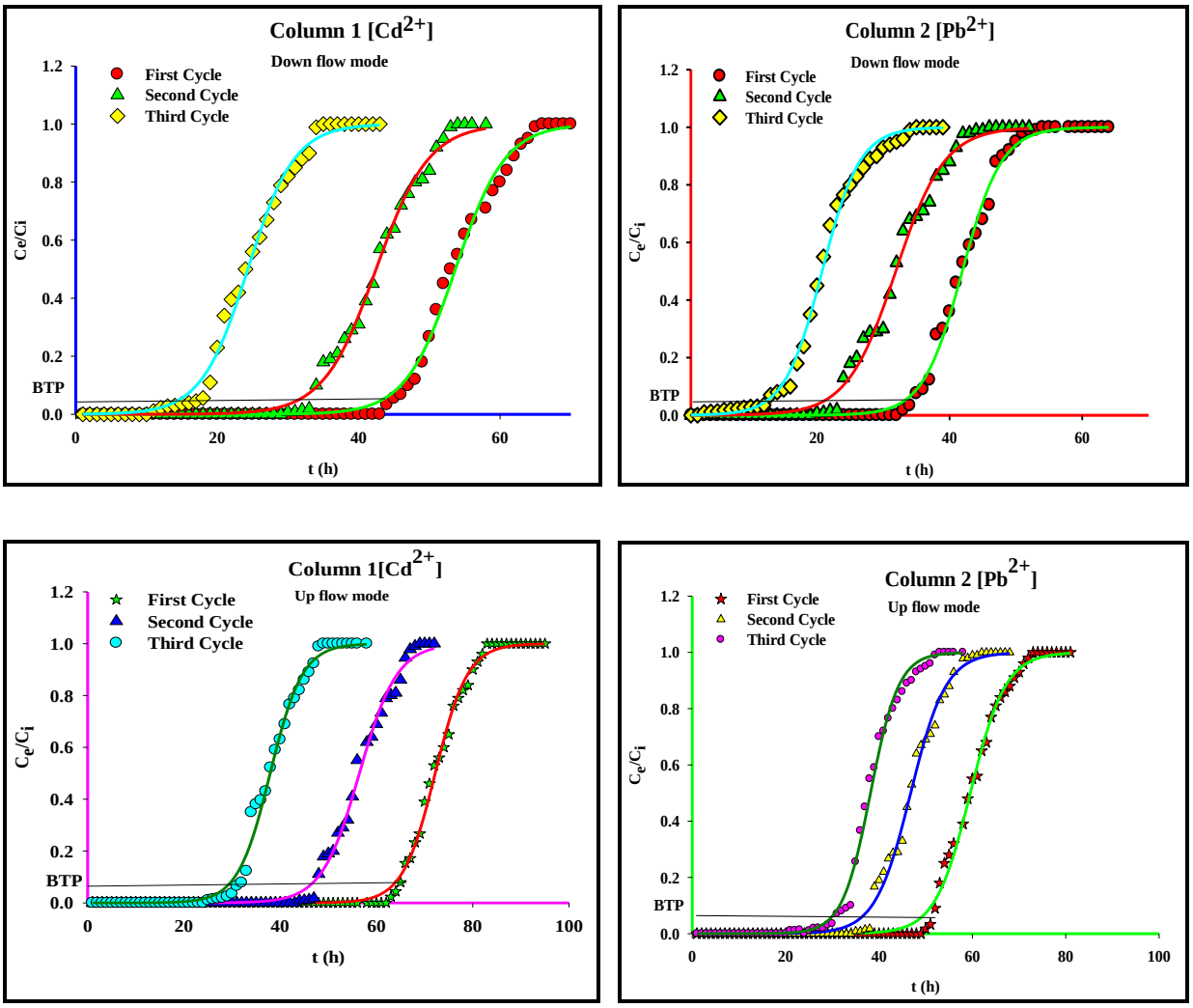

Figure 4: Down flow/ up flow biosorption of Cd^{2+} and Pb^{2+} from paint manufacturing industrial wastewater by ANDB packed columns at pH 5.0 and 6.0 respectively

The value of Thomas rate constant (k_{TH}), metal uptake capacity (q_e), breakthrough point and water treatment capacity are given in Table 5. From the data mentioned in Table 5, it can be summarized that the value of Thomas rate constant have not changed significantly but the total metal uptake capacity, breakthrough time and volume of treated water showed a variation between the two modes as well as among the three cycles carried out. The metal uptake capacity, breakthrough time and volume of water treated in both the columns were maximum in the first cycle and their value decreases in second and third cycle. It could be due to the partial blocking

of the active sites of ANDB in first and second cycle or the regeneration of the exhausted biosorbent could not be obtained 100% or it could be due to the deterioration of the ANDB by acid washing during its regeneration process.

Table 5: Thomas model parameters for Cd^{2+} and Pb^{2+} biosorption from paint manufacturing industrial waste water in down flow/ flow mode.

Columns (DF/UF)	Cycles (DF/UF)	q_e (mg g^{-1})		BTP (h)		Volume of Water Purified (mL)		% Removal of Cd^{2+}		% Removal of Pb^{2+}	
		DF	**UF**	**DF**	**UF**	**DF**	**UF**	**DF**	**UF**	**DF**	**UF**
Column 1 (Influent pH=5.0)	1st	673	722	43	64	2580	3840	93	100	28	32
	2nd	532	565	32	47	1920	2820	84	94	19	23
	3rd	305	379	15	31	900	1860	73	89	14	17
Column 2 (Influent pH= 6.0)	1st	525	596	33	51	1980	3060	0.0	0.0	60	68
	2nd	399	468	21	38	1260	2280	6.0	4.5	54	63
	3rd	260	382	13	30	780	1800	10.2	7.6	49	57

(The value of k_{TH} in both the columns was 0.0013 to 0.0017).

Further, comparing down flow and up flow modes, it was seen that in case of later, the metal uptake capacity, breakthrough time and volume of water treated was better than the down flow mode. This enhancement in the performance of the column in up flow mode may be due to increase in the residency time of the metal solution in the column while moving against the gravitational force and also due to the diffusion of the metal ions into the interior of the biosorbent utilizing the biosorbent binding sites completely.

After the third cycle, the exhausted biomass was removed from the columns and taken in 1000 mL beaker. The 200 mL of 1.0 M HCl was added to it and the mixture was agitated on the shaker for 2h. The mixture was than filtered and again agitated with 200 ml of demonized water

for same duration. Finally the biomass was filtered, dried and EDX analysis confirmed the absence of Cd^{2+} and Pb^{2+}. This powder was used as a manures in the rice fields.

6.3.3.3 Comparison of biosorption of Cd^{2+} in synthetic and paint manufacturing industrial wastewater

The comparison of biosorption of Cd^{2+} in synthetic solution (single metal ion system) containing Cd^{2+} only and paint manufacturing industrial wastewater (multi metal ion system) containing Cd^{2+}, Pb^{2+} and other anions was studied in up flow mode. Figure 5 shows the behavior of breakthrough curves for the same.

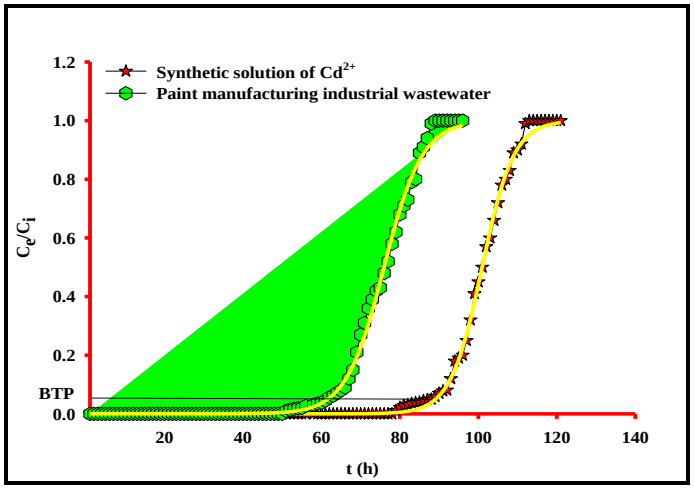

Figure 5: Breakthrough curves of biosorption of Cd^{2+} in synthetic solution and paint manufacturing industrial wastewater by ANDB packed column columns (pH 5.5, bed depth=12.0 cm, flow rate= 1.0 mL min^{-1}).

It was observed from Table 6 that Cd^{2+} biosorption was 100% in case of synthetic solution and it decreases to 95% in case of industrial wastewater. Additionally, the breakthrough point was also reduced to 63 h from 89 h. This may be ascribed due to various metal ions of different size, creating more competition for the adsorption sites and blocking the same. However, the uptake capacity (q_e = 720 mg g^{-1}) in industrial wastewater was still reasonably good indicating the efficacy of the ANDB for the removal of Cd^{2+}, even from multi ion solution.

Table 6: Thomas model parameters of Cd^{2+} biosorption in synthetic solution and paint manufacturing industrial wastewater by ANDB

Metal system	k_{Th} (mL min^{-1} mg)	q_e (mg g^{-1})	R^2	BTP (h)	% Removal of Cd^{2+}	Volume of Water purified (mL)
Single	0.0012	870	0.99	89	100	16,020
Multiple	0.0010	720	0.99	63	95	11,340

6.4 Conclusions

Aspergillus niger decomposed biomass was found to be a promising biosorbent for desalinating $Cd^{2+}$and Pb^{2+} from synthetic, paint manufacturing industrial wastewater due to its easy availability, high metal uptake capacity and reusability in repeated cycles.

The main focus in this chapter was column studies (down flow and up flow) so that the biosorbents as well as the process can be used at large scale in purifying industrial contaminated water. At optimized pH, contact time (flow rate) and temperature the column studies were conducted with paint manufacturing industrial wastewater.

It was observed that metal removal and overall water purification was maximum in up flow mode. Further the effect of co-ions in industrial wastewater was studied on biosorption of Cd^{2+} by comparing the biosorption of the same in synthetic and industrial wastewater. It was seen that the biosorption was more effective in synthetic solution (single metal system) but on the whole the biosorption was also better in industrial wastewater (multi metal system). Finally it can be concluded that ANDB has demonstrated the sequestering of metal ions from industrial effluents and has the potential to be used as an alternative adsorbent at large commercial scale.

References

Akara, S.T.; Gorgulu, A.; Anilan, B.; Kaynak, Z. and Akara, T., Investigation of the biosorption characteristics of lead(II) ions onto Symphoricarpus albus: batch and dynamic flow studies; *J. Hazard. Mater.*; **2009**,165, 126–133.

Amarasinghe, B. M. W. P. K. and Williams, R. A.; Tea waste as a low cost adsorbent for the removal of Cu and Pb from wastewater; *Chem. Eng. J.;* **2007**, *132*, 299–309.

Awofolu, O.R.; Okonkwo, J.O.; Merwe, R.R.; Badenhorst, J. and Jordaan, E.; A new approach to chemical modification protocols of Aspergillus niger and sorption of lead ion by fungal species, *Electronic Journal of Biotechnology*; **2006**, 9, 341–348.

Boudrahem, F.; Aissani-Benissad, F. and Aıˈt-Amar, H.; Batch sorption dynamics an equilibrium for the removal of lead ions from aqueous phase using activated carbon developed from coffee residue activated with zinc chloride; *Journal of Environmental Management;* **2009**, 90, 3031–3039.

Garg, V. K.; Gupta, R.; Yadav, A.B. and Kumar, R.D.; Dye removal from aqueous solution by adsorption on treated sawdust; *Bioresour. Tech;* **2003**, 89 (2): 121–124.

Garg, U.; Kaur, M.P.; Jawa, G.K.; Sud, D. and Garg, V.K. Removal of cadmium(II) from aqueous solution by adsorption on agricultural waste biomass, *J. Hazard. Mater.;* **2008**, 154, 1149–1157.

Galun, M.; Keller, P.; Malki, D.; FeldsteinH, Galun, E.; Siegel, S. and Siegel, B.; Recovery of uranium (VI) from solution using precultured Penicillium biomass; *Water Air Soil Pollut;* **1983**; 20, 221–32.

Galun, M.; Galun, E.; Siegel, B.Z.; Keller, P.; Lehr, H. and Siegel, SM.; Recovery of metal ions from aqueous solutions by Penicillium biomass: kinetic and uptake parameters; *Water Air Soil Pollut* .; **1987**, 33, 359–371.

Gundogdu, A.; Ozdes, D.; Duran, C.; Bulut, V.N.; Soylak, M. and Senturk, H.B.; Biosorption of Pb(II) ions from aqueous solution by pine bark (*Pinus brutia Ten*.); *Chem. Eng. J;* **2009**, 153, 62–69.

Hashim, M.A. and Chu, K.H.; Biosorption of cadmium by brown, green and red seaweeds, *Chem. Eng. J.;* **2004**, 97, 249–255.

Huang, C. and Huang, CP.; Application of Aspergillus oryzae and Rhizopus oryzae for Cu(II) removal; *Water Res*.; **1996**, 30, 1985–1990.

Jacques, R.A.; Lima, E.C.; Dias, S.L.P.; Mazzocato, A.C. and Pavan, F.A.; Yellow passion fruit shell as biosorbent to remove Cr(III) and Pb(II) from aqueous solution; *Sep Purif Technol*.; **2007** 57: 193–198.

Kapoor, A.; Viraraghavan,T. and Cullimore, D.R.; Removal of heavy metals using the fungus Aspergillus niger; *Bioresource Technol;* **1999**, 70, 95–104.

Krishnani, K.K.; Meng, X.; Christodoulatos, C. and Boddu, V.M.; Biosorption mechanism of nine different heavy metals onto biomatrix from rice husk.; *J. Hazard. Mater.;* **2008**, 153, 1222–1234.

Mullen, M.D.; Wolf, D.C.; Ferris, F.G.; Beveridge, T.J.; Flemming, C.A. and Bailey, G.W.; Bacterial sorption of heavy metals; *Appl Environ Microbiol.;* **1989**, 54, 3143–3149.

Naiya, T.K.; Bhattacharya, A.K. and Das, S.K.; Biosorption of Pb(II) by sawdust and neem bark from aqueous solutions; *Environ. Prog.*; **2008**, 27, 313–328.

Park, D.; Yun, Y.; Jo, J.H. and Park, J.M.; Mechanism of hexavalent chromium removal by dead fungal biomass of *Aspergillus niger*; *Water Research*; **2005**, 39, 533–540.

Pehlivan, E.; Altun, T. and Parlayıcı, S.; Utilization of barley straws as biosorbents for Cu^{2+} and Pb^{2+} ions; *J. Hazard. Mater*.; **2009**, 164, 982–986.

Sari, A. and Tuzen, M.; Kinetic and equilibrium studies of biosorption of Pb(II) and Cd(II) from aqueous solution by macrofungus (*Amanita* rubescens) biomass; *J. Hazard. Mater.;* **2009**, 164, 1004–1011.

Smith, A.H.; The Mushroom Hunter's Field Guide, Revised and Enlarged; The University of Michigan Press; Ann Arbor; **1963**, 67.

Sheng, P.X.; Ting, Y.P.; Chen, P. and Hong, L.; Sorption of lead, copper, cadmium, zinc and nickel by marine algal biomass: characterization of biosorptive capacity and investigation of mechanisms; *J. Colloid Interface Sci.;* **2004**, 275, 131–141.

Tsezos, M. and Velosky. B.; The mechanism of thorium biosorptionby Rhizopus arrhizus. *Biotechnol Bioeng.;* **1982**, 29, 955–969.

Tobin, J.M.; Cooper, D.G. and Neufeld, R.J.; Uptake of metal ions by Rhizopus arrhizus; Appl *Environ Microbiol*; **1984**, 47, 821–824.

Vimala, R. and Das, N.; Mechanism of Cd(II) adsorption by macrofungus *Pleutrotus platypus, Journal of Environmental science;* **2011**, 23(2), 288–293.

Vaghetti, J.C.P.; Lima, E.C.; Royer, B.; da Cunha, B.M.; Cardoso, N.F.; Brasil, J.L. and Dias, S.L.P.; Pecan nutshell as biosorbent to remove Cu(II), Mn(II) and Pb(II) from aqueous solutions; *J. Hazard. Mater.*; **2009**, 162, 270–280.

Yu, Q.; Matheickal, J.T.; Yin, P. and Kaewsarn, P.; Heavy metal uptake capacities of common marine macro algal biomass; *Water Res.;* **1999**, 33 (6), 1534–1537.

Zouboulis, A.I.; Matis, K.A.; Lanara, B.G. and Neskovic, C.L.; Removal of Cadmium from Dilute Solutions by Hydroxyapatite. II. Flotation Studies; *Sep. Sci. Technol*.; **1997**, 32, 1755–1767.

Chapter 7

Conclusions and Futuristic Aspects

Contents

Abstract

The outcomes from chapter 3 to 6 have been concluded, compared and correlated in this chapter. The future aspects of biosorbents from agricultural wastes for the removal of heavy metal ions along with other organic contaminants, dyes have also been discussed in this chapter.

7.1 Conclusions from the present studies

In the present study four biosorbents (*Arachis hypogea* shell powder, *Trifolium alexandrnium* biomass powder, *Eucalyptus sp.* saw dust and *Aspergillus niger* decomposed *Citrus limetta* peels powder) of agricultural origin were employed for the removal of six metal ions (Cr^{6+}, Ni^{2+},Cu^{2+}, Zn^{2+}, Pb^{2+} and Cd^{2+}) from synthetic and industrial wastewater. The wastewater of electroplating, lead acid battery and paint manufacturing industry was studied along with synthetic solution. The characterizations of the biosorbents were done using FTIR, SEM-EDX analysis. The biosorption experiments were conducted in batch as well as column modes under optimized conditions. The effect of solution pH, contact time, initial metal ion concentration, biosorbent dose, temperature, kinetics and isotherm modeling was studied in the batch mode. The mechanism of metal biosorption was studied with the help of point of zero charge, chemical blocking of the function groups and total cationic contents of the biosorbent. It was found that biosorption was mainly chemical in nature, including ion exchange and metal complexation on the surface of the biosorbents.

The column studies were performed with varying bed depth, flow rate and metal ion concentrations in down flow and up flow mode. The BDST and Thomas model were applied to the data obtained during column studies to evaluate the metal uptake capacity, breakthrough point and water purification capacity of the column. The HCl, H_2SO_4 , HNO_3, NaOH and EDTA were used as the desorbing agents for the exhausted biosorbents. The brief of each chapter is given as under.

i. **In chapter 3,** activated *Arachis hypogea* shell powder was applied for removal of Cr^{6+} from synthetic and electroplating industrial effluents in batch and column operations.

ii. Kinetics, thermodynamics and isotherm modeling was studied in the batch mode with synthetic solutions and breakthrough points were studied in column mode using electroplating wastewater.

iii. The maximum biosorption capacity of Cr^{6+} in batch process was found to be 111.11 mg g^{-1} at pH 2 and the kinetics data was best fitted with pseudo-second-order model. The thermodynamic parameters viz., Gibbs free energy (ΔG°), enthalpy (ΔH°), and entropy (ΔS°) changes were also calculated, and the observed values supported the spontaneity of the biosorption process.

iv. Thomas and bed depth service time model were applied to study the breakthrough curves at different flow rates and bed depths and the best results were obtained when Cr^{6+} solution of 50 mgL^{-1} concentration was used in a bed depth of 20 cm with a flow rate of 2.0 mL min^{-1} at 2 pH.

v. **Chapter 4**, In this chapter two biosorbents (*Arachis hypogea* shell powder and *Eucalyptus sp.* saw dust) were used in five different combinations, for the removal of Pb^{2+} from synthetic and lead acid battery wastewater.

vi The point of zero charge of the different combinations were studied in order to explain the adsorption of Pb^{2+} at pH 6.0.

vii. The FTIR, SEM, EDX and chemical blocking of the combination was done to expose the functional groups mostly responsible for the removal of Pb^{2+} ions.

viii Column studies were carried out using lead battery wastewater at different flow rates and bed depths. Thomas and bed depth service time model were applied to predict the breakthrough curves and breakthrough service time. The Pb^{2+} uptake capacity ($q_{e=}$ 540.41) was obtained using bed depth of 35.0 cm and a flow rate of 1.0 $mLmin^{-1}$ at 6.0 pH.

ix. **In Chapter 5,** *Trifolium alexandrnium* biomass powder, *Arachis hypogea* shell powder and *Eucalyptus sp.* saw dust were used in four different combinations for the bioremediation of Ni^{2+}, Cu^{2+} and Zn^{2+} from electroplating industrial effluent

x. The FTIR spectra and chemical blocking reveals that carboxyl and hydroxyl functional groups were mostly accountable for the removal of Ni^{2+}, Cu^{2+} and Zn^{2+}.

xi. The release of Na^{+}, K^{+}, Mg^{2+} Ca^{2+}, and H^{+} from the one of combination A with the equivalent uptake of Ni^{2+}, Cu^{2+} and Zn^{2+} supported ion exchange as the foremost mechanism of adsorption.

xii. The adsorbents used in different combinations were attractive and are alternative options for desalinating the heavy metal from industrial effluents containing multiple ions.

xiii. **Chapter 6**, highlights the application of *Aspergillus niger* decomposed *Citrus limetta* peels powder for desalinating $Cd^{2+}$and Pb^{2+} metal ions from synthetic and dye/paint manufacturing industrial wastewater.

xiv. The main focus in this chapter was column studies (down flow and up flow) so that the biosorbents as well as the process can be used at large scale in purifying industrial contaminated water. At optimized pH, contact time (flow rate) and temperature the column studies were conducted with paint manufacturing industrial wastewater.

xv. It was observed that metal removal and overall water purification was maximum in up flow mode. Further the effect of co-ions in paint manufacturing industrial wastewater on biosorption of Cd^{2+} was studied by comparing the biosorption of the same in synthetic solution and industrial wastewater. It was seen that the biosorption was more effective in synthetic solution (single metal system) but on the whole the biosorption was comparatively better in industrial wastewater (multi metal system) also.

xvi. ANDB was found to be most promising biosorbent for desalinating $Cd^{2+}$and Pb^{2+} metal ions from synthetic, paint manufacturing industrial wastewater due to its low cost, easy availability, high metal uptake capacity and reusability in repeated cycles.

7.3 Futuristic approach

i. In present thesis, only four agricultural residues have been studied and tested for the removal of only six metal ions. The biosorption of other toxic metal ions viz., Mercury, Arsenic, Molybdenum, Cobalt and Uranium could also be tested in near future.

ii. Other than metal ions, the removal of certain dyes and organic pollutants can also be studied.

iii. In the present work, the use of column studies both with up flow and down flow modes have been discussed. This approach can be tested at large scale industrial wastewater treatment.

iv. As shown in this study, the use of adsorbents in different combinations have improved the adsorption capacity and this idea can be used in utilizing different adsorbents already studied. The combination of different adsorbents can be utilized to prepare an ion exchanger with multi metal removing capacity. Moreover these low cost agricultural adsorbents can be used for the industrial effluent treatment in developing countries.

List of publications

1. Joginder Singh, Amjad Ali and Vinit Prakash; Removal of lead(II) from synthetic and batteries wastewater using agricultural in batch/column studies; *IJEST;* DOI:10.1007/s 13762-013-0326-9.[I.F: 1.88]

2. Joginder Singh, Amjad Ali and Raman Kumar; Removal of Ni^{2+}, Cu^{2+} and Zn^{2+} Using Different Agricultural Residues: Kinetics, Isotherm Modeling and Mechanism via Chemical blocking; *Asian Journal of Chemistry*; **2013**, 25 (11), 1–10. [I.F: 0.3]

3. Joginder Singh and Amjad Ali; Kinetics; Thermodynamics and Breakthrough Studies of Biosorption of Cr (VI) Using *Arachis hypogea* Shell Powder; *Research Journal of Chemistry and Environment;* **2012**, 16 (1), 69–79. [I.F: 0.66]

4. Joginder Singh; Gagandeep Kaur; Amjad Ali; Breakthrough Studies of Biosorption of Cr (VI) and Cu (II) from Aqueous Solutions Using *Eucalyptus cameldulensis* Charcoal through Column Operations, *Universal Journal of Environmental Research and Technology*; **2012**, 2 (3), 154–160.

5. Joginder Singh; Renu Sharma and Amjad Ali; Application of *Acacia karroo* Charcoal for Desalinating Ni (II) and Zn (II) from Aqueous Solutions in Batch Mode; *Water Reuse and Desalination*, DOI: 10.2166/wrd.2013.062

6. Rajvinder Kaur; Joginder Singh; Rajshree Khare and Amjad Ali; Biosorption the Possible Alternative to Existing Conventional Technologies for Sequestering Heavy Metal Ions from Aqueous Streams; A Review: *Universal Journal of Environmental Research and Technology;* **2012**, 2 (4), 325–335.

7. Rajvinder Kaur; Joginder Singh; Rajshree Khare; Swaranjit Singh and Amjad Ali; Batch Sorption Dynamics; Kinetics and Equilibrium studies of Cr(VI);

Ni(II) and Cu(II) from Aqueous phase Using Agricultural Residues; *Applied Water Science*, DOI 10.1007/s13201-012-0073-y.

8. Rajvinder Kaur; Rajshree Khare; Joginder Singh and Amjad Ali; Fixed bed column operations for the biosorption of Cu (II) from synthetic and electroplting wastewater using Syzygium cumini leaves powder; *Current Trends in Biotechnology and Chemical Research*, **2011**, 1(2) 73–79.

Manuscript under preparation

1. Joginder Singh, Amjad Ali and Vinit Prakash; Application of *Aspergillus niger* decomposed *Citrus limetta* peel powder for desalinating heavy metal ions from paint industry waste water: Batch and up flow column studies manuscript to be submitted in IJEST.

2. Joginder Singh and Amjad Ali, Activated *Arachis hypogea* with enhanced metal sorption capacity from synthetic and industrial wastewater, manuscript ready for submission.

3. Joginder Singh, Pooja Devi and Amjad Ali, Evaluation of Adsorption Potential of Arachis hypogea peel powder for Basic blue 9 and Acid orange 52 from aqueous solutions, manuscript ready for submission.

Publication in Conferences

1. Joginder Singh, Rajvinder Kaur, Rajshree Khare and Amjad Ali, FT-IR, Kinetics, Thermodynamics, Isotherm modeling, and Breakthrough studies for the biosorption of Ni (II) and Cu (II) from aqueous solutions using *Populus deltoides* leaves powder, "Recent Advances in Chemical sciences (ICRACS-2013)" organized by Department of Chemistry, Arya Post Graduate College, Panipat during **2013,** Feb. 24-26.

2. Joginder Singh and Amjad Ali, Removal of Hexavalent Chromium from aqueous systems using *Citrous Limonium* peel powder in AICTE sponsored national conference on Environmental Degradation: Effects, Challenges & Remedies (EDECR-2010) organized by JCDM College of Engineering, Sirsa during Feb. 25-27, 2010.

3. Joginder Singh and Amjad Ali, Thermodynamics and Breakthrough studies of Biosorption of Cr (VI) from Aqueous solution using Activated *Arachis hypogea* shell powder, presented in DST, AICTE, UGC sponsored National Conference on " Emerging Trends In Chemistry- Biology interface (ETCBI-2011) organized Department of Chemistry D.S.B Campus, Kumaun University, Nainital during 03-05 November 2011.

4. Joginder Singh and Amjad Ali, Sequestring heavy metal ions from lead battery effluent using agricultural residue Citrus Limonium peel powder and Eucalyptus cameldulesis in different combinations, presented paper in the AICTE sponsored National Conference on Environmental Pollution Challenges Ahead and their solutions (EPCAS-2012), organized by Global Research Institute of Management and Technology, Radaur, during April 21-22, 2012.